

FFI RAPPORT

**Time Referencing in Offshore Survey
Systems**

Bjørn Jalving, Einar Berglund

FFI/RAPPORT-2006/01666

Time Referencing in Offshore Survey Systems

Bjørn Jalving, Einar Berglund

FFI/RAPPORT-2006/01666

FORSVARETS FORSKNINGSINSTITUTT
Norwegian Defence Research Establishment
P O Box 25, NO-2027 Kjeller, Norway

P O BOX 25

N0-2027 KJELLER, NORWAY

REPORT DOCUMENTATION PAGE

SECURITY CLASSIFICATION OF THIS PAGE
 (when data entered)

1) PUBL/REPORT NUMBER FFI/RAPPORT-2006/01666 1a) PROJECT REFERENCE FFI-IV/341901	2) SECURITY CLASSIFICATION UNCLASSIFIED 2a) DECLASSIFICATION/DOWNGRADING SCHEDULE -	3) NUMBER OF PAGES 120		
4) TITLE Time Referencing in Offshore Survey Systems				
5) NAMES OF AUTHOR(S) IN FULL (surname first) Bjørn Jalving, Einar Berglund				
6) DISTRIBUTION STATEMENT Approved for public release. Distribution unlimited. (Offentlig tilgjengelig)				
7) INDEXING TERMS IN ENGLISH: <table style="width: 100%; border: none;"> <tr> <td style="width: 50%; vertical-align: top;"> a) <u>Survey system</u> b) <u>Time referencing</u> c) <u>Time stamping</u> d) <u>Clock synchronization</u> e) <u>Timing accuracy requirements</u> </td> <td style="width: 50%; vertical-align: top;"> IN NORWEGIAN: a) <u>Kartleggingssystem</u> b) <u>Tidsreferering</u> c) <u>Tidsstempling</u> d) <u>Klokkesynkronisering</u> e) <u>Spesifikasjoner på tidsnøyaktighet</u> </td> </tr> </table>			a) <u>Survey system</u> b) <u>Time referencing</u> c) <u>Time stamping</u> d) <u>Clock synchronization</u> e) <u>Timing accuracy requirements</u>	IN NORWEGIAN: a) <u>Kartleggingssystem</u> b) <u>Tidsreferering</u> c) <u>Tidsstempling</u> d) <u>Klokkesynkronisering</u> e) <u>Spesifikasjoner på tidsnøyaktighet</u>
a) <u>Survey system</u> b) <u>Time referencing</u> c) <u>Time stamping</u> d) <u>Clock synchronization</u> e) <u>Timing accuracy requirements</u>	IN NORWEGIAN: a) <u>Kartleggingssystem</u> b) <u>Tidsreferering</u> c) <u>Tidsstempling</u> d) <u>Klokkesynkronisering</u> e) <u>Spesifikasjoner på tidsnøyaktighet</u>			
THESAURUS REFERENCE:				
8) ABSTRACT <p>The accuracy of offshore survey sensors such as multibeam echo sounders, GPS, ultra-short baseline acoustic navigation systems and attitude sensors is steadily increasing. Integration of high-precision survey and navigation sensors depends on accurate time referencing. The offshore survey community is increasingly experiencing that time referencing accuracy and integration issues are limiting the accuracy offered by the individual sensors themselves.</p> <p>Methods for merging of asynchronous measurements and strategies for clock synchronization are discussed. Operational principles and correct time stamping of key acoustic sensors are presented.</p> <p>Errors in time referencing leads to position errors in final survey products. Based on derived error models of surface survey systems and underwater survey systems, timing accuracy requirements can be calculated from specifications on position accuracy. Timing accuracy requirements in the order of 1 ms were computed.</p> <p>Besides hard requirements on timing accuracy and data output rate a broad approach is needed to ensure high timing accuracy. The report suggests requirements covering time referencing, clock synchronization, time stamping, timing accuracy, merging of asynchronous measurements, data output rate, sensor latency, data acquisition, data recording, time integrity, and sensor mounting.</p>				
9) DATE 2006-06-07	AUTHORIZED BY This page only Nils Størkersen	POSITION Director of Research		

ISBN 82-464-1011-3

UNCLASSIFIED

SECURITY CLASSIFICATION OF THIS PAGE
 (when data entered)

CONTENTS

	Page
1	INTRODUCTION..... 11
2	OBJECTIVES..... 11
3	INTENDED READERSHIP..... 12
4	BACKGROUND ON TIME REFERENCING..... 12
4.1	Introduction to time referencing..... 12
4.2	Importance of time referencing..... 12
4.3	Effect of time referencing errors 13
4.4	Proposed requirements versus IHO standards 13
4.5	Outline of this report..... 14
5	GLOSSARY 15
6	TIME REFERENCING..... 18
6.1	Coordinated universal time (UTC)..... 18
6.2	Merging of asynchronous measurements 18
6.3	Clock synchronization and time stamping 19
6.3.1	Distributed clock synchronization and time stamping..... 19
6.3.2	Centralized clock synchronization and time stamping..... 20
6.3.3	Hybrid clock synchronization and time stamping..... 21
6.4	Methods for clock synchronization 22
6.4.1	GPS UTC 1 PPS (pulse per second)..... 22
6.4.2	Ethernet methods..... 23
6.5	Data output rate 24
6.6	Time integrity..... 25
7	TIME STAMPING OF ACOUSTIC SENSORS 25
7.1	Multibeam echo sounder 26
7.2	Doppler velocity log..... 28
7.2.1	Measurement characteristics 28
7.2.2	DVL timing overview..... 29
7.3	GPS-USBL 31
8	MATHEMATICAL MODELING OF SURVEY SYSTEMS 33
8.1	Nomenclature..... 33
8.2	Surface survey system 35
8.2.1	Introduction 35
8.2.2	Heave..... 36

8.2.3	Problem description	36
8.2.4	Assumptions	37
8.2.5	MBE measurement	37
8.2.6	GPS measurement	37
8.2.7	Geo-referencing of the MBE footprint	38
8.3	Underwater survey system	38
8.3.1	Survey vessel	39
8.3.2	Underwater vehicle	40
9	TIMING ACCURACY REQUIREMENTS	41
9.1	Determining timing accuracy	41
9.1.1	Surface survey system	41
9.1.2	Underwater survey system timing.....	42
9.1.3	Platform dynamics	43
9.2	Surface survey system requirements	44
9.2.1	DTM position requirement	44
9.2.2	Timing accuracy	46
9.3	Underwater survey system requirements	46
9.3.1	Decoupled position requirements	46
9.3.2	MBE ripples	47
9.3.3	Underwater vehicle position ripples	47
9.3.4	Underwater vehicle position offset.....	49
9.3.5	Timing accuracy	50
9.4	Summary of underlying principles for timing requirements	50
10	DYNAMIC BEHAVIOR OF TIMING ERRORS.....	51
11	RECOMMENDED REQUIREMENTS ON TIME REFRENCING	55
11.1	Time reference	55
11.1.1	Time reference (C Req)	55
11.1.2	Time format (C Req).....	55
11.2	Clock synchronization.....	56
11.2.1	Clock synchronization (Non-C Req)	56
11.2.2	Methods for clock synchronization (Non-C Req)	56
11.2.3	Clock synchronization accuracy (C Req)	57
11.2.4	Clock synchronization during data acquisition (C Req)	57
11.2.5	Documentation (C Req)	57
11.3	Time stamping	57
11.3.1	Time stamping (C Req).....	57
11.3.2	Time stamp accuracy (C Req)	57
11.3.3	Documentation on time stamping (C Req).....	58
11.3.4	Latency (C Req)	58
11.3.5	Documentation on latency (C Req).....	58
11.3.6	Hard real-time (C Req)	58
11.4	Timing accuracy	58
11.4.1	Surface survey system timing accuracy (C Req)	59
11.4.2	Underwater survey system timing accuracy (C Req).....	59

11.5	Merging of asynchronous measurements	60
11.5.1	Methods for merging of asynchronous measurements (C Req)	60
11.5.2	Interpolation	60
11.5.3	Merging of data samples closest in time (C Req)	60
11.5.4	Interpolation of position data (C Req)	60
11.6	Data output rate and sensor latency	60
11.6.1	Data output rate and latency in a real-time GPS-USBL system (C Req)	60
11.6.2	Data output rate and latency in real-time MBE surveys (C Req)	61
11.6.3	Data output rate and latency in near real-time and post-processed MBE surveys (C Req)	61
11.6.4	Sensor failure (C Req)	62
11.7	Data acquisition and data recording	62
11.7.1	Post-processing (C Req)	62
11.7.2	Raw data (C Req)	62
11.7.3	Raw data time information (C Req)	62
11.7.4	Data acquisition system time stamps	62
11.7.5	Raw data documentation (C Req)	63
11.7.6	Data acquisition integrity (C Req)	63
11.7.7	Documentation on data acquisition integrity (C Req)	63
11.7.8	Data recording integrity (C Req)	63
11.7.9	Documentation on data recording integrity (C Req)	63
11.7.10	Tracability (C Req)	63
11.7.11	Metadata (C Req)	63
11.8	Time integrity	64
11.8.1	Time integrity (C Req)	64
11.8.2	Documentation (C Req)	64
11.9	Sensor mounting	64
11.9.1	Surface survey ship lever arms (Non-C Req)	64
11.9.2	Underwater vehicle lever arms (Non-C Req)	65
11.9.3	Accurate and repeatable sensor mounting (Non-C Req)	65
11.9.4	Rigid sensor fixtures (C Req)	65
11.9.5	Vibrations (C Req)	65
11.9.6	Documentation (C Req)	65
12	REFERENCES	65
A	INTRODUCTION TO TIMING ERRORS AND ASSUMPTION ON SYNCHRONOUS MEASUREMENTS	67
A.1	Introduction to timing errors	67
A.2	Assumption on synchronous measurements	67
A.3	Error characteristics of an interpolated measurement	69
B	TIMING ERRORS IN SURFACE SURVEY SYSTEMS	71
B.1	Introduction	71
B.2	Error in GPS measurement at MBE measurement time	72
B.3	Error in orientation estimate at MBE measurement time	73

B.4	MBE measurement.....	74
B.5	Total beam positioning error due to timing error	74
B.6	Covariance analysis	76
C	TIMING ERRORS IN UNDERWATER SURVEY SYSTEMS.....	78
C.1	Introduction.....	78
C.2	Survey vessel	79
C.3	Underwater vehicle	80
C.3.1	Error in GPS-USBL measurement at MBE measurement time.....	80
C.3.2	Error in underwater vehicle orientation estimate at MBE measurement time	81
C.4	Total beam positioning error due to timing errors	82
12.1.1	Complete description	82
12.1.2	Categorization and simplification	84
C.5	Covariance analysis	86
C.5.2	Underwater vehicle position offset.....	87
C.5.3	Underwater vehicle position ripples	87
C.5.4	MBE ripples	88
D	LARGE SURVEY VESSEL EXAMPLE	89
D.1	Description.....	89
D.2	Vessel coordinates	89
D.3	Dynamics.....	90
D.4	Effect of timing errors.....	91
E	SMALL SURVEY VESSEL EXAMPLE	95
E.1	Description.....	95
E.2	Vessel coordinates	95
E.3	Dynamics.....	96
E.4	Effect of timing errors.....	97
F	AUV EXAMPLE	101
F.1	Description.....	101
F.2	Vessel coordinates	101
F.3	Deep-water dynamics.....	102
F.4	Effect of timing errors.....	105
G	ROV EXAMPLE	112
G.1	Description.....	112
G.2	Vessel coordinates	112
G.3	Dynamics.....	113

G.4	Effect of timing errors	114
H	WORK GROUP MEMBERS.....	120

Time Referencing in Offshore Survey Systems

Acknowledgement

This report has been written in co-operation with the work group on time referencing within the Norwegian offshore survey community. The report has benefited from comments from all work group members: Arne Indreeide (Statoil), Arne Ofstad (Norwegian Hydrographic Service), Jan Didrik Andersen (Deep Ocean), Rolf Arne Ueland (Blom Maritime), Tor Arne Paulsen (Acergy) and Jan Arvid Ingulfsen (Geoconsult).

The authors are grateful for proofreading and written suggestions from Arne Ofstad, Arne Indreeide and Tom Glancy (Statoil).

The report has benefited from comments and suggestions from Niels Jørgen Vase (Eiva), Edgar Johansen (Kongsberg Seatex AS), Erik Hammerstad (Kongsberg Maritime), Julian Bell (Geoconsult), Kenneth Gade (FFI) and Espen Hagen (FFI). Though, they are not accountable for this report.

1 INTRODUCTION

Within the Norwegian offshore survey community, a work group with representatives from Statoil, Norwegian Hydrographic Service, Blom Maritime, Deep Ocean, Acergy and Geoconsult (part-time) has addressed the need for improved accuracy on time referencing. The Norwegian Defence Research Establishment, FFI, has on behalf of the group written this report. The work group members are listed in Appendix H.

The objective of the work group has been to derive well-founded specifications on time referencing in offshore survey systems. With increased focus on timing accuracy, the ultimate goal is improved sensors, acquisition and processing systems, and procedures. This should result in better data quality in final survey products.

The primary application area for the proposed requirements is *detailed seabed mapping for the offshore industry*. The main goal of the requirements is to get rid of *ripple errors* in the final survey products.

2 OBJECTIVES

The objectives of this report are as follows:

- Explain the process and steps involved in time referencing
- Discuss error sources in time referencing
- Discuss timing issues in typical survey sensors
- Quantify the effect of timing errors in offshore survey systems
- Recommend requirements for improved data quality in offshore surveys

The last objective is of critical importance if the work associated with the compilation of this document is to have a practical value. Evaluation and implementation of requirements for improved data quality is the responsibility of the time group and the offshore survey community.

3 INTENDED READERSHIP

Intended readership of this report falls into a number of categories:

- Scientists and engineers involved in research and development of sensors and systems that are used in offshore survey systems
- Field and support engineers / technicians
- Field surveyors
- Survey managers

All the above-mentioned personnel have a requirement to be informed in matters relating to time referencing. Inevitable, there is a range of technical abilities across the various categories. This presents a practical problem in determining the appropriate structure for this report.

The report includes all necessary mathematical notation and background such that those who possess the required skills can access the detailed error models and calculations on timing accuracy requirements. However, in the interest of readers not interested in these details, the body of the document is predominantly text-based with references to mathematical workings in the appendices.

4 BACKGROUND ON TIME REFERENCING

4.1 Introduction to time referencing

Time referencing together with related terms, are formally defined in Chapter 5. For now we can take this term to mean the process of associating time with a particular measurement. This may be, for example, the time that a depth reading was taken. Accurate knowledge of the time of the measurement is required in order to relate it to other associated data, typical position and orientation.

4.2 Importance of time referencing

The key sensor in detailed seabed surveying is the multibeam echo sounder. The accuracy of multibeam echo sounders, GPS and attitude sensors has improved steadily. Integrating such high-precision survey and navigation sensors into complex survey systems is a non-trivial task. The operators as well as the end-users are increasingly experiencing that integration issues are limiting the accuracy offered by the individual sensors themselves. The work group has acknowledged that accurate time referencing is a key integration issue requiring special attention.

Merging of asynchronous measurements in survey systems is described in Section 6.2.

4.3 Effect of time referencing errors

Errors in time referencing eventually lead to positioning errors in the final survey products. A digital terrain model has two types of positioning errors:

1. *Offset error*
2. *Ripple error*

Timing errors scale with the speed of the survey vehicle and cause position offset errors. The error is called offset error, because for instance a more or less constant error in MBE timing will cause a more or less constant position error in the terrain model (given constant vehicle speed).

Timing errors scale with the angular velocity of the survey vehicle and result in time varying attitude errors with zero mean. These attitude errors cause ripple position errors that are well visible in sun-illuminated terrain models. In Figure 10.4, ripple position errors are illustrated. The dynamic behavior of ripple errors is discussed in Chapter 10.

If one applies different smoothing techniques on the digital terrain model to get rid of the ripples, there is a risk that true topographic features will be filtered as well. Instead of losing valuable information, it is better to assure high timing accuracy when recording and processing survey data. To get rid of ripple errors, is the main driving force for the requirements suggested in Chapter 11.

4.4 Proposed requirements versus IHO standards

In Chapter 11 a set of recommendations to achieve high timing accuracy is given. Besides hard requirements on timing accuracy and data output rate, the chapter includes requirements on several aspects of offshore survey systems:

- Clock synchronization
- Time stamping
- Timing accuracy
- Merging of asynchronous measurements
- Data output rate
- Sensor latency
- Data acquisition
- Data recording
- Time integrity
- Sensor mounting

The International Hydrographic Office (IHO) has developed a set of standards for hydrographic surveys, (6). As this report, the standards include recommendations on many aspects of seabed surveying. The standards also include requirements on horizontal accuracy

and depth accuracy. The accuracy requirements are dependent on the type of survey. Surveys are classified as Special Order, Order 1, Order 2 and Order 3. Special Order surveys are surveys of specific areas with minimum underkeel clearance and where bottom characteristics are potentially hazardous to vessels, for instance harbors. Special order surveys has a 1m (1σ) horizontal position accuracy requirement and a 0.00375 (1σ) depth factor accuracy requirement on depth.

In Chapter 9 it is shown how the timing accuracy requirements in this report are derived from DTM position accuracy requirements. The depth accuracy requirement in this report is one order of magnitude stricter than the IHO standard. This report has equal requirements on horizontal and vertical accuracy, while the IHO standards operate with looser requirements on horizontal accuracy. However, the IHO standards have requirements for the total positioning error and do not address the problems with ripples in DTMs specifically. Nor do the IHO standards address the primary focus area of this report; *detailed seabed mapping for the offshore industry*. The rationale for the timing accuracy requirements in this report is to get rid of ripples errors, to the benefit of underwater engineering. Requirements for total DTM position errors are not discussed. The requirements were chosen to match the available sensor accuracies. The underlying principles for calculating the requirements are summarized in Table 9.6. The work group welcomes suggestions to this report and the requirements.

The following general comments can be made on the IHO standards:

- In the preface to the IHO standards, it is said that the principal aim of the publication is to specify *minimum* standards for hydrographic surveys.
- The standards must be agreed by all national hydrographic offices.
- The principal use of the standards is hydrographic surveys intended for the compilation of nautical charts. The principal use of nautical charts is to ensure safe sea traffic.
- The IHO standards date back to 1998.

4.5 Outline of this report

The report starts with a presentation of key terms, abbreviations and acronyms in Chapter 5.

In Chapter 6 coordinated universal time (UTC), which is the natural time reference in survey systems, is presented. Then a discussion on methods for merging asynchronous measurements in a survey system follows. Since a survey system consists of several different sensors and systems, clock synchronization of the various components are important. The strategies for clock synchronization dictate where measurement time stamping shall take place. In Section 6.4, methods for clock synchronization are presented. The chapter concludes with discussions on data output rate and time integrity.

Chapter 7 is devoted time stamping of acoustic sensors. Understanding the nature of acoustic measurements, and time stamp these correctly is as important as clock synchronization.

In Chapter 8 a generic surface survey system and a generic underwater survey system are modeled mathematically. These models provide a mathematical definition of the survey problem, and a foundation for developing error models in Appendices B and C. The error

models show how timing errors result in position offset errors and position ripple errors in the terrain model.

In Chapter 9 it is suggested that timing accuracy requirements are derived from requirements on positioning accuracy in the terrain models. The end user is only interested in the accuracy of the terrain models, and using the error models in Appendices B and C, resulting requirements on the timing accuracy can be calculated. The offshore survey community should agree on the suggested requirements on positioning accuracy.

Chapter 11 is the main product of the report presenting recommended requirements on time referencing. These include specifications on clock synchronization, time stamping, timing accuracy, merging of asynchronous measurements, data output rate and latency, data acquisition and data recording, time integrity, and sensor mounting.

Input data to the timing accuracy calculations are typical dynamics for small and large surface vessels, ROVs and AUVs, typical sensor placement in these survey platforms and water depth. Increased dynamics cause stricter specifications on timing accuracy. The same is the case with larger sensor lever arms and water depth. In Appendices D, E, F and G, examples on large surface vessel, small surface vessel, AUV and ROV are presented.

5 GLOSSARY

Definitions:

Accuracy	The extent to which a measured or enumerated value agrees with the true value.
Attitude compensation	Transformation of a measurement in a sensor reference frame to a horizontal (North – East – Down) reference frame. High frequency attitude data is required for attitude compensation.
Clock synchronization	Clock synchronization is referring every clock in a multi-component system to a common time reference.
Digital terrain model	Digital representation of a surface model of the seafloor as determined by interpolating a grid of depths in between the observed depth samples.
Error	The difference between an observed or computed value of a quantity and the ideal or true value of that quantity.
Latency	The time delay from physical sensor measurement to processed data availability on the sensor output port.
Lever arm	Three-dimensional position vector from a sensor reference point (or from a ship reference point) to another sensor reference point. The lever arm is normally decomposed in the ship reference frame.
Measurement	A physical observation. A measurement should be as raw as possible, but still practical for further use. The nature of the observation should not be altered by higher order

processing, for instance filtering.

Metacenter

The intersection of vertical lines through the center of buoyancy of a floating body when it is at equilibrium and when it is inclined.

The location of the metacenter is an indication of the stability of a floating body.

For a submerged underwater vehicle, the metacenter coincides with the center of buoyancy. For a surface ship, the metacenter is higher than the center of buoyancy and the center of gravity.

A ship or underwater vehicle rotates around its metacenter. In this report, the origin of the vehicle reference frame is defined to be in the metacenter. Also, specifications on translational speed are referred to the metacenter.

Metadata

Data about a data set and usages aspect of it. Metadata is data implicitly attached to a collection of data. Examples of metadata are data accuracy, data set title and sensor identification.

Navigation

Navigation is the process of directing movement from one point to another. A navigation system is the means by which position and direction is assessed when moving from one point to another.

Positioning

Position referencing of data in a reference frame.

Real-time

A real-time system responds in a (timely) predictable way to unpredictable external stimuli arrivals. In the context of this document; a processor responsible for time stamping reacts within a given predictable time interval when a measurement arrives.

Hard real-time

- No lateness greater than a pre-defined duration is accepted under any circumstances
- Necessary requirement for accurate time stamping of sensor measurements

Soft real-time

- Moderate lateness is accepted
- Necessary requirement for on-line survey processing

Sensor

A sensor is an instrument that reacts to certain physical conditions or impressions and provides information (measurement) on these.

System

Integration of two or more sensors.

Time integrity

Time integrity in a survey system is the ability to provide early warnings to the operators when any sensor or processing system should not be used due to degraded

	timing accuracy.
Time referencing	Time referencing is the assignment of a sensor measurement to its true measurement time in system time (UTC time). Time referencing encompasses time stamping and clock synchronization.
Time stamp	A measurement is normally a complex physical process. The time stamp tells when the physical measurement took place. If the measurement is an averaging process, and not an instantaneous event, the time stamp shall be the best approximate value. Time stamping can be relative a local clock, thus differing the term from time referencing.
Timing accuracy	Short for time referencing accuracy

Some of the definitions are taken from (6).

Abbreviations and acronyms:

AINS	Aided Inertial Navigation System
AUV	Autonomous Underwater Vehicle
DTM	Digital Terrain Model
DVL	Doppler Velocity Log
GMT	Greenwich Mean Time (= Universal Time (UT))
GNSS	Global Navigation Satellite System
GPS	Global Positioning System
IHO	International Hydrographic Organization
IMU	Inertial Measurement Unit
INS	Inertial Navigation System (in this document, the term INS is also used for attitude and heading reference systems)
LAN	Local Area Network
LXI	LAN eXtensions for Instrumentation
MBE	MultiBeam Echo Sounder
NMEA	National Marine Electronics Association
NTP	Network Time Protocol
ppm	parts per million
PPS	Pulse Per Second
PTP	Precision Time Protocol
RFC	Request For Comments (Internet document series. Defines IP networks.)
ROV	Remotely Operated Vehicle
SNTP	Simple Network Time Protocol
SSBL	Super Short Base Line system (= USBL)
TP	Transponder (in this document it is not distinguished between transponder and responder)
USBL	Ultra Short Base Line system (= SSBL)
UTC	Coordinated Universal Time
UV	Underwater Vehicle (term for ROV, towfish and AUV)
WAN	Wide Area Network

6 TIME REFERENCING

Time referencing is the assignment of a sensor measurement to its true measurement time in system time (UTC time). This chapter presents the elements in time referencing; universal time, time stamping and clock synchronization. The chapter also presents methods for merging of asynchronous measurements, which motivates the need for accurate time referencing. Data output rate and time integrity is also discussed.

6.1 Coordinated universal time (UTC)

Coordinated universal time (UTC) is equivalent to mean solar time at the prime meridian (0° longitude), formerly expressed in Greenwich mean time (GMT). UTC is commonly used, and recommended as the time reference for survey work. The GPS system uses precise knowledge of time in its measurements, and is used as a reliable source for correct time.

The GPS time reference is computed based on data from the accurate atomic clocks in each GPS satellite, and from the relative travel times from each satellite to the receiver. GPS time reflects the number of seconds since January 6 1980. GPS time does *not* account for leap seconds, i.e. it differs from UTC time by an integer number of seconds (13 seconds by January 1 1999). This is compensated for by the GPS receivers, which output true UTC time.

Leap seconds are added at midnight on June 30 or December 31, to account for the irregularity in Earth's rotation around the Sun. They cause the last minute of that day in UTC time to have 59 or 61 seconds. The handling of leap seconds varies between systems and is a potential cause of data corruption. Leap seconds are announced several months in advance.

6.2 Merging of asynchronous measurements

A survey system merges time referenced asynchronous measurements into geo-referenced measurements of water depth, and other acoustic or seismic properties. Timing of asynchronous measurements is in Figure 6.1 illustrated for a surface survey system.

A common reference to absolute time is the main key for combining observations from the various sensors and subsystems (see Section 6.1). Equally important is accurate time referencing of each measurement. Accurate time referencing requires time synchronized components, and accurate time stamping within each component (see Section 6.3).

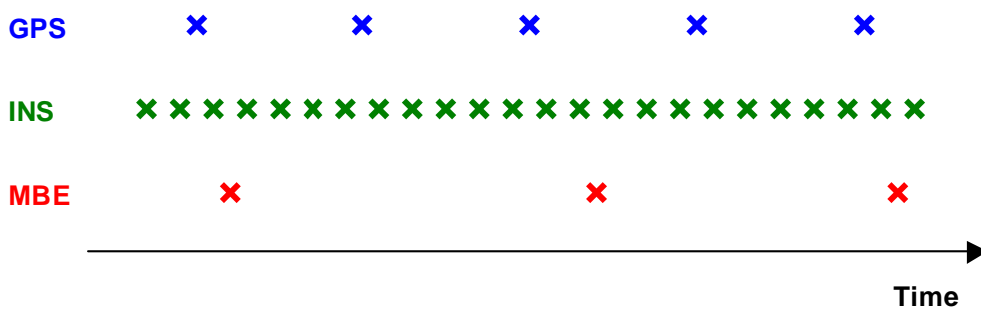


Figure 6.1 Illustration of asynchronous measurements in a surface survey system

Different techniques for merging asynchronous data exist:

1. *Merging of data samples closest in time*
2. *Interpolation*
3. *Extrapolation*

Merging of data samples closest in time requires a sufficiently high data rate to ensure that no significant error is introduced by the measurement period. In Chapter 11.6 specifications on data rate is given. A motion sensor (gyrocompass) is typical capable of producing attitude data at high frequency. An integrated inertial navigation system is typical capable of producing both position and attitude data at high frequency. This allows for

- Combination of high frequency attitude data and MBE raw measurements into a beam swath. See Section 7.1 for details.
- Combination of high frequency ship position data and a MBE swath into a digital terrain model (DTM)

Interpolation is required if the specifications on data output rates in Section 11.6 are not met. For instance lower frequency attitude data can be interpolated to the MBE transmit and receive times. Likewise, lower frequency GPS position data can be interpolated to the MBE swath time stamp. The sensor sampling time must be sufficient to capture the dynamics of the platform (see Section 6.5).

Extrapolation introduces inaccuracy compared to interpolation, and should thus be avoided.

It is important to differ between real-time, near real-time and post-processing use of sensor data. Interpolation is only possible in near real-time or post-processing.

6.3 Clock synchronization and time stamping

It is important to distinguish between data acquisition and data processing. Data acquisition involves precise time stamping and storing of measurements and time stamps. Online or offline data processing combines measurements into survey products.

There are two fundamental approaches to clock synchronization and time stamping:

1. *Distributed clock synchronization and time stamping*. Every sensor is synchronized to reference time (UTC) through to a timeserver. Every sensor time stamps its measurements.
2. *Centralized clock synchronization and time stamping*. The data acquisition system is synchronized to reference time (UTC). The measurements are time stamped in the data acquisition system.

A general requirement to clock synchronization is that sensor time does not change significantly during data acquisition.

6.3.1 Distributed clock synchronization and time stamping

Figure 6.2 illustrates distributed clock synchronization and time stamping. Each sensor clock is individually synchronized to a time reference. Different methods for clock synchronization are described in Section 6.4. If GPS UTC is used directly to synchronize each sensor, the Time Server block in the figure can be omitted. If one of the Ethernet methods described in Sections

6.4.2.1, 6.4.2.2 and 6.4.2.3 are used, a Time Server synchronized to GPS UTC will typically be responsible for time synchronizing of every sensor (client) on the network.

In principle, the Data Acquisition and Survey Processing system in Figure 6.2 does not have to be time synchronized. However, in practice it will normally be, since for instance comparison of sensor time stamps with own time allows for increased time integrity as discussed in Section 6.6.

In distributed clock synchronization, one can have more than one time server in the system, and sensors can be connected to different time servers. However, due to reliability and maintenance, the number of time servers should be low.

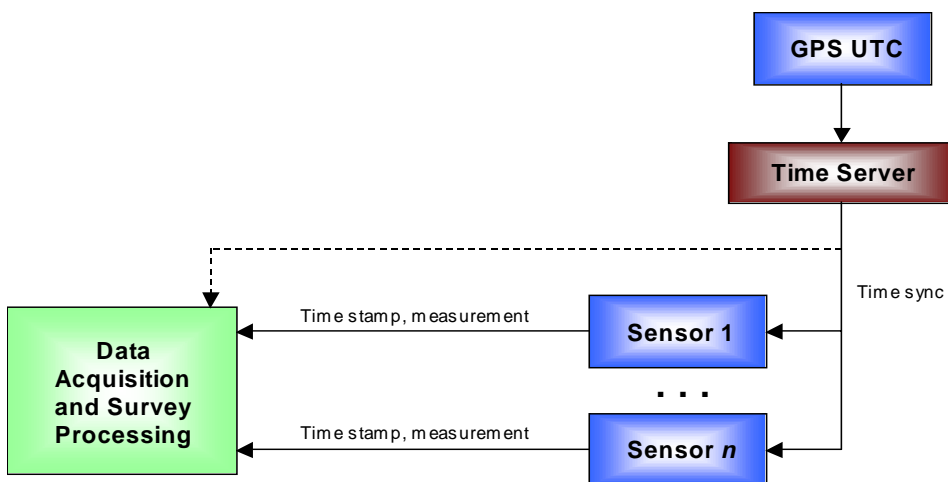


Figure 6.2 Conceptual illustration of distributed clock synchronization and time stamping. Each sensor is individually synchronized to a Time Server. Each sensor time stamps its measurements in UTC.

A practical problem with distributed clock synchronization is that many sensors used in survey systems today do not have time synchronization capabilities. This is for instance the case for most motion sensors, inertial measurement units, pressure sensors and Doppler velocity logs.

Error sources in a system with distributed clock synchronization and time stamping include

1. Error in clock synchronization of each sensor
2. Error in internal sensor timing of physical measurement (time stamping). Refer to Chapter 7.

6.3.2 Centralized clock synchronization and time stamping

A conceptually different approach is illustrated in Figure 6.3, where the sensors are not time synchronized, but directly interfaced to a clock synchronized data acquisition system. The data acquisition system time stamps each incoming stream of sensor data using its central clock. Instead of a time stamp, the sensor measurement must come with latency. The latency must either be known and repeatable (typical for a motion sensor) or computed for each measurement and part of the data interface (typical for an acoustic sensor). Apart from the sensor latency, the data acquisition system must also compensate for transmission delay and its own driver response time.

In principle the central clock in the data acquisition system can be “free running” as long as all measurements are time referenced to the same clock, but in practice the data acquisition system is synchronized to UTC.

Error sources in this system include

1. Error in internal sensor timing of physical measurement (time stamping)
2. Error in calculation of latency in the sensor (or lack of calculation)
3. Error in clock synchronization of the data acquisition system
4. Error in compensation of transmission time
5. Unpredictable interrupt response time in the data acquisition system (real-time requirements)
6. Hardware / software limitations in large systems (typically limited resources in hardware to handle time stamping of all sensors to the central clock)

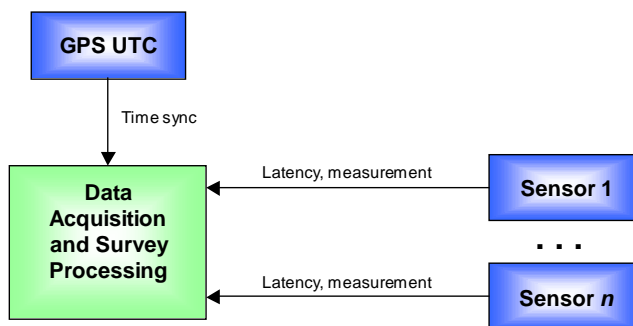


Figure 6.3 Conceptual illustration of centralized clock synchronization and time stamping. The data acquisition system is synchronized to UTC. The measurements are time stamped in the data acquisition system. Each sensor must determine its latency.

6.3.3 Hybrid clock synchronization and time stamping

A practical way to cope with the case that some sensors do not come with clock synchronization capabilities is to install dedicated time stamp hardware (“Time box”) responsible for time stamping. This is illustrated in Figure 6.4. The Time Box must be synchronized to a Time Server and have hard real-time interrupt response time. The Time Box puts a global time stamp on the input data message (compensating for transmission time and interrupt latency) before forwarding it to the Data Acquisition system. The Survey Processing system must subtract the sensor data latency from the Time Box time stamp when processing the data.

The alternative to dedicated time stamp hardware is to have a hard real-time data acquisition system.

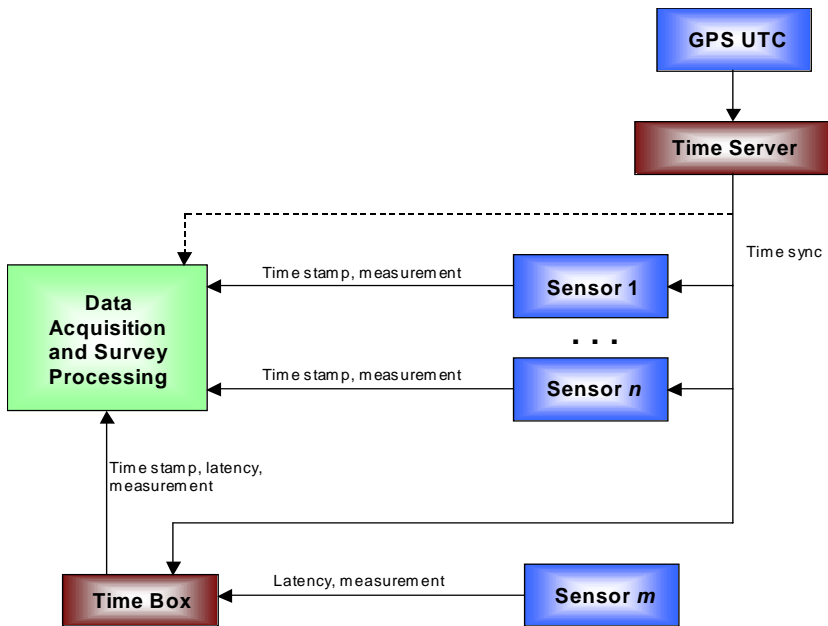


Figure 6.4 A hybrid survey system consisting of sensors capable of clock synchronization together with a dedicated Time Box, which time stamps a sensor that only outputs measurement and latency. The Time Box is required since the Data Acquisition system does not have hard real-time characteristics.

6.4 Methods for clock synchronization

Alternative methods for time synchronization in integrated survey systems are described in the following. In every case, GPS is the ultimate source for UTC time.

6.4.1 GPS UTC 1 PPS (pulse per second)

A GPS receiver outputs a 1 PPS signal every integer second of UTC. There is no standard on shape, duration and polarity of the 1 PPS pulse. This makes it difficult to distribute and use PPS as a means of synchronization for instruments in a survey system. Since the 1 PPS signal represents a one second clock tick, complete UTC time information must be obtained on a separate data line.

The recommended time synchronization output from a GPS receiver is the Trimble compatible 1 PPS + UTC protocol. This consists of a continuous sequence of extremely short pulses at every integer second, accompanied by a *UTC string* emitted on a serial line 500 ms before every integer second. The UTC string contains the date and time of the next 1 PPS pulse. The UTC string also includes a flag to indicate whether the GPS receiver is properly synchronized to GPS time.

Some GPS receivers are unable to transmit UTC strings, and direct customers to use NMEA 0183 standard ZDA or RMC strings instead. The ZDA standard does not define the relation between the 1 PPS pulse and the ZDA telegram. Thus, GPS suppliers recommending ZDA must document their use of the standard.

On sensor level, the implementation of 1 PPS synchronization must be well documented. Since there are few standards for the 1 PPS signals, the sensor must have a user configurable signal

polarity for the 1 PPS input port. The sensor must be able to detect pulses down to $1\mu\text{s}$ duration having a 100 ns rise time and a 3V level. The handling of the full date and the time information in the timestamp must be correct and well documented.

The stability of the 1 PPS signal vary with GPS receivers. Only high quality GPS receivers should be used as a time reference.

6.4.2 Ethernet methods

Correct time and distribution of time in networks and computer systems is important for correct operation. In power distribution, telecommunication and plant automation, distributed systems with real time requirements have often based their communication solutions on fieldbuses. However, due to the continuous price decrease, high bandwidth and availability, switched Ethernet is now a preferred alternative for many applications. In these systems there is a technological trend to time stamp measurements at the source where they are collected.

For Ethernet methods to work, the PC must have a network card suitable for NTP, SNTP or P1588 PTP. Applications running on the PC must use the clock in the network card. According to one Norwegian supplier of timing products, (5), an accuracy of $1\mu\text{s}$ is achievable if the servers are implemented in the Ethernet switches and time stamping of incoming and outgoing time packets is performed at lowest possible level in the OSI protocol stack of both the server and the client implementations. The accuracy is claimed to be in the range of $10\mu\text{s}$ if the time client implementation is based on time stamping in the Ethernet software driver.

6.4.2.1 Network Time Protocol (NTP)

NTP is a client / server time synchronization protocol defined in RFC 1305 (the Request for Comments (RFC) document series is a set of technical notes and standards about the Internet, see (12). RFC defines IP networks.). NTP was designed for time synchronization of computers in a wide area network (WAN). It is the de-facto standard for time synchronization of computer systems on the Internet. NTP client software is available on all major computer platforms, and is included as standard on Windows computers. The timing accuracy depends on network delay and jitter, and is typically 10-50 ms on a WAN and 2-3 ms on a local area network (LAN).

NTP works with four time stamps, two at the client and two at the server. NTP estimates the drift rate and frequency characteristics of the client clock and slowly adjust the clock to correct time. The estimation process takes some time, but the client clock is normally set to correct time from a NTP server at boot up. However, it means that an out-of-sync system (for instance a sensor that has recently been powered on) should be given some time to adjust to the correct time before data acquisition is initialized. The lack of instant synchronization can also be an issue when a leap second is added.

There is some debate on how long it takes to adjust the time. According to OnTime, NTP, SNTP and PTP all need a few minutes to get time synchronization accuracy better than $1\mu\text{s}$, but better accuracy than 1 ms is achieved instantaneously.

6.4.2.2 Simple NTP (SNTP)

Simple NTP is a variant of NTP utilizing server broadcasts to reduce network load. OnTime has developed patented technology that achieves the same time synchronization accuracy with SNTP as PTP.

6.4.2.3 IEEE 1588 Precision Time Protocol (PTP)

IEEE 1588 PTP is a new standard for distribution and synchronization of time in a local area network and is the most accurate Ethernet-based timing available, (10). The PTP standard is intended for precision clock synchronization of networked measurement systems and control systems. The protocol is designed to enable the synchronization of systems that include clocks of different precision, resolution and stability. Sub-microsecond accuracy can be achieved with minimal network and local clock computing resources, and with little administrative attention from the user.

There are several ways in which PTP can be implemented, ranging from user-level software control, to kernel-level driver modifications, to hardware implementations utilizing dedicated FPGA devices.

Use of PTP requires instruments and sensors that can be interfaced to a LAN. Developers of new survey equipment should seriously consider using PTP for time synchronization to UTC.

LXI is an open standard for interfacing instruments to a LAN. LXI is short for LAN eXtensions for Instrumentation. LXI implements IEEE 1588. Although clearly outside the scope of this report, the survey industry is encouraged to consider the LXI standard, (9).

6.5 Data output rate

A sensor has to be sampled with twice the highest frequency component of the signal. If high frequency components are not of interest and a lower sampling frequency is chosen, the signal must be low-pass filtered to avoid aliasing (down-sampling).

Modern motion sensors include embedded processors performing regular calculations. The motion sensors themselves must adhere to basic signal and sampling theory for their internal sensors. The physical bandwidth of the internal sensors must match the sampling frequency. Inertial measurement units (sensor units consisting of three gyros and three accelerometers) typically output rate and acceleration as delta-orientation and delta-velocity over the sampling interval. This avoids problems with aliasing (but creates other challenges such as coning and sculling compensation).

The data output rate of the motion sensor should match the vehicle dynamics. For attitude compensation, *a sampling frequency ten times the highest vehicle frequency of interest is a sound requirement*. For large vehicle attitude rates, a low data rate exhibits similar characteristics as sensor latency when using attitude measurements to position a beam vector, even though no aliasing occurs.

The data rate determines whether interpolation is required in survey processing. The easiest solution for a survey processing system is to have sufficient data rate on its various sensors to allow merging of data samples closest in time (refer to Section 6.1). Real-time MBE transmit

beam steering is an example of an application where sufficient data output rate is required, and interpolation is not possible.

6.6 Time integrity

Time integrity is the ability to provide timely warnings to the operators when the sensor or system should not be used due to degraded time accuracy.

Methods for achieving time integrity include

- Sensors
 - Warning message if problems in synchronizing to universal time
 - Warning message in case of processor overload or degraded hard real-time performance
- System components
 - Warning message if problems in synchronizing to universal time
 - Comparison of time information from every input sensor
 - Comparisons of time synchronized measurements from redundant sensors, e.g. two motion sensors or two GPS receivers.
 - Time difference between sensor input datagram and data acquisition system clock should be relatively small, stable and low variance for sensors like GPS and motion sensors.
 - Supervision on time status from every input sensor.

Examples of system components are:

- Data acquisition systems
- Multibeam echo sounders with position and attitude input for real-time swath calculations
- USBL system with GPS and motion sensor input for real-time production of combined GPS-USBL data.
- Aided inertial navigation systems with input from various aiding sensors

The time integrity methods should be dedicated functionality in survey sensors and systems. But time integrity is also an inherent part of systems for clock synchronization, such as PTP, and should be exploited.

7 TIME STAMPING OF ACOUSTIC SENSORS

Time stamping of acoustic sensors is complicated. For instance, a two way travel time and a bearing measurement have different time stamps. In this chapter correct time stamping of multibeam echo sounder, ultra short base line acoustic navigation system and Doppler velocity log is addressed.

Time stamping of non-acoustic sensors is an equally important issue in survey systems. The workings of non-acoustic survey sensors are not detailed in this report, but the timing accuracy requirements determined in Chapter 9 apply for all survey sensors.

7.1 Multibeam echo sounder

Figure 7.1 shows the observation geometry of a multibeam echo sounder. The effective beam footprint is the intersection between transmit and receive beam patterns. The beam range and thus the two-way travel time for each beam are dependent on the beam angle. The MBE transmits a short pulse and then receives signal echoes for a longer time interval. Typical two-way travel times for shallow water and deep water surveys on a flat seafloor are shown in Figure 7.2. In 50 m water depth, there is a 60 ms time interval between reception of the first beam to hit bottom and end of reception of an outer 60° beam echo. In 2000 m water depth, the corresponding reception period is 2.7 s. The vehicle attitude will normally change significantly during reception of one swath, thus high frequency attitude data is required to position the footprint relative to the ship.

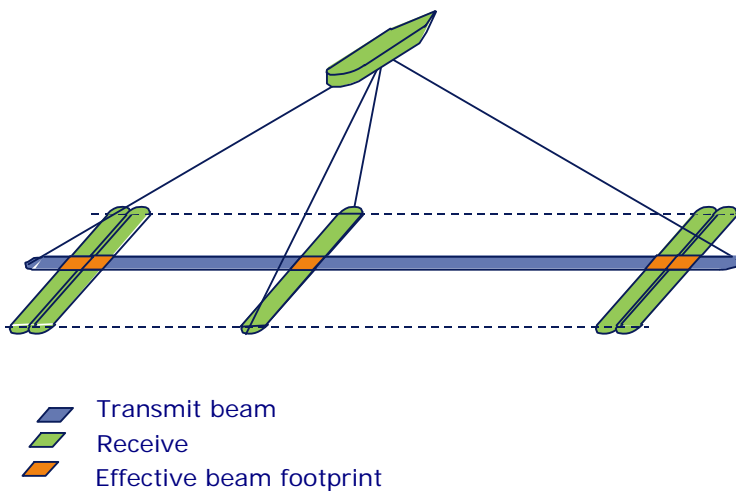


Figure 7.1 Illustration of the observation geometry of a multibeam echo sounder (courtesy of Kongsberg Maritime)

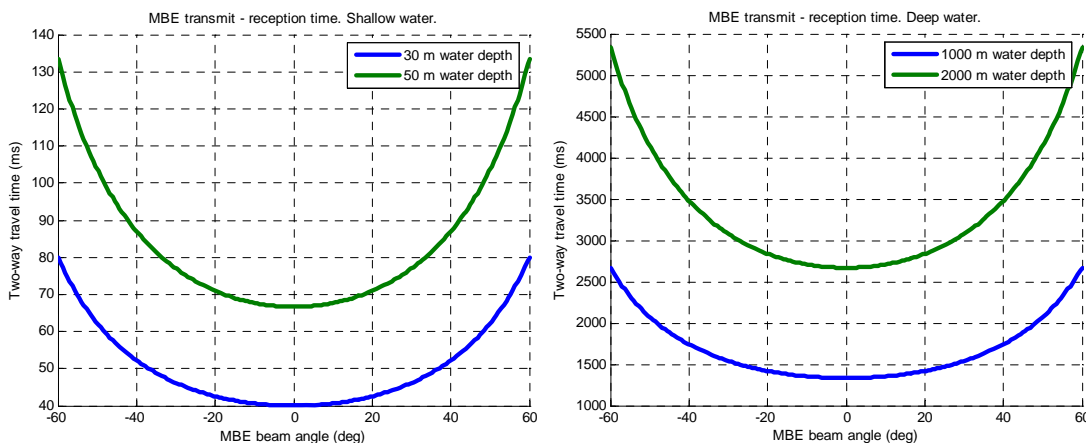


Figure 7.2 MBE transmit-reception time for shallow water and deep water, assuming flat seafloor.

Figure 7.3 and Figure 7.4 illustrate MBE timing. The following definitions are used:

t_{Tx} MBE transmit time

$t_{Rx,center}$ MBE reception time of first beam to hit bottom
 $t_{Rx,outer}$ MBE reception time of outer beams
 $t_{Rx,n}$ MBE reception time of beam n

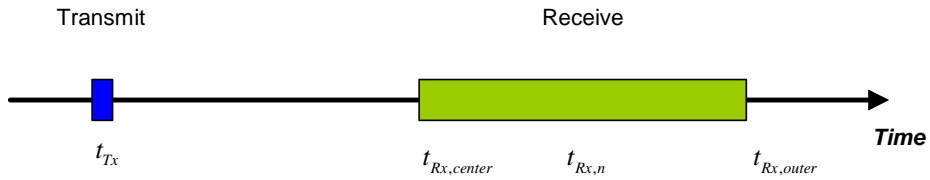


Figure 7.3 Time axis illustration of an MBE transmit-receive sequence.

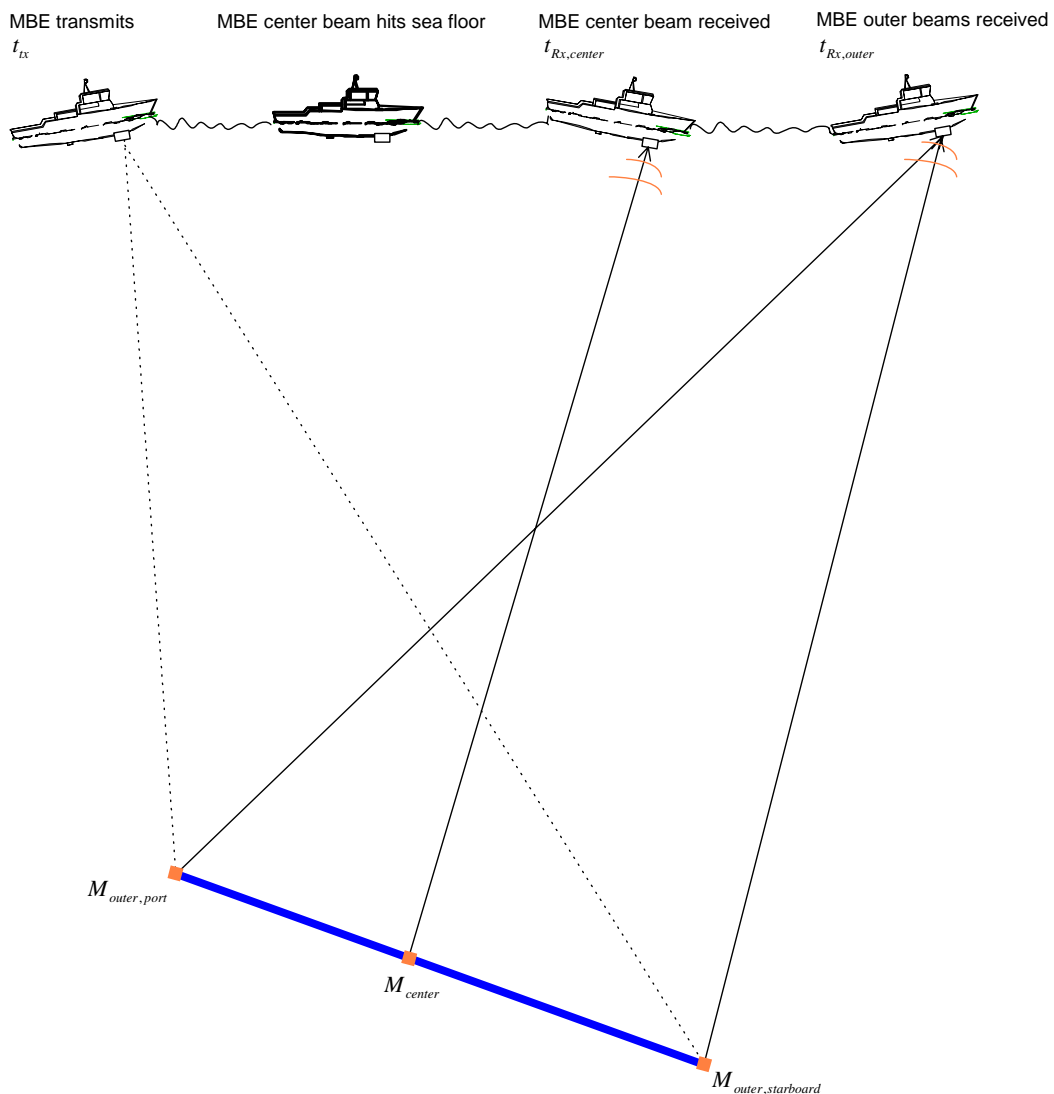


Figure 7.4 Illustration of MBE timing. Center beam means the first beam to hit bottom.

Raw MBE data consists of:

- t_{Tx} (ping time)

- Steered pitch angle
- {range, beam angle, $t_{Rx,n} - t_{Tx}$ } for each beam $1 \dots n$.

MBE beam angle is angle around the x-axis of B_{MBE} (see Table 8.1). Some MBEs come with active transmit beam steering in pitch. This angle must be logged in the raw data.

In a survey set-up, an MBE is accompanied by a motion sensor or an inertial navigation system providing high frequency heave and attitude data. Thus, heave and attitude estimates are available at ping time (t_{Tx}) and each beam reception time ($t_{Rx,n}$). Accurate attitude at t_{Tx} is necessary to determine the position of the narrow transmit beam on the sea floor. And attitude and beam angle at $t_{Rx,n}$ is necessary to position the effective beam footprint inside the narrow transmit beam (see Figure 7.1). Position at t_{Tx} and change in position from t_{Tx} to $t_{Rx,n}$ are also required to process MBE data.

Processed MBE data consists of:

- MBE transmit time (t_{Tx})
- MBE position (global Earth referenced) at transmit time
- Three dimensional x, y, z position of each beam relative to the MBE position at transmit time. The relative position is decomposed in the MBE reference frame at transmit time.

Following the notation defined in Section 8.1 and defining $B_{MBE}(t_{Tx})$ as the position of the MBE at transmit time and M_n as the position of one single MBE beam footprint on the seafloor, the processed MBE data can be described as

- t_{Tx}
- $\hat{\mathbf{p}}_{EB_{MBE}(t_{Tx})}^E$
- $\hat{\mathbf{p}}_{B_{MBE}(t_{Tx})M_n}^{B_{MBE}(t_{Tx})}$ for each beam n

Note that the relative beam position is decomposed in $B_{MBE}(t_{Tx})$.

A sound velocity profile is required to accurately calculate beam range $\left| \mathbf{p}_{B_{MBE}(t_{Tx})M_n}^{B_{MBE}(t_{Tx})} \right|$ from the time measurements. These calculations include refraction (ray bending).

Some MBE systems store both processed and raw MBE data, as well as sound velocity profile and time referenced attitude and position data. Thus, MBE data can be post-processed, if one for instance wants to correct for motion sensor latency or a different sound velocity profile.

7.2 Doppler velocity log

7.2.1 Measurement characteristics

Measured Doppler shift is the sum of Doppler shift at transmission (t_{Tx}) and reception (t_{Rx}). Thus, measured velocity \tilde{v} can be expressed as:

$$\tilde{v}(t_{Tx} + (t_{Rx} - t_{Tx})/2) \approx \frac{v(t_{Tx}) + v(t_{Rx})}{2} \quad (1)$$

Correct time stamping of this average measurement is in the middle of transmission and reception.

In a navigation system, the DVL measurement is normally treated as an instant measurement valid at the given time stamp. Since the DVL measurement in reality is the average of the velocity at t_{Tx} and t_{Rx} , a measurement error is introduced if the acceleration changes in the measurement interval. This is illustrated in Figure 7.5. For typical ROV and AUV dynamics, this effect seems to be negligible.

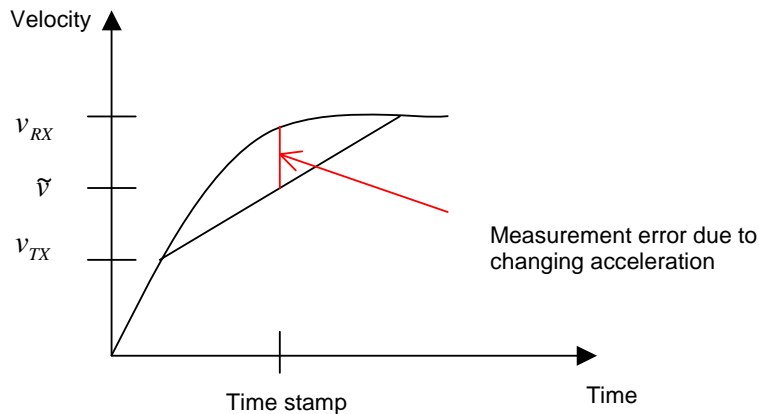


Figure 7.5 DVL measurement error due to averaging effect

7.2.2 DVL timing overview

In Figure 7.6 transmission, reflection and reception of the DVL transmit pulse is illustrated. The measurement is taken from the midpoint of the reflected signal. For the RDI WHN Doppler velocity logs the default pulse length is 30% of the two way travel time to the sea bottom.

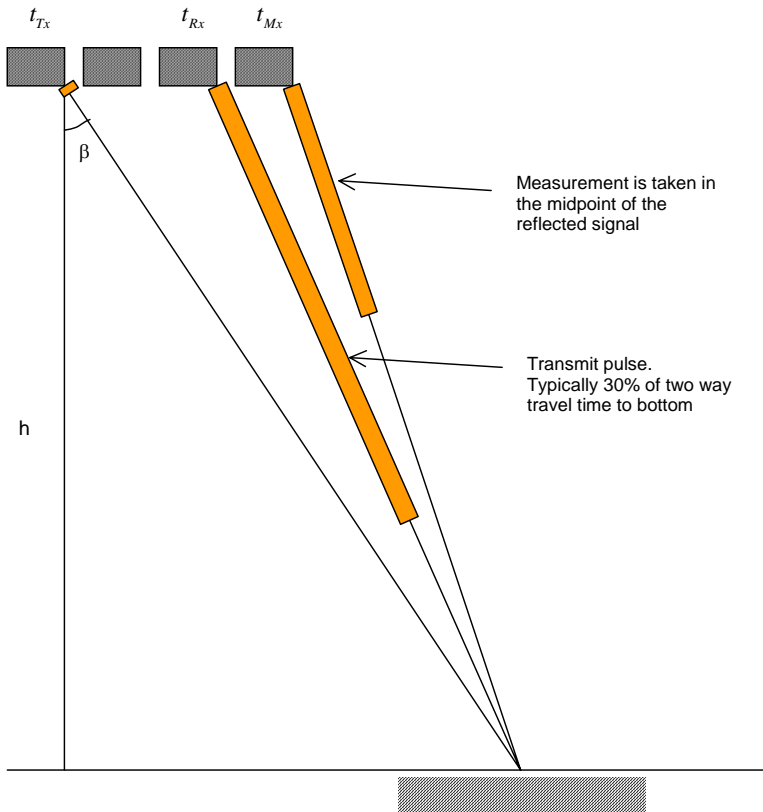


Figure 7.6 Illustration of DVL pulses in water. The figure is based on information on the RDI WHN Doppler velocity logs.

In Figure 7.7 a time axis is shown. The following abbreviations are used:

t_{Tx}	DVL transmit time
t_{Rx}	DVL receive time
t_{Mx}	Doppler shift measurement time
t_{Ex}	End of pulse receive time
t_{DVL}	Correct time stamp. Midpoint of transmit pulse reflection from sea bottom.
$t_{Tx,SL}$	Start serial line transmission
$t_{Rx,SL}$	Data acquisition system receives start of serial line telegram

In the figure, DVL process time is defined as the delay between end of pulse reception (t_{Ex}) and transmission of the serial line ensemble data ($t_{Tx,SL}$). When the data acquisition system receives a DVL serial line telegram, it reads its own current time, $t_{Rx,SL}$. To achieve acceptable navigation performance, it needs t_{DVL} in its own time reference. This can be achieved in two obvious ways. Either, the DVL must output latency ($t_{Tx,SL} - t_{DVL}$) in its data telegram or the DVL must be time synchronized to the same time reference at the data acquisition system and time stamp the measurement with t_{DVL} .

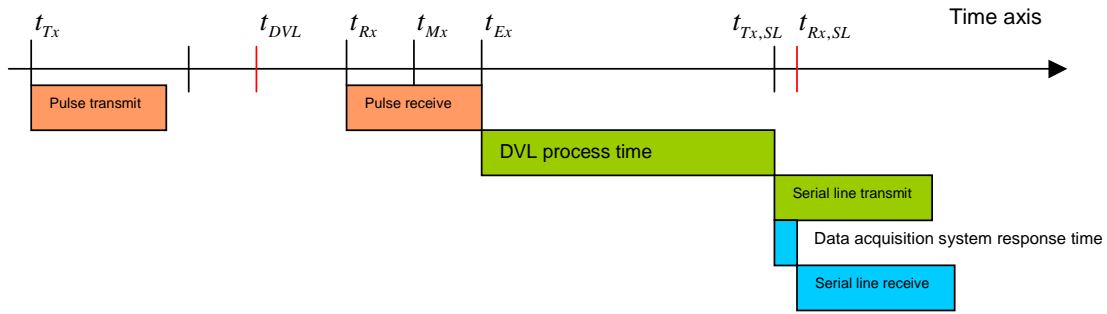


Figure 7.7 Time axis illustration of DVL timing

7.3 GPS-USBL

A USBL system can either output relative position between its transceiver and transponder, or if integrated with GPS, global position estimates of the transponder. The USBL must be integrated with a motion sensor or INS, to correct for survey vessel attitude. In underwater mapping operations with ROV, AUV or towfish, global GPS-USBL position measurements are of interest. A conceptual GPS-USBL system is shown in Figure 7.8.

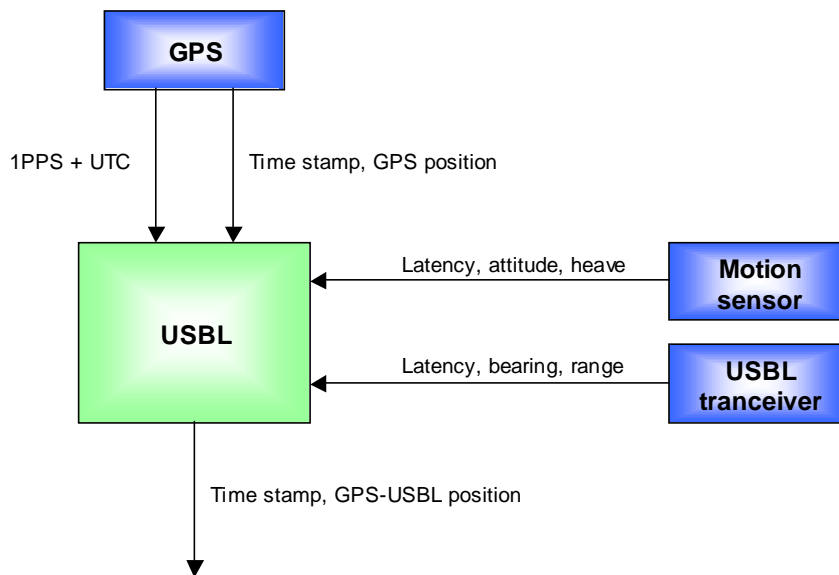


Figure 7.8 Conceptual illustration of a GPS-USBL system. Input of sound velocity profile is not illustrated. A GPS-USBL system normally runs in real-time, but it can also be run in post-processing.

Correct time stamping of the GPS-USBL measurements is crucial for position accuracy. In Figure 7.9, timing of an USBL system in *transponder mode* is illustrated. Transponder mode means that the survey vessel interrogates the transponder on the underwater vehicle at regular intervals. The following definitions are used:

$t_{Tx,ship}$	Survey vessel transmit time
$t_{Rx,UV}$	Underwater vehicle receive time
$t_{Tx,UV}$	Underwater vehicle transmit time

$t_{Rx,ship}$ Survey vessel receive time

Range, $|\tilde{\mathbf{p}}_{B_{USBL}B_{TP}}^{B_{USBL}}|$, is found by measuring two-way travel time

$$|\tilde{\mathbf{p}}_{B_{USBL}B_{TP}}^{B_{USBL}}| = \frac{(t_{Rx,ship} - t_{Tx,ship} - (t_{Tx,UV} - t_{Rx,UV})) \cdot c}{2} \quad (2)$$

where c is sound velocity. The transponder reaction time, $t_{Tx,UV} - t_{Rx,UV}$, is normally constant and known. The complete sound velocity profile should be compensated for. Two-dimensional USBL bearing is measured in the survey vessel at $t_{Rx,ship}$. Importantly, the bearing measurements reflect the underwater vehicle position at $t_{Tx,UV}$. When combining USBL and GPS, the GPS measurement at $t_{Rx,ship}$ must be used, but the combined measurement is valid at $t_{Tx,UV}$.

The example is typical for an AUV application with the USBL run in transponder mode. For ROV and towfish, the underwater vehicle transponder can be triggered electronically (via and umbilical/cable) and only a one-way acoustic travel time is measured. This is often referred to as responder mode. AUVs can also be run in beacon mode. In beacon mode, the AUV transmits at regular interval without any triggering. The surface ship can only measure bearing, but gets depth information from the AUV depth sensor, thereby having enough information to calculate a position fix.

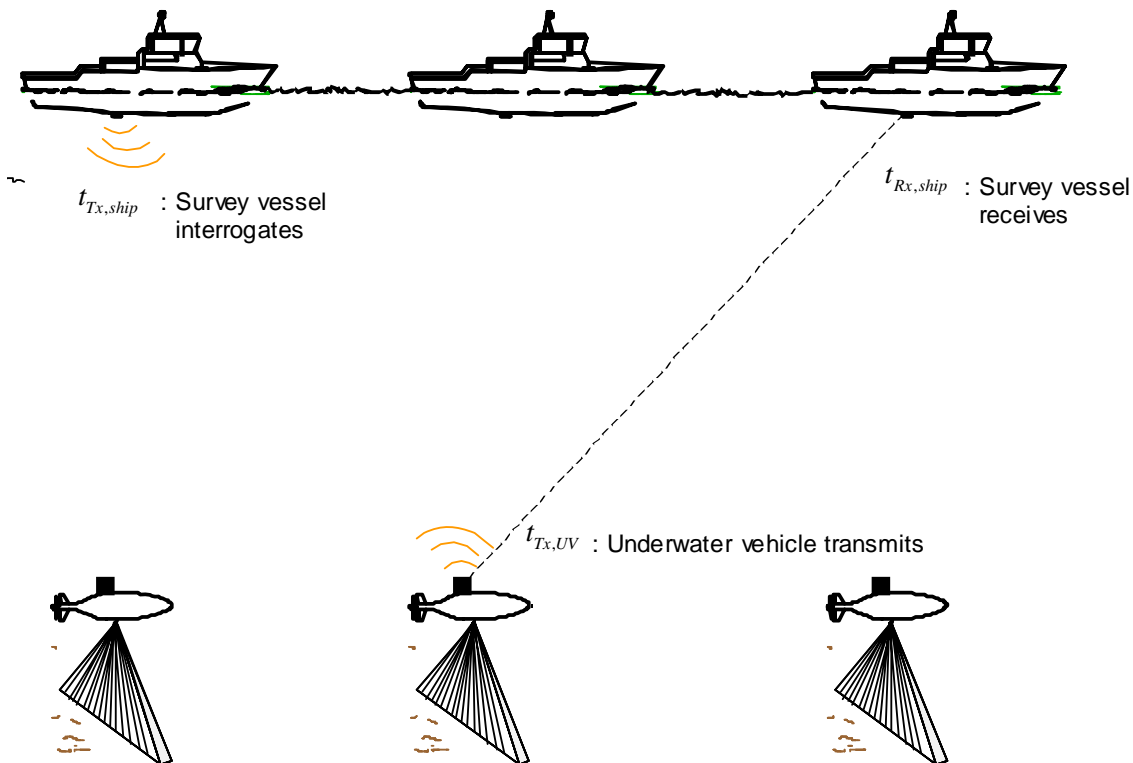


Figure 7.9 Illustration of USBL timing in transponder mode.

In Figure 7.10 asynchronous arrival of GPS, attitude and USBL data is illustrated. Attitude data typically comes with 100 Hz, GPS data with 1 – 10 Hz and USBL data with 0.2 – 2 Hz, depending on water depth. The attitude data is used for USBL beam arm attitude compensation and GPS lever arm and attitude compensation. USBL systems normally interpolate the lever arm and attitude compensated GPS data to $t_{Rx,ship}$ before adding USBL and GPS.

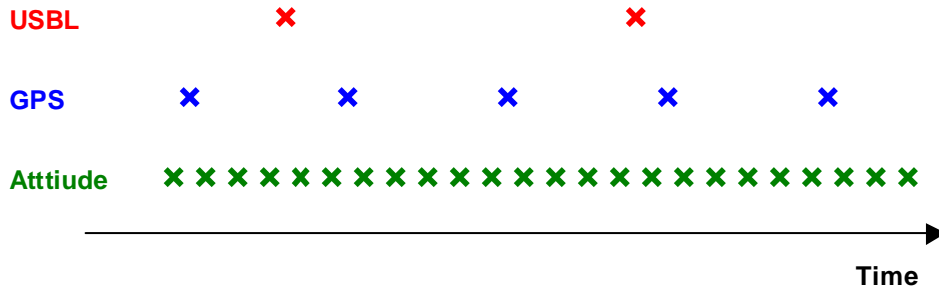


Figure 7.10 Illustration of asynchronous measurements in a GPS-USBL system

For a real-time underwater navigation system, the GPS-USBL position measurement is by nature delayed in time. Thus, the integrated navigation system must be capable of handling delayed measurements. This requires accurate time stamping, a common time reference and a buffer of old navigation data in the integrated navigation system, typically a 10 – 15 s history for deep-water operations (handling delay in USBL measurement and delay in acoustic transmission to the underwater vehicle).

8 MATHEMATICAL MODELING OF SURVEY SYSTEMS

8.1 Nomenclature

To model the sensor integration problem and derive an error budget on timing errors, we define the coordinate systems in Table 8.1. These coordinate systems are in accordance with the definitions in (3).

The survey and navigation sensors have different positions and orientations. Reference systems for each sensor are defined in Table 8.2. The reference systems define both location and orientation. The origin is in the reference point of the sensor.

The position vector from the origin of coordinate system A to the origin of coordinate system B , decomposed in coordinate system C , is denoted p_{AB}^C . Use of tilde \tilde{p}_{AB}^C denotes a measurement of p_{AB}^C . Use of hat \hat{p}_{AB}^C denotes a calculated value based on one or more measurements. No embellishment means a true value.

Symbol	Description
I	<i>Name:</i> Inertial

	<p>Position: Not relevant</p> <p>Orientation: Not relevant</p> <p>Comments: The system is the inertial space as defined by Newton, i.e. inertial sensors measure relative to this system.</p>
<i>E</i>	<p>Name: Earth</p> <p>Position: The origin coincides with Earth's center (geometrical center of ellipsoid model).</p> <p>Orientation: The <i>x</i>-axis points towards north (the <i>yz</i>-plane coincides with the equatorial plane), the <i>y</i>-axis points towards longitude +90° (east).</p> <p>Comments: The system is Earth-fixed (rotates and moves with the Earth).</p>
<i>B</i>	<p>Name: Body</p> <p>Position: The origin is in the vehicle's reference point.</p> <p>Orientation: The <i>x</i>-axis points forward, the <i>y</i>-axis to the right (starboard), and the <i>z</i>-axis in the vehicle's down direction.</p> <p>Comments: The system is fixed to the vehicle.</p>
<i>N</i>	<p>Name: North-East-down (local)</p> <p>Position: The origin is directly beneath or above the vehicle (<i>B</i>), at Earth's surface (surface of ellipsoid model).</p> <p>Orientation: The <i>z</i>-axis is pointing down. The <i>x</i>-axis points towards north, and the <i>y</i>-axis points towards east.</p> <p>Comments: When moving relative to the Earth, the system rotates about its <i>z</i>-axis to allow the <i>x</i>-axis to always point towards north.</p>
<i>L</i>	<p>Name: Local, Wander azimuth (Foucault-version)</p> <p>Position: The origin is directly beneath or above the vehicle (<i>B</i>), at Earth's surface (surface of ellipsoid model).</p> <p>Orientation: The <i>z</i>-axis is pointing down. Initially the <i>x</i>-axis points towards north, and the <i>y</i>-axis points towards east, but as the vehicle moves they are not rotating about the <i>z</i>-axis (their angular velocity relative to the Earth has zero component along the <i>z</i>-axis).</p> <p>Comments: The <i>L</i>-system is equal to the <i>N</i>-system except for the rotation about the <i>z</i>-axis, which is always zero for this system. Hence, at a given time, the only difference between the systems is an angle between the <i>x</i>-axis of <i>L</i> and the north direction; this angle is called the <i>wander azimuth</i> angle. If the movement of the vehicle is within a limited geographical area and not close to any of the poles, the wander azimuth angle is very small ($L \approx N$). The <i>L</i>-system is well suited for general calculations as it is non-singular.</p>
<i>M</i>	<p>Name: Map</p> <p>Position: The position of one single multibeam echo sounder beam footprint on the seafloor. (Beam number <i>n</i>.)</p> <p>Orientation: Not relevant</p> <p>Comments: In this report this coordinate system is used to denote the position of one multibeam echo sounder beam footprint on the seafloor. The origin is Earth fixed and does not move with the vehicle.</p>

Table 8.1 Definitions of coordinate systems

Body system	Description
B_{ship}	Surface vessel reference frame. Origin is in metacenter.
B_{UV}	Underwater vehicle reference frame. Origin is in metacenter.
B_{MBE}	Multibeam echo sounder transducer head
B_{USBL}	Ultra short base line system transducer (on surface vehicle)
B_{TP}	Ultra short base line system transponder (on underwater vehicle)
B_{GPS}	GPS antenna
B_{INS}	Defined by the inertial measurement unit of the inertial navigation system
B_{depthm}	Pressure sensor
B_{DVL}	Doppler velocity log

Table 8.2 Definitions of sensor reference systems. The origin is in the reference point of the sensor.

The surface vessel reference frame, B_{ship} , and the underwater vehicle reference frame, B_{UV} , are assumed to have their origins in the metacenter. Thus, in this analysis the surface vessel and the underwater vehicle rotate around their reference frames.

8.2 Surface survey system

8.2.1 Introduction

In Figure 8.1 a surface survey system is schematically illustrated. On survey vessels, there is considerable diversity in navigation sensor equipment. Many vessels have a dedicated gyrocompass (motion sensor) or a dual GPS antenna for heading combined with a motion sensor for roll and pitch. In the figure, a single GPS receiver and an inertial navigation system (INS) capable of estimating roll, pitch, heading, velocity and position are shown. The main objective of the navigation system is to position each MBE footprint accurately in geographic coordinates (E). In this section, the positioning of a MBE footprint is modeled mathematically. The sensor outfit and the mathematical modeling in this report probably differ somewhat from actual systems. However, the presented model is valid for deriving a generic error budget for a surface survey system.

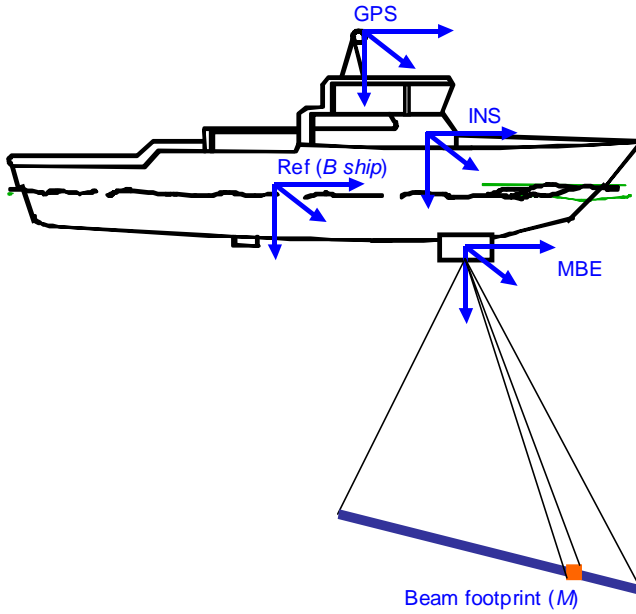


Figure 8.1 Illustration of sensor coordinate systems in a surface survey system

8.2.2 Heave

Motion sensors and gyrocompasses usually come with specialized algorithms for measuring heave. A digital terrain model (DTM) must be referred to a defined datum. The parameter of interest is the vertical distance from N to B_{ship} , $p_{NB_{ship},z}^N$. If the WGS-84 datum is used, and N is defined to follow the surface of this ellipsoid, the distance between N and B_{ship} must be determined to refer the digital terrain model to WGS-84. In the equations below, it is assumed that the GPS system measures ship height with sufficient accuracy. If using heave estimates from a motion sensor, one should be aware that these are normally derived using frequency based filtering techniques that can introduce a time shift.

The main argument for assuming heave measured by GPS is to simplify the principal analysis on time accuracy in this report. Discussing obtainable heave accuracy for GPS and motion sensor is outside the scope of this report.

8.2.3 Problem description

The multibeam echo sounder measures range (two-way acoustic travel time) and bearing to a beam footprint (M) on the seafloor in its B_{MBE} body system. Relative the MBE, the position of the footprint can be expressed as $\tilde{p}_{B_{MBE}M}^{B_{MBE}}$. To arrive at a final digital terrain model (bathymetric map), the footprint must be transformed into Earth fixed coordinates (E), mathematically described as \hat{p}_{EM}^E . From this vector, latitude, longitude and depth of the footprint can be derived.

8.2.4 Assumptions

Since the scope of this report is time synchronization error analysis, we assume that the orientation of the inertial navigation system (B_{INS}) and the multibeam echo sounder (B_{MBE}) relative to the body reference frame (B_{ship}) is perfectly known. That means that the rotation matrices $R_{B_{ship}B_{MBE}}$ and $R_{B_{ship}B_{INS}}$ are error-free. Normally, these rotation matrices are found by a static survey of the vessel at dock. The relative orientation error between the INS and the MBE ($R_{B_{INS}B_{MBE}}$) can be found by a conventional patch test, (4). For a discussion on the whole range of MBE related error sources see (1) and (2).

The ship lever arms from B_{GPS} to B_{ship} , $p_{B_{GPS}B_{ship}}^{B_{ship}}$, and from B_{ship} to B_{MBE} , $p_{B_{ship}B_{MBE}}^{B_{ship}}$, are assumed perfectly surveyed.

8.2.5 MBE measurement

Since $R_{B_{ship}B_{MBE}}$ is known, the MBE measurement can be directly decomposed in the B_{ship} reference frame

$$\tilde{p}_{B_{MBE}M}^{B_{ship}} = R_{B_{ship}B_{MBE}} \tilde{p}_{B_{MBE}M}^{B_{MBE}} \quad (3)$$

The $\tilde{p}_{B_{MBE}M}^{B_{ship}}$ vector should be decomposed in the North East down (N) system. We also want to express the position of M relative to the origin of the ship reference frame (B_{ship}). This transformation is also called MBE attitude and lever arm compensation. It is given by

$$\hat{p}_{B_{ship}M}^N = \hat{R}_{NB_{ship}} \left(p_{B_{ship}B_{MBE}}^{B_{ship}} + \tilde{p}_{B_{MBE}M}^{B_{ship}} \right) \quad (4)$$

where $\hat{R}_{NB_{ship}}$ is a rotation matrix representing the attitude estimate (roll, pitch, heading) of the inertial navigation system and $p_{B_{ship}B_{MBE}}^{B_{ship}}$ is the lever arms from the ship reference frame (B_{ship}) to the MBE (B_{MBE}).

8.2.6 GPS measurement

We now have the position of M (beam footprint) relative to B_{ship} ($\hat{p}_{B_{ship}M}^N$) in the North East down reference frame, but we need to geo-reference it, i.e. we need to find \hat{p}_{EM}^E . GPS measures the position of the GPS antenna (B_{GPS}) relative to the Earth (E): $\tilde{p}_{EB_{GPS}}^E$. Since the MBE measurement has been transformed to the ship reference point (B_{ship}), we want to do the same thing with the GPS measurement. GPS lever arm compensation from B_{GPS} to B_{ship} in North East down is given by

$$\hat{p}_{B_{GPS}B_{ship}}^N = \hat{R}_{NB_{ship}} p_{B_{GPS}B_{ship}}^{B_{ship}} \quad (5)$$

By adding the $\hat{p}_{B_{GPS}B_{ship}}^N$ lever arms to the GPS measurement in B_{GPS} , we get the global position of B_{ship}

$$\hat{\mathbf{p}}_{EB_{ship}}^E = \tilde{\mathbf{p}}_{EB_{GPS}}^E + \hat{\mathbf{R}}_{EN} \hat{\mathbf{R}}_{NB_{ship}} \mathbf{p}_{B_{GPS}B_{ship}}^{B_{ship}} \quad (6)$$

\mathbf{R}_{EN} is the rotation matrix from N to E . \mathbf{R}_{EN} can be derived from $\tilde{\mathbf{p}}_{EB_{GPS}}^E$.

8.2.7 Geo-referencing of the MBE footprint

By adding GPS position in B_{ship} (equation (6)) with relative MBE footprint in B_{ship} (equation (4)), we get a position estimate of the MBE footprint in geographic coordinates

$$\hat{\mathbf{p}}_{EM}^E = \tilde{\mathbf{p}}_{EB_{GPS}}^E + \hat{\mathbf{R}}_{EN} \hat{\mathbf{R}}_{NB_{ship}} \left(\mathbf{p}_{B_{GPS}B_{ship}}^{B_{ship}} + \mathbf{p}_{B_{ship}B_{MBE}}^{B_{ship}} + \tilde{\mathbf{p}}_{B_{MBE}M}^{B_{ship}} \right) \quad (7)$$

$$\hat{\mathbf{p}}_{EM}^E = \tilde{\mathbf{p}}_{EB_{GPS}}^E + \hat{\mathbf{R}}_{EN} \hat{\mathbf{R}}_{NB_{ship}} \left(\mathbf{p}_{B_{GPS}B_{MBE}}^{B_{ship}} + \tilde{\mathbf{p}}_{B_{MBE}M}^{B_{ship}} \right) \quad (8)$$

where $\hat{\mathbf{p}}_{EM}^E$ represents the desired geo-referencing of the MBE footprint.

In Section A.3 equation (8) will be analyzed with respect to time synchronization errors.

8.3 Underwater survey system

In Figure 8.2 an underwater survey system is illustrated. Several different platforms and technologies can be categorized as an underwater survey system, including:

- ROV
- AUV
- Towfish

Even though these systems have different dynamics and different vehicle to survey vessel geometry, they share the same mathematical description that only differs in parameters.

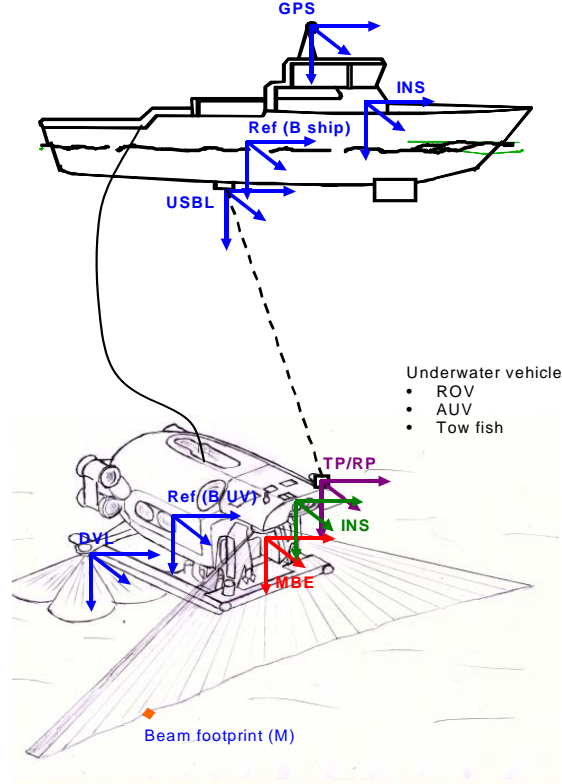


Figure 8.2 Illustration of sensor coordinate systems in an underwater survey system.

8.3.1 Survey vessel

For the purpose of deriving a generic error budget, the survey vessel is assumed to have a GPS and INS as in Section 8.2. The USBL system is the primary sensor, needed to measure the position of the underwater vehicle relative to the survey vessel. USBL measures the position of the underwater vehicle transponder B_{TP} in its B_{USBL} body system. This measurement can be expressed as $\tilde{\mathbf{p}}_{B_{USBL}B_{TP}}^{B_{USBL}}$. $\tilde{\mathbf{p}}_{B_{USBL}B_{TP}}^{B_{USBL}}$ must be transformed into Earth fixed coordinates, $\hat{\mathbf{p}}_{EB_{TP}}^E$, before it can be used as a position measurement in the underwater vehicle. This is analogous to transforming the $\tilde{\mathbf{p}}_{B_{MBE}M}^{B_{MBE}}$ MBE beam footprint into Earth coordinates in Section 8.2.

Since the scope of this report is time synchronization error analysis, we assume that the orientations of the INS ($B_{INS,ship}$) and the USBL (B_{USBL}) relative to the ship reference frame (B_{ship}) are perfectly known. That means that the rotation matrices $\mathbf{R}_{B_{ship}B_{USBL}}$ and $\mathbf{R}_{B_{ship}B_{INS,ship}}$ are error-free. The orientation between the INS and the ship reference frame can be found by a static survey of the vessel at dock. The relative orientation between the INS and the USBL is typically found in a USBL transducer alignment. A normal procedure is to deploy a transponder on the seafloor and position the vessel at four cardinal points and on top of the transponder with four headings, (8).

The ship lever arms from B_{GPS} to B_{ship} , $\mathbf{p}_{B_{GPS}B_{ship}}^{B_{ship}}$, and from B_{ship} to B_{USBL} , $\mathbf{p}_{B_{ship}B_{USBL}}^{B_{ship}}$, are assumed perfectly surveyed.

Following the same steps as in Section 8.2, a combined GPS-USBL position measurement of the underwater vehicle transponder can be derived

$$\hat{\mathbf{p}}_{EB_{TP}}^E = \tilde{\mathbf{p}}_{EB_{GPS}}^E + \hat{\mathbf{R}}_{EN} \hat{\mathbf{R}}_{NB_{ship}} \left(\mathbf{p}_{B_{GPS}B_{USBL}}^{B_{ship}} + \tilde{\mathbf{p}}_{B_{USBL}B_{TP}}^{B_{ship}} \right) \quad (9)$$

$\hat{\mathbf{R}}_{NB_{ship}}$ is the rotation matrix representing the orientation estimate of the ship navigation system. $\hat{\mathbf{R}}_{EN}$ can be derived from the GPS position measurement.

The major error components in this equation with respect to time synchronization include

- *GPS position measurement*, $\tilde{\mathbf{p}}_{EB_{GPS}}^E$.
- *USBL attitude compensation*, $\hat{\mathbf{R}}_{NB_{ship}} \tilde{\mathbf{p}}_{B_{USBL}B_{TP}}^{B_{ship}}$.
- *Ship lever arms compensation*, $\hat{\mathbf{R}}_{NB_{ship}} \mathbf{p}_{B_{GPS}B_{USBL}}^{B_{ship}}$.

See Section C.2 for error modeling.

8.3.2 Underwater vehicle

The underwater vehicle navigation system runs in real-time and / or in post-processing. In either case, its position measurement is the combined GPS-USBL position $\hat{\mathbf{p}}_{EB_{TP}}^E$ calculated in the survey vessel and modeled in equation (9).

As shown in Figure 8.1, the underwater vehicle is equipped with a multibeam echo sounder measuring range and bearing to a beam footprint (M) on the seafloor: $\tilde{\mathbf{p}}_{B_{MBE}M}^{B_{MBE}}$. The main objective of the underwater vehicle navigation system is to position this footprint in geographic coordinates, $\hat{\mathbf{p}}_{EM}^E$.

As for the survey vessel, the rotation matrices $\mathbf{R}_{B_{UV}B_{MBE}}$ and $\mathbf{R}_{B_{UV}B_{INS}}$ and the underwater vehicle lever arms $\mathbf{p}_{B_{TP}B_{UV}}^{B_{UV}}$ and $\mathbf{p}_{B_{UV}B_{MBE}}^{B_{UV}}$ are assumed perfectly surveyed.

Geo-referencing of the MBE beam footprint is derived in similar manner to that described in Section 8.2. We get

$$\hat{\mathbf{p}}_{EM}^E = \hat{\mathbf{p}}_{EB_{TP}}^E + \hat{\mathbf{R}}_{EN} \hat{\mathbf{R}}_{NB_{UV}} \left(\mathbf{p}_{B_{TP}B_{MBE}}^{B_{UV}} + \tilde{\mathbf{p}}_{B_{MBE}M}^{B_{UV}} \right) \quad (10)$$

$\hat{\mathbf{R}}_{NB_{UV}}$ is the orientation estimate of the underwater vehicle navigation system. $\hat{\mathbf{R}}_{EN}$ can be derived from the GPS-USBL position measurement.

Equation (10) can be re-written as

$$\hat{\mathbf{p}}_{EM}^E = \hat{\mathbf{p}}_{EB_{TP}}^E + \hat{\mathbf{R}}_{EN} \hat{\mathbf{R}}_{NB_{UV}} \mathbf{p}_{B_{TP}B_{UV}}^{B_{UV}} + \hat{\mathbf{R}}_{EN} \hat{\mathbf{R}}_{NB_{UV}} \left(\mathbf{p}_{B_{UV}B_{MBE}}^{B_{UV}} + \tilde{\mathbf{p}}_{B_{MBE}M}^{B_{UV}} \right) \quad (11)$$

If the underwater vehicle has an integrated inertial navigation system located in B_{UV} , the inertial navigation system will be aided with the lever arm compensated position measurement

$$\tilde{\mathbf{p}}_{EB_{UV}}^E = \tilde{\mathbf{p}}_{EB_{TP}}^E + \hat{\mathbf{R}}_{EN} \hat{\mathbf{R}}_{NB_{UV}} \mathbf{p}_{B_{TP}B_{UV}}^{B_{UV}} \quad (12)$$

The MBE beam position relative to B_{UV} is given by

$$\hat{\mathbf{p}}_{B_{UV}M}^E = \hat{\mathbf{R}}_{EN} \hat{\mathbf{R}}_{NB_{UV}} \left(\mathbf{p}_{B_{UV}B_{MBE}}^{B_{UV}} + \mathbf{p}_{B_{MBE}M}^{B_{UV}} \right) \quad (13)$$

This re-formulation is introduced because the integrated inertial navigation system is able to filter some of the ripple noise from a timing error in $\tilde{p}_{EB_{UV}}^E$. Thus, we can put less strict position error requirements on $\tilde{p}_{EB_{UV}}^E$ than $\hat{p}_{B_{UV}M}^E$, and consequently come up with less strict requirements on timing accuracy. The inertial navigation system has complementary information on the vehicle dynamics, which allows for filtering of $\tilde{p}_{EB_{UV}}^E$. Of the seabed topography, $\hat{p}_{B_{UV}M}^E$, no complementary information is normally available.

In Appendix C, errors in equation (11) will be analyzed with respect to time synchronization errors.

9 TIMING ACCURACY REQUIREMENTS

In Section 4.4 it is discussed how the requirements developed in this report for detailed seabed surveys for the offshore industry relate to the International Hydrographic Organization's (IHO) standards for hydrographic surveys.

9.1 Determining timing accuracy

9.1.1 Surface survey system

In Figure 9.1 it is shown how the surface survey system timing requirements are determined.

The key part is the timing error model for a surface survey system in Appendix B. The error model requires input of characteristic vessel dynamics. It was decided to apply the error model on two cases: *Large survey vessel* and *Small survey vessel*. In Appendices D and E the example vessels are described including data on lever arms and characteristic dynamics. The Norwegian Hydrographic Service provided data on S/L Sjøtroll while Deep Ocean provided data on M/V Edda Fonn.

The timing requirements are based on the MBE beam footprint accuracy requirements discussed in Section 9.2. The resulting timing accuracy requirements are calculated using the covariance analysis in Section B.6.

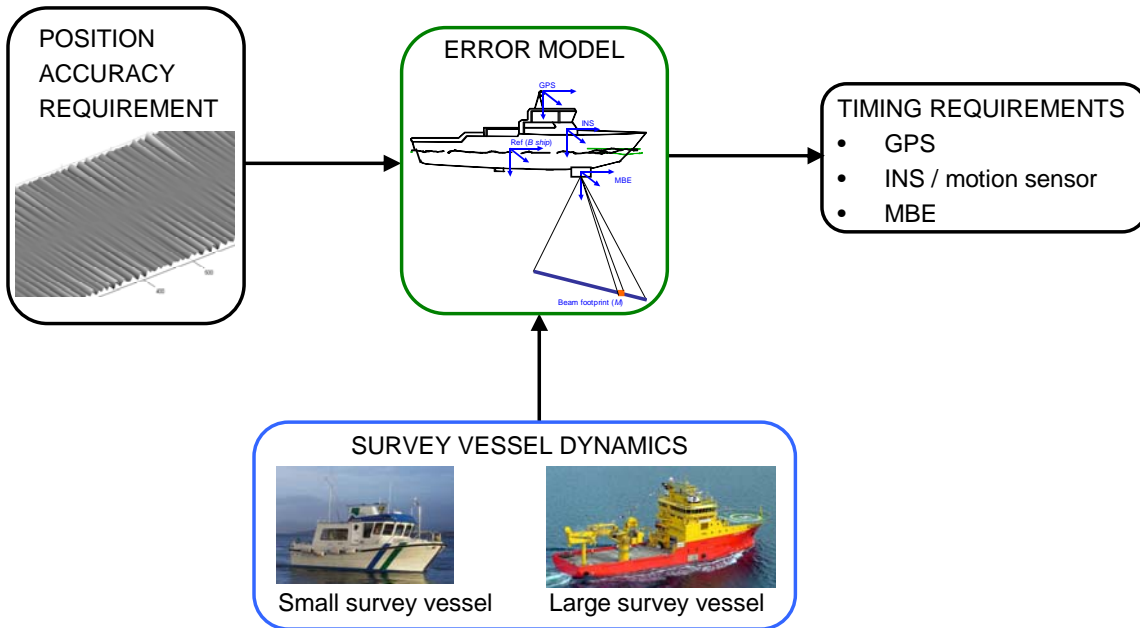


Figure 9.1 Illustration of how surface survey system timing requirements are determined

9.1.2 Underwater survey system timing

Figure 9.2 shows how the underwater survey system timing requirements are determined.

In Appendix C the error model for timing errors in underwater survey systems is given. The error model requires input of characteristic dynamics for both a surface vessel and an underwater vehicle. M/V Edda Fonn serves as example for the surface vessel. For the underwater vehicle, both ROV and AUV have been examined. See Appendices F and G for lever arms and characteristic dynamics. Deep Ocean provided data on HiROV 3000, while FFI provided data on HUGIN 3000.

The accuracy requirements in Section 9.3 are deliberately decoupled to avoid over-specification. The timing accuracy requirements are calculated using the covariance analysis in Section C.5.

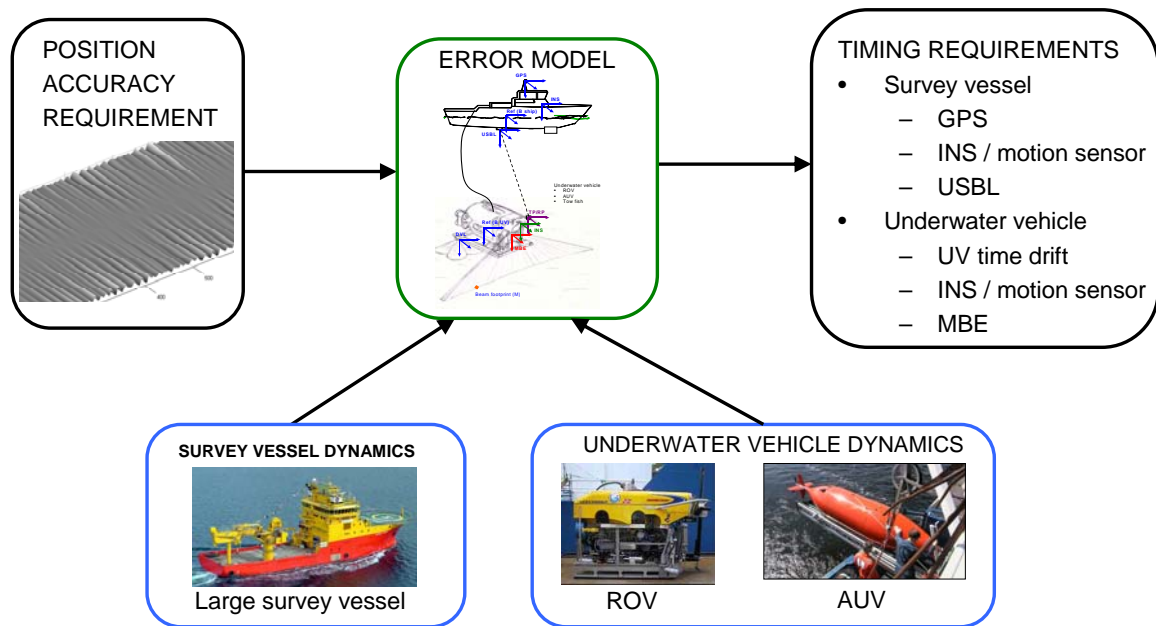


Figure 9.2 Illustration of how underwater survey system timing requirements are determined

9.1.3 Platform dynamics

The dynamic data required for the error models is time series of

- 3 dimensional translational velocity: \mathbf{v}_{EB}^B
- 3 dimensional angular velocity: $\boldsymbol{\omega}_{NB}^B$

A ship or underwater vehicle rotates around its metacenter. Thus, the error models are based on translational speed in the metacenter, opposed to any other point on the vehicle where angular velocity also causes a velocity component.

For the surface vessels, the sea state is largely determining the angular velocities. The data was recorded during relatively rough sea. The idea is to have specifications that ensure high data quality even in rough seas. Several methods for choosing representative numbers for vehicle speed and angular velocity can be envisaged. We have chosen to specify the largest values in the example time series. This corresponds to a *requirement for full mapping accuracy in all relevant sea states throughout a survey.*

For an AUV, the dynamics are dependent on water depth, sea state, bottom topography (an AUV typically runs at constant altitude) and number and type of heading turns. An AUV operating in shallow water and rough sea has higher degree of dynamics than an AUV operating in deep water. Presently, the use of AUVs in shallow water is mostly for military applications, and the shallow water case has thus been omitted in this report. Dynamics of ROV operations in shallow water has similarly been omitted.

In Table 9.1 the four cases for studying timing accuracy requirements are summarized.

Case	Example	Water depth	Speed	Acoustics
<i>Surface survey system</i>				
Large survey vessel	M/V Edda Fonn	300 m water depth	2.5 m/s	60° MBE beam angle
Small survey vessel	S/L Sjøtroll	100 m water depth	4 m/s	60° MBE beam angle
<i>Underwater survey system</i>				
AUV deep water Survey vessel	M/V Edda Fonn	3000 m AUV depth	2.0 m/s	0° USBL beam angle
AUV	HUGIN 3000	30 m AUV altitude	2.0 m/s	60° MBE beam angle
ROV deep water Survey vessel	M/V Edda Fonn	3000 m ROV depth	1.5 m/s	0° USBL beam angle
ROV	HiROV 3000	30 m ROV altitude	1.5 m/s	60° MBE beam angle

Table 9.1 Four survey system cases used for deciding relevant timing accuracy specifications.

9.2 Surface survey system requirements

9.2.1 DTM position requirement

MBE beam positioning error due to sensor attitude error and systems installation attitude error scale with MBE beam range, $\left| \mathbf{p}_{B_{MBE}M}^{B_{MBE}} \right|$. It is reasonable that a requirement on the accuracy of MBE beam position error also scale with MBE beam range. The requirements on MBE beam position error are specified in the ship reference system, $\delta \mathbf{p}_{EM}^{B_{ship}}$.

For the central beam, the vertical error, $\delta p_{EM,z}^{B_{ship}}$, is small. At 45° MBE beam angle, the horizontal and vertical components of a roll error is equal. The covariance analysis is done for 60° MBE beam angle. There are equal requirements for vertical accuracy and horizontal accuracy. This is in contrast to the IHO standards for hydrographic surveys, see Section 4.4.

The positioning accuracy of an MBE beam footprint is typically limited by the basic error sources listed in Table 9.2. In the table typical parameters for each error source are given. *Requiring that timing errors shall not compromise the accuracy offered by basic error sources in a surface survey system*, the requirement on timing accuracy is set to 2.5 times less than typical INS and motion sensor orientation accuracy:

$$\sigma(\delta \mathbf{p}_{EM}^{B_{ship}}) < \text{rad}(0.01^\circ) \cdot \begin{bmatrix} \left| \mathbf{p}_{B_{MBE}M}^{B_{MBE}} \right| \\ \left| \mathbf{p}_{B_{MBE}M}^{B_{MBE}} \right| \\ \left| \mathbf{p}_{B_{MBE}M}^{B_{MBE}} \right| \end{bmatrix} \quad (14)$$

$\sigma(\delta p_{EM}^{B_{ship}})$ is the standard deviation of $\delta p_{EM}^{B_{ship}}$. In Figure 9.3, the requirement is plotted for MBE beam ranges up to 600 m (600 m beam range corresponds to 60° beam angle in 300 m water depth).

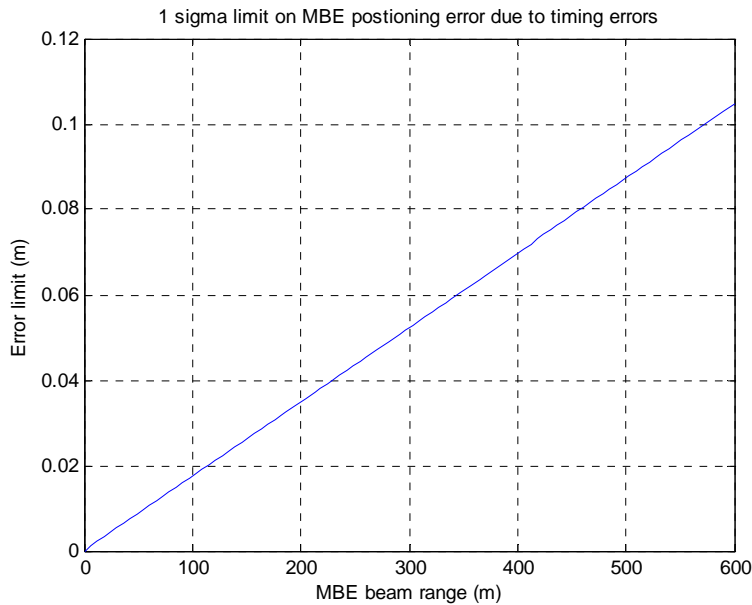


Figure 9.3 1σ requirement on MBE beam positioning error in a surface survey system due to timing errors. The requirement is plotted for beam range up to 600 m. In 300 m water depth, an MBE beam 60° out of the vertical has 600 m range.

A more relaxed approach would have been to relate the timing specifications to the MBE beam width, which is typically 0.5° – 2°. However, accurate attitude in the order of 0.1° (and thus implicitly accurate time stamping) is believed to be required to get rid of dynamic errors (rippling) in the terrain models. The dynamics of the rippling is determined by the periods in the ocean wave spectrum and the dynamics of the survey platform. See Chapter 10 for a description on the dynamic effects of timing errors.

Error source	Typical value
GPS	
- Horizontal accuracy	0.1 m (1 σ)
- Vertical accuracy	0.15 m (1 σ)
INS or motion sensor	
- Roll and pitch accuracy	0.025° (1 σ)
- Heading accuracy	0.2° (1 σ)
INS and MBE installation and calibration accuracy	0.05° (1 σ)
MBE	
- Beam width	1.0°
- Range resolution	2.5 cm

Table 9.2 Typical values for basic error sources in a surface survey system. MBE performance is dependent on an accurate sound velocity profile. The GPS values apply for modern kinematic systems.

9.2.2 Timing accuracy

The small survey vessel and large survey vessel cases are summarized in Table 9.1. For the small survey vessel case, 100 m water depth and 4 m/s vessel speed were assumed. For the large survey vessel case, the numbers were 300 m water depth and 2.5 m/s vessel speed. In both cases, the MBE beam ranges are much larger than the ship lever arms. The calculated timing accuracy requirements are strictest for the small survey vessel, which have the highest dynamics. The timing requirements are summarized in Table 9.3.

Timing accuracy requirement (1 σ)	Small survey vessel	Large survey vessel
Multibeam echo sounder	0.57 ms	2.3 ms
Inertial navigation system / motion sensor	0.62 ms	2.4 ms

Table 9.3 Timing accuracy requirements (1 σ) for surface survey systems. The requirements are calculated using the covariance analysis in Section B.6.

9.3 Underwater survey system requirements

9.3.1 Decoupled position requirements

The MBE beam position in an underwater survey system, $\hat{\mathbf{p}}_{EM}^E$, is the sum of the GPS-USBL position estimate of the underwater vehicle, $\hat{\mathbf{p}}_{EBUV}^E$, and the positioning of the MBE beam relative the underwater vehicle, $\hat{\mathbf{p}}_{B_{UV}M}^E$:

$$\hat{\mathbf{p}}_{EM}^E = \hat{\mathbf{p}}_{EBUV}^E + \hat{\mathbf{p}}_{B_{UV}M}^E \quad (15)$$

In Appendix C the MBE beam position error due to timing errors, $\delta \mathbf{p}_{EM}^E$, has been derived:

$$\delta \mathbf{p}_{EM}^E = \delta \mathbf{p}_{EB_{UV},offset}^E + \delta \mathbf{p}_{EB_{UV},ripple}^E + \delta \mathbf{p}_{B_{UV}M,ripple}^E \quad (16)$$

$\delta \mathbf{p}_{EB_{UV},offset}^E$ is position offset error due to translational speed and time difference between clocks in surface vessel and underwater vehicle. $\delta \mathbf{p}_{EB_{UV},ripple}^E$ is underwater vehicle position ripples due to ship angular rate and timing errors in USBL and INS. $\delta \mathbf{p}_{B_{UV}M,ripple}^E$ are ripples in attitude compensated MBE data due to UV angular rates and timing errors in MBE and UV INS.

Requirements for all three error components are derived separately in the underwater vehicle and ship reference frames: $\delta \mathbf{p}_{EB_{UV},offset}^{B_{ship}}$, $\delta \mathbf{p}_{EB_{UV},ripple}^{B_{UV}}$ and $\delta \mathbf{p}_{B_{UV}M,ripple}^{B_{UV}}$.

9.3.2 MBE ripples

For $\delta \mathbf{p}_{B_{UV}M,ripple}^{B_{UV}}$ we follow the same reasoning as in Section 9.2 and come up with an analogous requirement:

$$\sigma(\delta \mathbf{p}_{B_{UV}M,ripple}^{B_{UV}}) < \text{rad}(0.01^\circ) \cdot \begin{bmatrix} \left| \mathbf{p}_{B_{MBE}M}^{B_{MBE}} \right| \\ \left| \mathbf{p}_{B_{MBE}M}^{B_{MBE}} \right| \\ \left| \mathbf{p}_{B_{MBE}M}^{B_{MBE}} \right| \end{bmatrix} \quad (17)$$

where $\sigma(\delta \mathbf{p}_{B_{UV}M,ripple}^{B_{UV}})$ is the standard deviation of $\delta \mathbf{p}_{B_{UV}M,ripple}^{B_{UV}}$, and $\left| \mathbf{p}_{B_{MBE}M}^{B_{MBE}} \right|$ is MBE beam range.

9.3.3 Underwater vehicle position ripples

In Table 9.4 basic error sources for a GPS-USBL system is listed. If the sound velocity profile is properly included in refraction calculations, the USBL direction error is mainly white noise for modern USBL systems. Underwater vehicles can be expected to be equipped with integrated navigation systems, typically aided inertial navigation systems, which are well suited for filtering out high frequency noise. The ship angular rate will make the timing error $\delta \mathbf{p}_{EB_{UV},ripple}^E$ appear as noise with zero mean. The noise frequency matches the frequency of the surface ship angular rates, which is considerable higher than the error drift in the underwater vehicle navigation system. $\delta \mathbf{p}_{EB_{UV},ripple}^E$ can thus relatively easy be filtered, utilizing the extra information on the underwater vehicle dynamics provided by the inertial navigation system. From this point of view one can require that a *survey vessel timing error shall not exceed the level of inherent white noise in the GPS-USBL position measurement*. This leads to the following requirement on $\delta \mathbf{p}_{EB_{UV},ripple}^{B_{ship}}$:

$$\sigma(\delta \mathbf{p}_{EB_{UV},ripple}^{B_{ship}}) < \text{rad}(0.1^\circ) \begin{bmatrix} \left| \mathbf{p}_{B_{USBL}B_{TP}}^{B_{USBL}} \right| \\ \left| \mathbf{p}_{B_{USBL}B_{TP}}^{B_{USBL}} \right| \\ NA \end{bmatrix} \quad (18)$$

where $\sigma(\delta \mathbf{p}_{EB_{UV}, ripple}^{B_{ship}})$ is the standard deviation of $\delta \mathbf{p}_{EB_{UV}, ripple}^{B_{ship}}$ and $|\mathbf{p}_{B_{USBL}B_{TP}}^{B_{USBL}}|$ is USBL range, i.e. distance between the survey vessel and the underwater vehicle. In Figure 9.4, the requirement is plotted for USBL ranges up to 3000 m.

The depth of the underwater vehicle is determined by a pressure sensor. Thus, the z-component of $\sigma(\delta \mathbf{p}_{EB_{UV}, ripple}^{B_{ship}})$ is not applicable when determining timing accuracy requirements for USBL, MBE and INS in the underwater vehicle. Pressure sensor analysis is not included in this report.

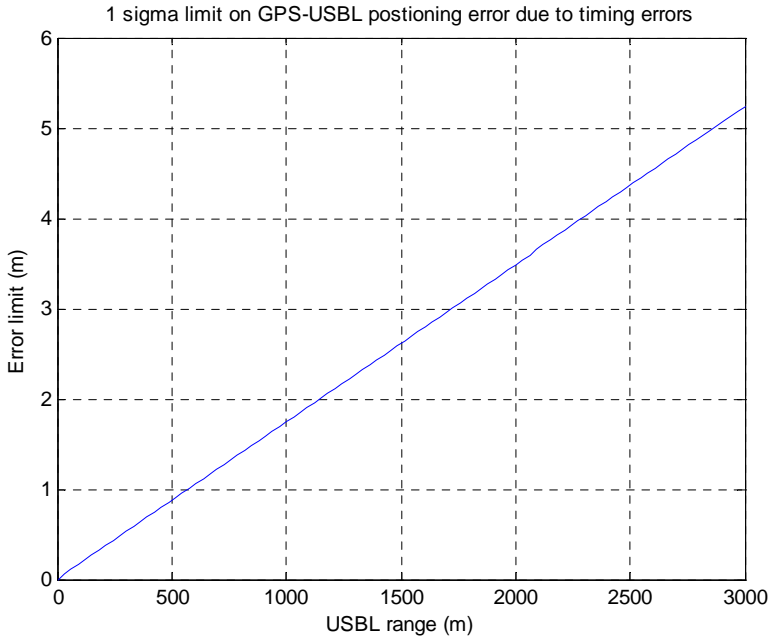


Figure 9.4 1σ requirement on GPS-USBL positioning error due to timing errors plotted for USBL ranges up to 3000 m.

The requirement for $\sigma(\delta \mathbf{p}_{B_{UV}M, ripple}^{B_{UV}})$ is a factor 10 stricter than the requirement for $\sigma(\delta \mathbf{p}_{EB_{UV}, ripple}^{B_{ship}})$. Normally, no apriori knowledge of the sea bottom is available, and consequently one risk to loose information if one filters the digital terrain model for dynamic ripples. On the other hand, an underwater vehicle inertial navigation system has complementary information on the dynamics of the underwater vehicle. This information can be utilized to filter the GPS-USBL measurement, $\hat{\mathbf{p}}_{EB_{TP}}^E$, without losing any true information.

If the assumption of an aided inertial navigation system in the underwater vehicle does not hold, one should require that timing errors shall not compromise the accuracy offered by basic error sources in the GPS-USBL system. An accurate USBL system has 0.1° (1σ) bearing accuracy. Requiring four times less timing errors, leads to the following requirement on

$\delta \mathbf{p}_{EB_{UV}, ripple}^{B_{ship}}$:

$$\sigma(\delta \mathbf{p}_{EB_{UV}, ripple}^{B_{ship}}) < \text{rad}(0.025^\circ) \begin{bmatrix} \mathbf{p}_{B_{USBL} B_{TP}}^{B_{USBL}} \\ \mathbf{p}_{B_{USBL} B_{TP}}^{B_{USBL}} \\ NA \end{bmatrix} \quad (19)$$

Error source	Typical value
GPS	
- Horizontal accuracy	0.1 m (1 σ)
- Vertical accuracy	0.15 m (1 σ)
USBL	
- Bearing accuracy	0.1 $^\circ$ (1 σ)
- Range accuracy	< 0.2 m
INS or motion sensor	
- Roll and pitch accuracy	0.025 $^\circ$ (1 σ)
- Heading accuracy	0.2 $^\circ$ (1 σ)
INS and USBL installation and calibration accuracy	0.05 $^\circ$ (1 σ)
MBE	
- Beam width	0.5 $^\circ$
- Range resolution	6 mm

Table 9.4 Basic error sources in a GPS-USBL system. MBE and USBL performance are dependent on an accurate sound velocity profile. More details on accuracy analysis of underwater survey systems can be found in (7).

9.3.4 Underwater vehicle position offset

The stationary underwater vehicle position offset is determined by translational speed the time difference between the surface vessel clock and the underwater vehicle clock. *The time drift in the underwater vehicle shall not compromise the accuracy offered by a high quality GPS system:*

$$\sigma(\delta \mathbf{p}_{EB_{UV}, offset}^{B_{UV}}) < \begin{bmatrix} 0.1 \text{ m} \\ 0.1 \text{ m} \\ NA \end{bmatrix} \quad (20)$$

This should only be an issue for AUVs, as the ROV clock can remain synchronized through the umbilical. 0.1 m position error translates to 50 ms time drift for an AUV traveling at 2 m/s. 50 ms time drift requires an accurate clock oscillator with 0.2 ppm drift rate for a 60 h AUV mission.

Since depth of the underwater vehicle is determined by a pressure sensor, the z-component of $\sigma(\delta \mathbf{p}_{EB_{UV}, offset}^{B_{UV}})$ is not applicable for this analysis.

9.3.5 Timing accuracy

The ROV and AUV cases are summarized in Table 9.1. Both the ROV and the AUV are assumed followed by a large survey vessel and traveling at 30 m altitude in 3000 m depth. ROV speed is assumed to 1.5 m/s. AUV speed is assumed to 2.0 m/s.

In Table 9.5 it is worth noticing that even if an AUV is a more stable platform than an ROV, it is also capable of more agile heading turns. Since the timing requirements are designed to guarantee full mapping accuracy for a whole mission, even in turns, the AUV has actually slightly stricter requirements on timing accuracy. See table caption for discussion on GPS-USBL timing accuracy requirements.

Timing accuracy requirement (1σ)	ROV	AUV
Ship USBL	6 ms (24 ms)	6 ms (24 ms)
Ship INS / motion sensor	6 ms (24 ms)	6 ms (24 ms)
Ship – UV time drift	NA	50 ms
Underwater vehicle INS	1.1 ms	0.8 ms
Underwater vehicle MBE	1.1 ms	0.8 ms

Table 9.5 Timing accuracy requirements (1σ) for underwater survey systems. The requirements are calculated using the covariance analysis in Section C.5. The 6 ms requirement for Ship USBL and Ship INS / motion sensor is based on an assumption of no inertial navigation system in the underwater vehicle, see equation (19). If the underwater vehicle has an aided inertial navigation system, the requirement can be as shown in brackets, refer to equation (18).

9.4 Summary of underlying principles for timing requirements

In order to arrive at the timing accuracy requirements in Table 9.3 and Table 9.5 a set of principles discussed in Sections 9.2 and 9.3 were decided. In Table 9.6, these principles are summarized. The principles are pivotal in determining the final timing accuracy requirements. Table 9.6 provides thus a background for a discussion on the timing accuracy requirements. The motivation for the principles is to eliminate ripples in final survey products.

Principle	Consequence
<i>The effect of timing errors shall not compromise the accuracy offered by basic error sources in a survey system.</i>	Due to accurate INS and motion sensors, DTM position accuracy requirement was set to 0.01° multiplied with MBE beam range. This results in strict timing accuracy requirements on MBE, INS and motion sensors.
<i>The timing specifications are not related to MBE beam width.</i>	Timing requirements were not moderated due to typical MBE beam widths of $0.5^\circ - 2^\circ$. Accurate attitude (and thus implicitly accurate time stamping) is believed to be required to get rid of dynamic errors (rippling) in the terrain models.
<i>An accurate sound velocity profile ensures optimal MBE and USBL performance.</i>	Timing requirements not moderated due to inaccurate sound velocity profile.
<i>Full mapping accuracy is required in all relevant sea states.</i>	Dynamic example data was taken from missions in rough seas. This results in stricter requirements than necessary for calm seas.
<i>Full mapping accuracy is required for all MBE beams.</i>	The timing requirements were calculated for 60° MBE beam angle.
<i>Full mapping accuracy is required in turns.</i>	High AUV turning rates used in timing accuracy calculations.
<i>For an underwater survey system, the survey vessel timing errors shall not compromise the accuracy offered by basic error sources in the GPS-USBL system</i>	Timing requirements for a GPS-USBL system are relatively strict, though less strict than the requirements for MBE attitude compensation since USBL bearing accuracy is less than INS orientation accuracy. If the underwater vehicle is equipped with an inertial navigation system, the requirements can be relaxed.
<i>Underwater vehicle offset error shall not compromise the accuracy offered by high quality GPS systems.</i>	Strict requirements on AUV time drift.

Table 9.6 Summary of underlying principles for deciding timing accuracy requirements

10 DYNAMIC BEHAVIOR OF TIMING ERRORS

The purpose of this section is to illustrate the dynamic behavior of DTM position errors caused by timing errors. In Figure 10.1 recorded roll rate, pitch rate and heading rate is shown for the small surface survey vessel example, S/L Sjøtroll. The red lines are the maximum rates that were determined in Appendix D.3 after investigation of a larger data set. The timing accuracy requirements in the previous chapter were computed using the maximum rates.

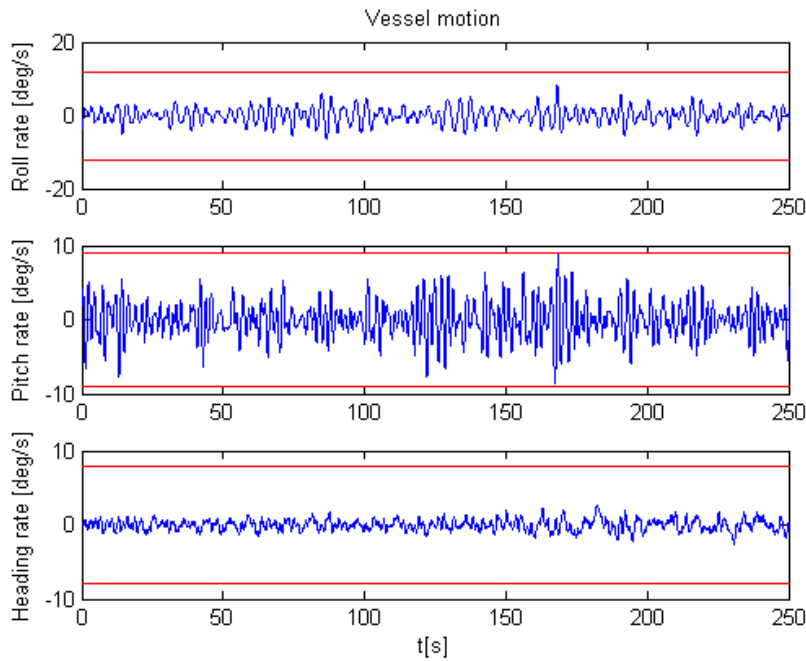


Figure 10.1 Roll, pitch and heading rate of S/L Sjøtroll. The red lines are the maximum rates that were determined in Appendix D.3 after investigation of a larger data set.

In Figure 10.2 MBE beam positioning error on a flat sea bottom has been computed with an assumed timing error of 20 ms both in the MBE and the INS. In 100 m water depth, an MBE beam 60° out of the vertical has a range of 200 m. At this beam range, the position accuracy requirement in equation (14) in Section 9.2 equals 0.035 m. We see that the maximum effect of a 20 ms timing error is close to 1 m and clearly breaks the positioning error requirements shown in the figure as red lines.

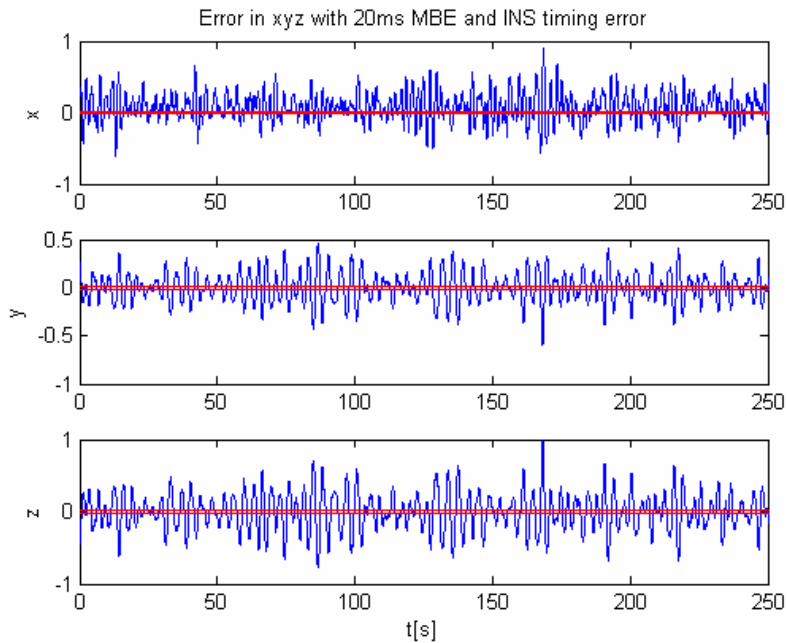


Figure 10.2 MBE positioning error in surface vessel reference frame on a flat seabed due to a 20 ms constant timing error in the MBE and a 20 ms constant timing error in the INS, in the opposite direction. The figure shows position error for a 200 m MBE beam 60° out of the vertical, water depth is 100 m. The red lines are required footprint position accuracy.

In Figure 10.3 the MBE beam position error has been computed with timing errors that are in accordance with the requirements in Table 9.3. Now, the beam position error is within the requirement.

In Figure 10.4 the MBE beam position error has been computed for all MBE beams that make up a DTM. The 3D terrain model is generated from the error models in Appendix B. It is simulated with the S/L Sjøtroll dynamics from Figure 10.1 and shows ripples that occur on a flat seabed due to 20 ms timing errors in the MBE and the INS.

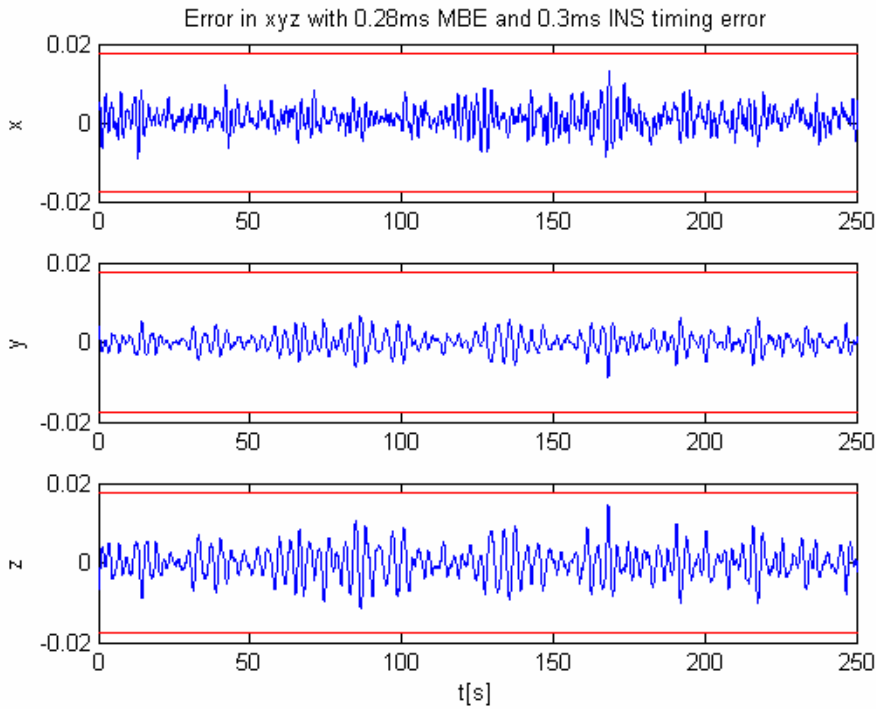


Figure 10.3 MBE positioning error in surface vessel reference frame on a flat seabed due to a 0.28 ms constant timing error for the MBE and a 0.3 ms constant timing error for the INS, in the opposite direction. The figure shows position error for a 200 m MBE beam 60° out of the vertical, water depth is 100 m. Red lines are required footprint position accuracy.

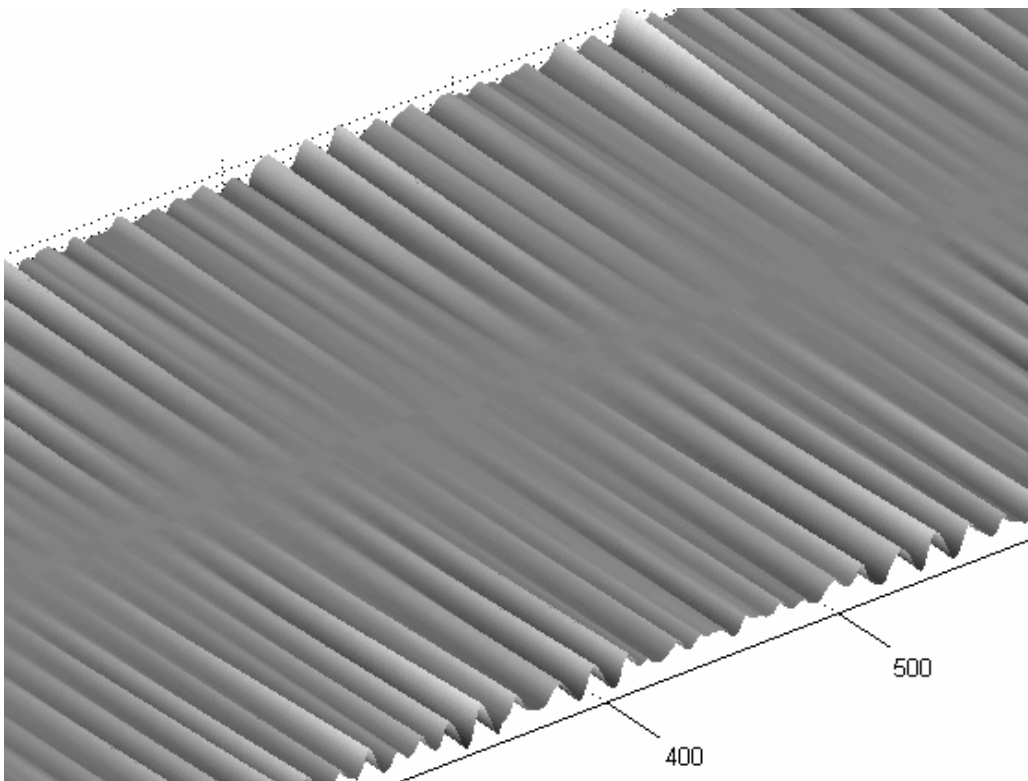


Figure 10.4 DTM ripples due to a constant 20 ms INS and MBE timing error for the small surface survey vessel example. The depth is 100 m. The z-axis is magnified by a

factor of 10. The magnitude of the vertical error for the outer 60° beams is shown in the z-axis in Figure 10.3. For the 60° beam, the error typically varies between ±0.5 m. For the central beam, the error on a flat seabed is 0 m. On a sloping seabed, time induced errors in pitch, will also cause vertical errors for the central beam.

11 RECOMMENDED REQUIREMENTS ON TIME REFERENCING

The purpose of this chapter is to recommend requirements for time referencing in survey systems used for *detailed seabed mapping in the offshore survey industry*. The main goal of the requirements is to get rid of *ripple errors* in the final survey products.

The requirements apply for all sensors, hardware systems, and software systems that form an integrated survey system. The requirements are stated in separate paragraphs with separate headings and numbers for each requirement. Descriptive text is used in sections to give intentions and explanations applicable to the requirement

The recommended requirements are divided into two groups:

1. *Shall: Compulsory Requirement (C Req)*
Requirements containing "shall" are to be fully met by every component in an offshore survey system.
2. *Should: Non-Compulsory Requirement (Non-C Req)*
Requirements containing "should" are medium-term development goals for vendors delivering products to the offshore survey industry. For short-term deliveries, the requirements should be fulfilled to the extent possible.

11.1 Time reference

11.1.1 Time reference (C Req)

All sensor data, processed data and metadata shall be referred to coordinated universal time (UTC).

11.1.2 Time format (C Req)

The time format shall have at least micro seconds (μs) resolution.

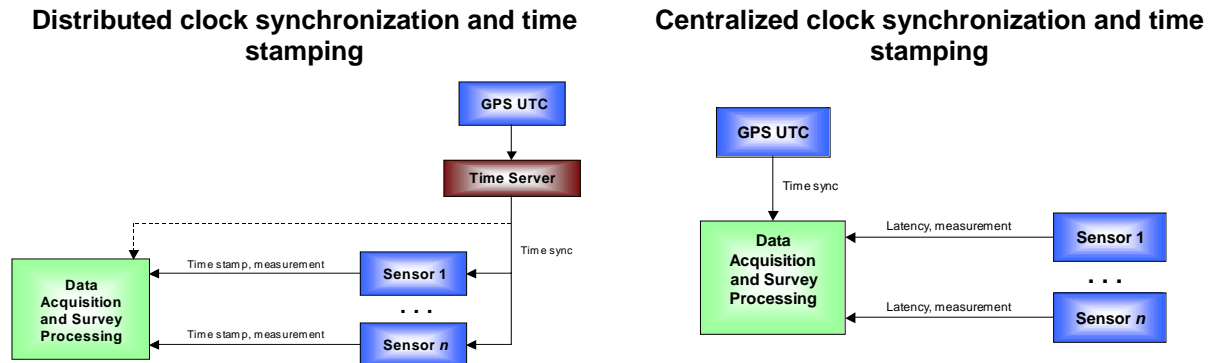
Time shall be represented by one single number.

If applicable, the time format should be given by the time format in the clock synchronization method (e.g. PTP, refer to Section 11.2.2).

An example of a reasonable time format is micro seconds since 1970.

11.2 Clock synchronization

In Figure 11.1 two general approaches to clock synchronization and time stamping discussed in Chapter 6 are summarized.



Timing errors:

1. Error in clock synchronization of each sensor.
2. Error in internal sensor timing of physical measurement (time stamping).

Timing errors:

1. Error in internal sensor timing of physical measurement (time stamping).
2. Error in calculation of latency in the sensor (or lack of calculation).
3. Error in clock synchronization of the data acquisition system.
4. Error in compensation of transmission time
5. Unpredictable interrupt response time in the data acquisition system
6. Hardware / software limitations in large systems (typically limited resources in hardware to handle time stamping of all sensors to the central clock)

Figure 11.1 Two general approaches to time synchronization and time stamping

11.2.1 Clock synchronization (Non-C Req)

Every sensor and component in an integrated survey system should be clock synchronized (see “Distributed clock synchronization and time stamping” in Figure 11.1).

As an intermediate solution, unsynchronized sensors can be handled by installing dedicated time hardware responsible for time stamping, as discussed in Section 6.3.3. Another solution is to have a hard real-time data acquisition system.

This requirement should be considered to be changed to a compulsory requirement (C Req) by the offshore industry in a few years.

11.2.2 Methods for clock synchronization (Non-C Req)

Components in a survey system should be capable of handling the following methods for clock synchronization:

- Precision time protocol (PTP)
- Network time protocol (NTP). PTP is preferred to NTP.

- UTC synchronization via a 1 PPS signal. Since there are few standards for PPS signals, the sensor shall have a user configurable signal polarity for the PPS input port. The sensor shall be able to detect pulses down to 1 μ s duration having a 100 ns rise time and a 3V level. The handling of the full date and time information in the timestamp shall be well documented.

11.2.3 Clock synchronization accuracy (C Req)

The list of timing errors in Figure 11.1 show that clock synchronization is only one of several error sources.

The clock synchronization errors shall be minimized so that the total timing error meets the requirements in Section 11.4.

11.2.4 Clock synchronization during data acquisition (C Req)

During data acquisition adjustment of sensor time shall be less than 1 ms over a period of 30 s.

11.2.5 Documentation (C Req)

Sensors and data acquisition systems usually use high-resolution timers in hardware to achieve satisfactory resolution on its time stamping. These hardware timers are usually referred to a time reference (time of day) in software. In clock synchronization, the software time reference is adjusted to an external time reference in UTC. Correct use of hardware timers and clock synchronization methods are necessary for obtaining required timing accuracy.

The methods for clock synchronization and achievable clock synchronization accuracy shall be well documented. This include:

- Information on which computer timers or clocks that are used for representing time
- Information on system calls that are used to access hardware counters
- Information on how the counter values are used to calculate an absolute time reference
- Information on how clock synchronization affects the absolute time reference
- Test results that document the accuracy of the clock synchronization

11.3 Time stamping

Time stamping is in many cases a larger error source than clock synchronization. Time stamping is a challenge for acoustic sensors because it is normally necessary to differ between transmit time, receive time, and measurement time. Details on correct time stamping of MBE, DVL and USBL are given in Sections 7.1, 7.2 and 7.3 respectively.

11.3.1 Time stamping (C Req)

Every clock-synchronized sensor shall time stamp the measurement at the time the measurement physically took place.

11.3.2 Time stamp accuracy (C Req)

The time stamp error shall be minimized so that the total timing error meets the requirements in Section 11.4.

11.3.3 Documentation on time stamping (C Req)

Documentation on time stamping shall include:

- A physical explanation of the measurement process
- A physical explanation of correct measurement time stamp
- Specification on accuracy of time stamping

11.3.4 Latency (C Req)

Latency is defined as the time delay from physical sensor measurement until the processed data is available on the sensor output port.

If the sensor does not have clock synchronization capabilities (see requirement in Section 11.2.1), it shall output a latency estimate.

If the latency is varying (typical for an acoustic sensor), it shall be part of the data message.

If the latency is known and repeatable (typical for a motion sensor), it shall at least be given in the documentation. Preferably, it should be part of the data message even if it is constant. This will counteract manual typing or procedure errors, and allow for change in latency in sensor upgrades.

11.3.5 Documentation on latency (C Req)

Documentation on latency shall include:

- Specification on accuracy of latency estimate
- Specification on variation of latency estimate

11.3.6 Hard real-time (C Req)

The processor responsible for time stamping shall fulfill hard real-time requirements.

11.4 Timing accuracy

A timing error is modeled as

$$\tilde{t}_{sensor} = t_{sensor} + \delta t_{sensor} \quad (21)$$

where \tilde{t}_{sensor} is sensor time stamp, t_{sensor} is true sensor measurement time and δt_{sensor} is time stamp error. δt_{sensor} is considered a statistical process with zero mean value. The various error sources contributing to δt_{sensor} are listed in Figure 11.1.

The motivation for the timing accuracy requirements is to eliminate ripples in final survey products. The underlying assumptions for calculating the requirements are summarized in Table 9.6.

11.4.1 Surface survey system timing accuracy (C Req)

The total timing error (sum of the different error contributors listed in Figure 11.1) shall not exceed the requirements in Table 11.1.

The GPS data shall use the GPS time stamp.

	Motion sensor / INS	MBE
Small survey vessel	1 ms	1 ms
Large survey vessel	2.5 ms	2.5 ms

Table 11.1 Timing accuracy requirements (1σ) for small and large surface survey vessels

11.4.2 Underwater survey system timing accuracy (C Req)

The underwater vehicle is assumed to operate in concert with a surface ship. For the components in the GPS-USBL system in the surface ship, the total timing error (sum of the different error contributors listed in Figure 11.1) shall not exceed the requirements in Table 11.2.

The GPS data shall use the GPS time stamp.

	Motion sensor / INS	USBL
Large survey vessel	6 ms (24 ms)	6 ms (24 ms)

Table 11.2 Timing accuracy requirements (1σ) for GPS-USBL systems in large surface survey vessels when part of an underwater survey system. Brackets: possible timing accuracy requirements if the underwater vehicle is equipped with an aided inertial navigation system.

For ROV and AUV survey systems, the total timing error (sum of the different error contributors listed in Figure 11.1) shall not exceed the requirements in Table 11.3.

	Ship – UV time drift	Motion sensor / INS	MBE
AUV	50 ms	1 ms	1 ms
ROV	NA	1 ms	1 ms

Table 11.3 Timing accuracy requirements (1σ) for ROV and AUV underwater survey systems

11.5 Merging of asynchronous measurements

A survey system merges asynchronous measurements into geo-referenced measurements of water depth, and other acoustic or seismic properties. Techniques for merging asynchronous data are:

1. *Merging of data samples closest in time*
2. *Interpolation*
3. *Extrapolation*

These methods are described in more detail in Section 6.2.

It is important to differ between real-time, near real-time and post-processing use of sensor data. In real-time applications, interpolation is in many cases not possible.

11.5.1 Methods for merging of asynchronous measurements (C Req)

Methods for merging final data in an offshore survey system shall be *merging of data samples closest in time* and/or *interpolation*.

Extrapolation shall not be used for merging asynchronous measurements.

11.5.2 Interpolation

The accuracy of the interpolation algorithm shall be documented.

11.5.3 Merging of data samples closest in time (C Req)

Merging of data samples closest in time shall only be allowed for final survey products if the average delay due to the finite data output rate and sensor latency is less than the timing accuracy requirements in Section 11.4.

11.5.4 Interpolation of position data (C Req)

Interpolation of GPS data in surface survey systems and GPS-USBL data in underwater survey systems shall be on position data that has been transformed to the ship's metacenter.

11.6 Data output rate and sensor latency

It is important to differ between real-time, near real-time and post-processing use of sensor data:

- In real-time applications without data buffering, interpolation is normally not possible, refer to Section 11.5.
- In near real-time and post-processing, sensor latency is no problem as long as it is accurately known and compensated for. In near-real time processing, data must be buffered for a sufficiently long period.
- In near-real time and post-processing, interpolation is normally applied to achieve the desired timing accuracy.

11.6.1 Data output rate and latency in a real-time GPS-USBL system (C Req)

For a real-time GPS-USBL system measuring position of an underwater vehicle, the following requirements shall apply:

Sensor	Minimum output rate	Max latency
Motion sensor / INS	50 Hz	5 ms
GPS / INS position	10 Hz	10 ms

Table 11.4 Minimum output rate and max latency for a real-time GPS-USBL system used to estimate position of AUV, ROV or tow fish in an underwater survey system. The requirements assume that the underwater vehicle is equipped with an aided inertial navigation system.

The finite sampling rate introduces an average delay of half a sampling interval, 10 ms for 50 Hz attitude data and 50 ms for 10 Hz position data. This gives an average delay of 15 ms for the attitude data and 60 ms for the position data. Compare these average delays with the GPS-USBL timing accuracy requirements in Section 11.4.2.

11.6.2 Data output rate and latency in real-time MBE surveys (C Req)

In a real time processing of MBE data, attitude data is sent to the MBE for transformation of raw MBE ranges to three dimensional x, y, z positions of each beam relative to the MBE position at transmit time.

The finite sampling rate introduces an average delay of half a sampling interval. The delay due to finite sampling rate and sensor latency shall not exceed the timing accuracy requirements in Sections 11.4.1 and 11.4.2.

11.6.3 Data output rate and latency in near real-time and post-processed MBE surveys (C Req)

In near real-time and post-processed MBE surveys, the time delays shall be compensated for.

The latency and the accuracy of the latency shall be well known, refer to requirements 11.3.4 and 11.3.5.

In near-real time and post-processed MBE surveys, interpolation shall be applied to achieve the timing accuracy requirements in Sections 11.4.1 and 11.4.2.

In near-real time processing, the data shall be buffered longer than the maximum time delay in the system.

The minimum data rate in near real-time and post-processing shall be determined by the dynamics of the vehicle and the accuracy of the interpolation algorithm. For near real-time and post-processed MBE surveys Table 11.5 shall define minimum requirements on data output rate.

Sensor	Minimum output rate
Motion sensor / INS	50 Hz
GPS / INS position	1 Hz

Table 11.5 Minimum output rates in near-real time and post-processed MBE surveys. In near real-time processing, the data shall be buffered longer than the maximum time delay in the system.

11.6.4 Sensor failure (C Req)

The sensor output rate shall be constant regardless of whether the sensor works or not.

Sensor failures or degraded performance shall be signaled immediately by setting an appropriate status field.

11.7 Data acquisition and data recording

11.7.1 Post-processing (C Req)

It shall be possible to reprocess the full set of recorded raw sensor data, even if final survey products normally are processed in real-time or near real-time.

11.7.2 Raw data (C Req)

For every survey sensor, the following information shall be stored:

- Time information in UTC (refer to Requirement 11.2.1)
 1. If distributed clock synchronization:
 - Sensor time stamp
 2. If clock synchronized data acquisition system:
 - Data acquisition system time stamp
 - Sensor latency
 3. If dedicated time stamping hardware:
 - Time Box time stamp
 - Sensor latency
- Raw measurement(s)
- Sensor status

11.7.3 Raw data time information (C Req)

Time information in raw data shall never be overwritten or changed.

11.7.4 Data acquisition system time stamps

Time stamps from a data acquisition system shall come in addition to the raw time stamps.

11.7.5 Raw data documentation (C Req)

The raw data format shall be documented in detail.

11.7.6 Data acquisition integrity (C Req)

Data acquisition integrity is defined as the ability of the data acquisition system to provide early warning when raw and processed sensor data is not received

There shall be continuous quality check on the data acquisition.

11.7.7 Documentation on data acquisition integrity (C Req)

Vendors shall specify their functionality for data acquisition integrity by three parameters:

- *Alert limit.* The number of bytes or parameters not received properly that will result in a warning.
- *Time-to-alarm.* Time elapsed from a data acquisition error to a warning is issued.
- *Integrity risk.* The probability that the alert limit is exceeded undetected.

The methods used for detecting data reception problems shall be documented.

11.7.8 Data recording integrity (C Req)

Data recording integrity is defined as the ability of the data recording system to provide early warning when raw and processed sensor data is not stored properly.

There shall be continuous quality check on the data recording process.

11.7.9 Documentation on data recording integrity (C Req)

Vendors shall specify their functionality for data recording integrity by three parameters:

- *Alert limit.* The number of bytes or parameters not recorded properly that will result in a warning.
- *Time-to-alarm.* Time elapsed from a data storing error to a warning is issued.
- *Integrity risk.* The probability that the alert limit is exceeded undetected.

The methods used for detecting data recording problems shall be documented.

11.7.10 Tracability (C Req)

The data recording system shall ensure easy tracability of data (desired data shall be easy to locate even after a long period of time).

11.7.11 Metadata (C Req)

All relevant information for processing sensor data shall be stored together with the raw data. Examples are sensor identification, sensor lever arms, sensor orientation and sensor accuracy data.

11.8 Time integrity

Time integrity is defined as the ability of a sensor or a system to provide early warning when degraded timing accuracy reduces the quality and the accuracy of the survey products. See Section 6.6 for a discussion on possible integrity checks.

A reason for degraded timing accuracy can be a problem with the clock synchronization. Another reason can be an internal sensor problem, for instance processor overload.

11.8.1 Time integrity (C Req)

There shall be continuous time integrity checking on every component in an offshore survey system.

Inherent time integrity functionality in standard methods for clock synchronization (e.g. PTP) shall be exploited.

11.8.2 Documentation (C Req)

Vendors shall specify their functionality for time integrity by three parameters:

- *Alert limit.* Size of time error that will result in a warning. The alert limit shall meet the timing accuracy requirements in Section 11.4.
- *Time-to-alarm.* Time elapsed from degraded timing accuracy to a warning is issued.
- *Integrity risk.* The probability that the alert limit is exceeded undetected.

The methods used for detecting problems shall be documented.

11.9 Sensor mounting

A lever arm is a three-dimensional position vector from one sensor reference point (or from a vehicle reference point) to another sensor reference point. The lever arm is normally decomposed in the vehicle reference frame. Position errors due to timing errors scale with the length of the lever arms.

11.9.1 Surface survey ship lever arms (Non-C Req)

In a surface survey system, the following lever arms should be considered minimized:

- Lever arm between GPS antenna and ship metacenter
- Lever arm between GPS antenna and MBE transducer
- Lever arm between GPS antenna and USBL transducer

Though, good locations with respect to GPS and MBE signal strength and signal to noise ratios are more important than small lever arms.

Co-location of INS / motion sensor with the MBE and USBL transducers will ease the calibration work in determining the relative orientation between the sensors.

11.9.2 Underwater vehicle lever arms (Non-C Req)

In an underwater vehicle, the following lever arms should be considered minimized:

- Lever arm between USBL transponder and underwater vehicle metacenter
- Lever arm between USBL transponder and MBE transducer

Though, good locations with respect to USBL and MBE signal strength and signal to noise ratios are more important than small lever arms.

Co-location of INS / motion sensor with the MBE will ease the calibration work in determining the relative orientation between the sensors.

11.9.3 Accurate and repeatable sensor mounting (Non-C Req)

Accurate and repeatable mounting of survey sensors should be ensured by use of dowel pins and dowel holes.

11.9.4 Rigid sensor fixtures (C Req)

Survey sensors shall be mounted on rigid fixtures.

11.9.5 Vibrations (C Req)

Survey sensors shall not be mounted in places with higher vibrations than the main vehicle frame.

11.9.6 Documentation (C Req)

Sensor mounting angles and lever arms shall be accurately measured and documented.

Sensor mounting angles and lever arms shall be part of the recorded metadata (refer to requirement 11.7.11.)

12 REFERENCES

- (1) J. E. Hughes Clarke, Dynamic Motion Residuals in Swath Sonar Data: Ironing out the Creases, *International Hydrographic Review*, March 2003.
- (2) J. E. Hughes Clarke, A reassessment of vessel coordinate systems: what is it that we are really aligning? *US Hydrographic Conference* 2003.
- (3) K. Gade, NavLab, a Generic Simulation and Post-processing Tool for Navigation. *European Journal of Navigation*, Volume 2, Number 4, November 2004, pp. 51-59.
- (4) Herlihy, D. R., Hillard, B. B., Rulon, T. D., 1989, National Oceanic and Atmospheric Administration Sea Beam "Patch Test" Manual: Ocean Mapping Section, Office of Charting and Geodetic Services.
- (5) Ø. Holmeide and T. Skeie, "Time synchronization in switched ethernet", www.ontimenet.com.
- (6) International hydrographic organization, "IHO standards for hydrographic surveys", 4th edition 1998, Special publication No 44, www.iho.shom.fr.

- (7) B. Jalving, K. Vestgård and N. Størkersen, Detailed Seabed Surveys with AUVs. Technology and Applications of Autonomous Underwater Vehicles, edited by G. Griffiths. Taylor & Francis, London and New York, ISBN 0-415-30154-8.
- (8) Kongsberg Maritime, Product description, HiPAP 500 system, High Precision Acoustic Positioning System, 2003.
- (9) LXI Web Site, <http://www.lxistandard.org/home>.
- (10) National Institute of Standards and Technology, IEEE 1588 Website, <http://ieee1588.nist.gov/>.
- (11) A. E. Ofstad, Verdier for hastigheter of vinkelhastigheter til bruk ved beregning av krav til tidssynkronisering, E-mail to B Jalving, August 2005.
- (12) Request for Comments (RFC) Editor, www.rfc-editor.org.

A INTRODUCTION TO TIMING ERRORS AND ASSUMPTION ON SYNCHRONOUS MEASUREMENTS

A.1 Introduction to timing errors

For a time-varying variable x , the error δx due to timing error δt_x is given by

$$\delta x = \frac{dx}{dt} \delta t_x \quad (22)$$

This is a first order approximation. Since we in this work are focusing on relatively small timing errors, the change in x can be assumed linear.

Considering one-dimensional examples, error δp in position p due to timing error δt_p is given by

$$\delta p = \frac{dp}{dt} \delta t_p = v \delta t_p \quad (23)$$

where v is speed. Error in orientation $\delta \theta$ in position θ due to timing error δt_θ is given by

$$\delta \theta = \frac{d\theta}{dt} \delta t_\theta = \omega \delta t_\theta \quad (24)$$

where ω is angular speed.

In this report the position error in the beam footprint, $\delta \mathbf{p}_{EM}^E$, due to timing errors in surface and underwater survey systems is derived. The resulting three dimensional models match the general theory in equation (22):

- Timing errors in position measurements is proportional to the vehicle velocity \mathbf{v}_{EB}^B .
- Timing errors in attitude is proportional to the vehicle angular rate $\boldsymbol{\omega}_{NB}^B$. Position errors due to timing induced attitude errors scale with ship lever arms and the sonar relative beam vector into position errors in the beam footprint.

A.2 Assumption on synchronous measurements

A time stamp error is modeled as

$$\tilde{t}_{sensor} = t_{sensor} + \delta t_{sensor} \quad (25)$$

where \tilde{t}_{sensor} is sensor time stamp, t_{sensor} is physical sensor measurement time and δt_{sensor} is the time stamp error. Equation (25) is valid for every measurement. δt_{sensor} is a stochastic process with zero mean value and standard deviation $\sigma(\delta t_{sensor})$.

When deriving the timing error, every measurement is referred to the MBE time stamp.

Following equation (25), the MBE time stamp is modeled as

$$\tilde{t}_{MBE} = t_{MBE} + \delta t_{MBE} \quad (26)$$

where \tilde{t}_{MBE} is MBE time stamp, t_{MBE} is true transmit or receive time (when the measurement actually took place) and δt_{MBE} is time stamp error. When modeling the surface and underwater survey systems in Section 8.2 and 8.3, we merged measurements with equal time stamps. This is illustrated in Figure 12.1 for a surface survey system.

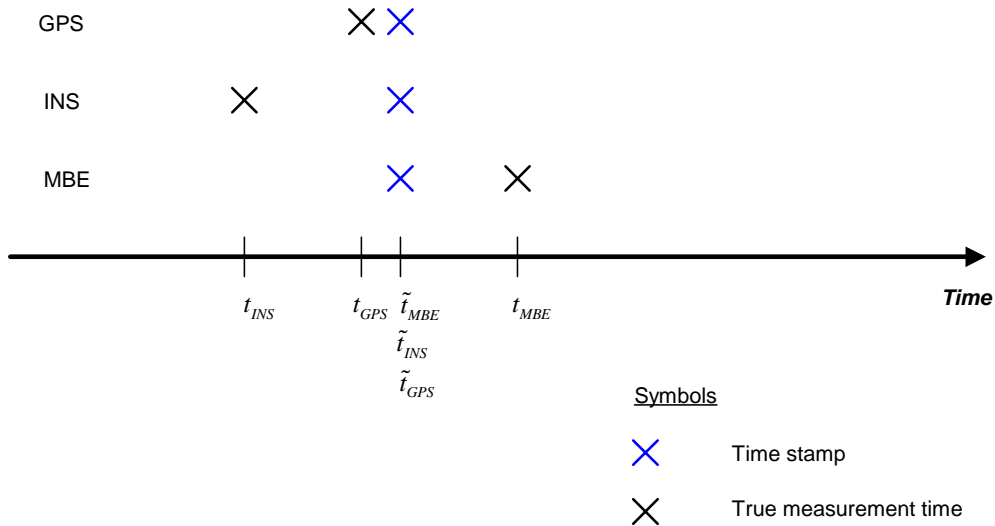


Figure 12.1 Synchronous measurements with equal time stamps were assumed when modeling the surface survey system in Section 8.2. The same assumption is used in the timing error analysis in Appendix B.

In reality, the sensors are asynchronous and thus the assumption $\tilde{t}_{MBE} = \tilde{t}_{INS} = \tilde{t}_{GPS}$ does not hold. In Section 6.2 we discussed different methods for merging asynchronous measurements. Interpolation is one obvious method. To be allowed to work with equal time stamps, we assume that every sensor measurement is interpolated to the MBE time stamp. This is illustrated in Figure 12.2.

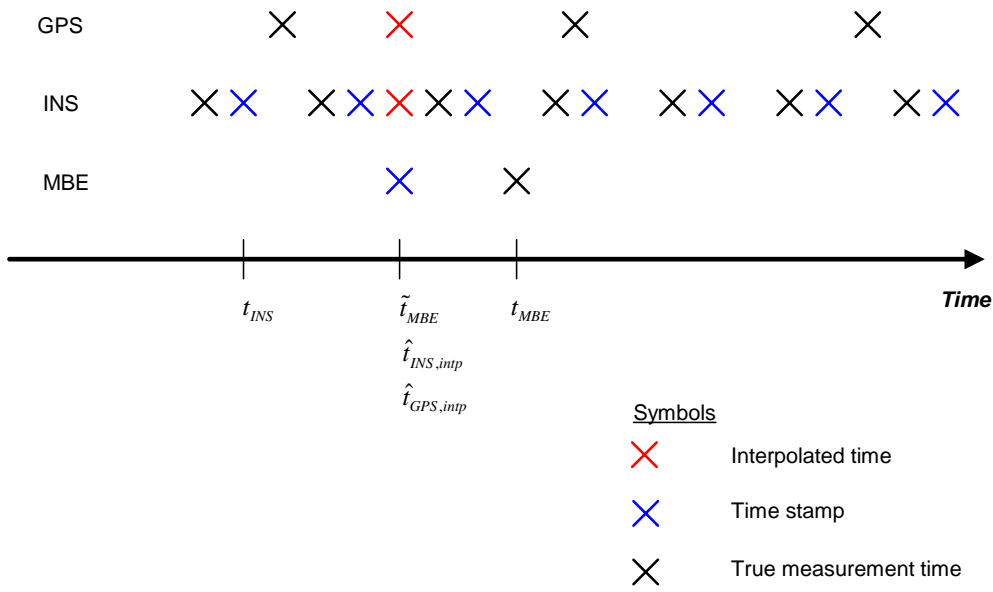


Figure 12.2 Interpolation to MBE measurement time in a surface survey system. Notice that no time error in GPS is assumed.

In the next section, we show that an interpolated value has the same stochastic properties as the physical value. Thus, we conclude that derivation of a timing error budget based on the assumption that all sensor time stamps are equal to the MBE time stamp is valid.

A.3 Error characteristics of an interpolated measurement

We define the sensor measurement \tilde{x}_i with time stamp $\tilde{t}_{x,i}$ as the measurement prior to \tilde{t}_{MBE} . Similarly, we define \tilde{x}_{i+1} with time stamp $\tilde{t}_{x,i+1}$ as the measurement after \tilde{t}_{MBE} . \hat{x}_{inp} is an interpolated value valid at \tilde{t}_{MBE} . \hat{x}_{inp} is found by weighting the two measurements \tilde{x}_i and \tilde{x}_{i+1} with their relative distance in time to \tilde{t}_{MBE} .

$$\hat{x}_{inp} = \frac{\tilde{t}_{x,i+1} - \tilde{t}_{MBE}}{\tilde{t}_{x,i+1} - \tilde{t}_{x,i}} \tilde{x}_i + \frac{\tilde{t}_{MBE} - \tilde{t}_{x,i}}{\tilde{t}_{x,i+1} - \tilde{t}_{x,i}} \tilde{x}_{i+1} \quad (27)$$

which can be re-arranged as

$$\hat{x}_{inp} = \frac{(\tilde{t}_{x,i+1} - \tilde{t}_{MBE}) \tilde{x}_i + (\tilde{t}_{MBE} - \tilde{t}_{x,i}) \tilde{x}_{i+1}}{\tilde{t}_{x,i+1} - \tilde{t}_{x,i}} \quad (28)$$

As described in the previous section, \tilde{x}_i and \tilde{x}_{i+1} come with time stamp errors

$$\begin{aligned} \tilde{t}_{x,i} &= t_{x,i} + \delta t_{x,i} \\ \tilde{t}_{x,i+1} &= t_{x,i+1} + \delta t_{x,i+1} \end{aligned} \quad (29)$$

To model the effect of the time stamp error, equation (29) and equation (26) is inserted into equation (28)

$$\hat{x}_{inp} = \frac{(t_{x,i+1} + \delta t_{x,i+1} - t_{MBE} - \delta t_{MBE}) \tilde{x}_i + (t_{MBE} + \delta t_{MBE} - t_{x,i} - \delta t_{x,i}) \tilde{x}_{i+1}}{t_{x,i+1} + \delta t_{x,i+1} - t_{x,i} - \delta t_{x,i}} \quad (30)$$

To simplify this equation, we assume $\delta t_{x,i} = \delta t_{x,i+1} = \delta t_x$. If the sampling period, $t_{x,i+1} - t_{x,i}$, is much larger than the variation in timing error between the two time steps, this is a safe assumption. Thus,

$$\hat{x}_{inp} = \frac{(t_{x,i+1} + \delta t_x - t_{MBE} - \delta t_{MBE}) \tilde{x}_i + (t_{MBE} + \delta t_{MBE} - t_{x,i} - \delta t_x) \tilde{x}_{i+1}}{t_{x,i+1} - t_{x,i}} \quad (31)$$

An interpolation without timing errors are given by

$$x_{inp} = \frac{(t_{x,i+1} - t_{MBE}) \tilde{x}_i + (t_{MBE} - t_{x,i}) \tilde{x}_{i+1}}{t_{x,i+1} - t_{x,i}} \quad (32)$$

We define the error in the interpolated value due to timing error as

$$\delta x_{inp} = \hat{x}_{inp} - x_{inp} \quad (33)$$

Inserting equation (30) and equation (32), we get

$$\delta x_{inp} = \frac{\tilde{x}_{i+1} - \tilde{x}_i}{t_{x,i+1} - t_{x,i}} (\delta t_{MBE} - \delta t_x) \quad (34)$$

Thus, error in interpolated value due to timing errors is given by

$$\delta x_{inp} = \frac{d\tilde{x}}{dt} (\delta t_{MBE} - \delta t_x) \quad (35)$$

which is the same expression as the error in a sensor measurement due to timing errors. Compare for instance with equation (56) in Section B.3. We have $\delta x_{inp} = \delta x$ and $\text{cov}(\delta x_{inp}) = \text{cov}(\delta x)$.

Since timing errors in an interpolated value share the same properties as timing errors in a measured value, it is safe to assume equal time stamps for every measurement when deriving error models. Thus, the timing accuracy specifications for the surface and underwater survey systems are valid.

B TIMING ERRORS IN SURFACE SURVEY SYSTEMS

B.1 Introduction

In Figure 12.3, a block diagram of the surface survey system is shown. We assume all sensor processing to be post-processing in the Data Acquisition and Survey Processing module. In practice, sensor processing could also be done in real-time in the MBE, or in a dedicated computer, provided necessary functionality and real-time data input. In the figure, we assume that the MBE and the INS are synchronized to UTC time.

We are only modeling errors due to timing errors. That is, we assume that every sensor produces a perfect measurement, but this measurement is time stamped erroneously.

We assume error-free time stamping of the GPS position measurement. Sources for time stamp errors in the INS / motion sensor are discussed in Section 6.3. Following the pattern in Section A.2, the INS time stamp error is modeled as

$$\tilde{t}_{INS} = t_{INS} + \delta t_{INS} \quad (36)$$

where \tilde{t}_{INS} is INS time stamp, t_{INS} is true INS measurement time and δt_{INS} is time stamp error.

To process the MBE data correctly, it is important to time stamp accurately both at transmit and receive time. Orientation is required at both transmit and receive. In equation (8), the MBE processing details discussed in Section 7.1, are simplified by modeling the MBE beam transformation as one operation in time. This simplification is valid, since pitch and heading is required at transmit time and roll at receive time.

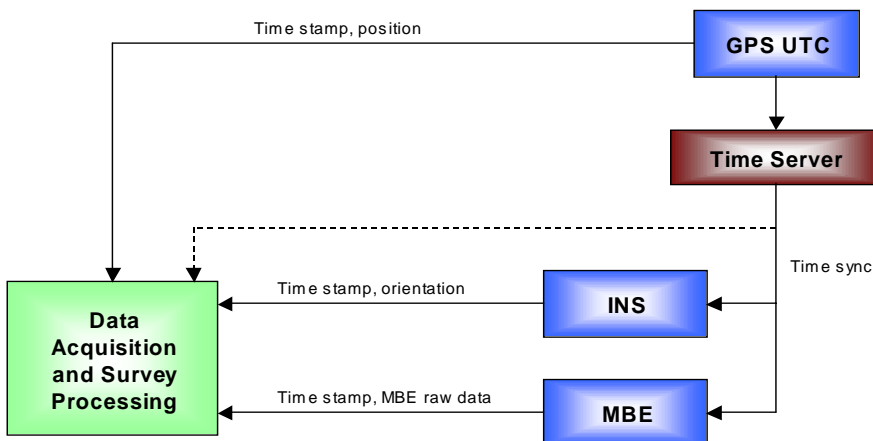


Figure 12.3 Block diagram of a generic surface survey system

Following the discussion in Sections A.2 and A.3, the GPS and INS measurements are referred to the MBE beam measurement and we assume equal time stamps for every sensor. Since GPS time stamping is assumed error-free, we have

$$\tilde{t}_{MBE} = \tilde{t}_{INS} = t_{GPS} \quad (37)$$

for every measurement. t_{GPS} is true GPS measurement time.

The true position \mathbf{p}_{EM}^E of the footprint is given by

$$\mathbf{p}_{EM}^E = \mathbf{p}_{EB_{GPS}}^E + \mathbf{R}_{EN} \mathbf{R}_{NB_{ship}} \left(\mathbf{p}_{B_{GPS}B_{MBE}}^{B_{ship}} + \mathbf{p}_{B_{MBE}M}^{B_{ship}} \right) \quad (38)$$

where $\mathbf{p}_{EB_{GPS}}^E$, \mathbf{R}_{EN} , $\mathbf{R}_{NB_{ship}}$, $\mathbf{p}_{B_{GPS}B_{ship}}^{B_{ship}}$, $\mathbf{p}_{B_{ship}B_{MBE}}^{B_{ship}}$, and $\mathbf{p}_{B_{MBE}M}^{B_{ship}}$ are true physical quantities at t_{MBE} .

The footprint position estimate is given by

$$\hat{\mathbf{p}}_{EM}^E = \mathbf{p}_{EM}^E + \delta \mathbf{p}_{EM}^E \quad (39)$$

where $\delta \mathbf{p}_{EM}^E$ is the position error due to timing errors.

B.2 Error in GPS measurement at MBE measurement time

Assuming equal time stamps (synchronous measurements), the error in the GPS measurement is equal to the distance the GPS antenna moves from the actual time of the physical MBE measurement t_{MBE} to the actual time of the GPS measurement t_{GPS} . The error is given by

$$\tilde{\mathbf{p}}_{EB_{GPS}}^E - \mathbf{p}_{EB_{GPS}}^E = \left(\frac{d}{dt} \mathbf{p}_{EB_{GPS}}^E \right) (t_{GPS} - t_{MBE}) \quad (40)$$

Since $t_{GPS} - t_{MBE}$ is small, we assume that $\mathbf{v}_{EB_{GPS}}^E$ is constant in this interval. The measured GPS position can be expressed as

$$\tilde{\mathbf{p}}_{EB_{GPS}}^E = \mathbf{p}_{EB_{GPS}}^E + \mathbf{v}_{EB_{GPS}}^E (t_{GPS} - t_{MBE}) \quad (41)$$

Substitution of equation (26) into equation (41) yields

$$\tilde{\mathbf{p}}_{EB_{GPS}}^E = \mathbf{p}_{EB_{GPS}}^E + \mathbf{v}_{EB_{GPS}}^E (t_{GPS} - \tilde{t}_{MBE} + \delta t_{MBE}) \quad (42)$$

Using equation (37)

$$\tilde{\mathbf{p}}_{EB_{GPS}}^E = \mathbf{p}_{EB_{GPS}}^E + \mathbf{v}_{EB_{GPS}}^E \delta t_{MBE} \quad (43)$$

In equation (43) $\tilde{\mathbf{p}}_{EB_{GPS}}^E$ is a function of GPS antenna velocity relative to Earth decomposed in the Earth reference frame, $\mathbf{v}_{EB_{GPS}}^E$. Instead we want to express $\tilde{\mathbf{p}}_{EB_{GPS}}^E$ as a function of ship velocity in the ship metacenter $\mathbf{v}_{EB_{ship}}^{B_{ship}}$ (notation is explained by the fact that in Table 8.2 the origin of the ship reference frame is specified to be in the metacenter). Since the ship rotates around its metacenter, the velocity of the GPS antenna is given by

$$\mathbf{v}_{EB_{GPS}}^E = \frac{d}{dt} \mathbf{p}_{EB_{GPS}}^E = \frac{d}{dt} \left(\mathbf{p}_{EB_{ship}}^E + \mathbf{p}_{B_{ship}B_{GPS}}^E \right) = \frac{d}{dt} \left(\mathbf{p}_{EB_{ship}}^E + \mathbf{R}_{EB_{ship}} \mathbf{p}_{B_{ship}B_{GPS}}^{B_{ship}} \right) \quad (44)$$

$$\mathbf{v}_{EB_{GPS}}^E = \frac{d}{dt} \mathbf{p}_{EB_{ship}}^E + \left(\frac{d}{dt} \mathbf{R}_{EB_{ship}} \right) \mathbf{p}_{B_{ship}B_{GPS}}^{B_{ship}} + \mathbf{R}_{EB_{ship}} \left(\frac{d}{dt} \mathbf{p}_{B_{ship}B_{GPS}}^{B_{ship}} \right) \quad (45)$$

where $\mathbf{p}_{B_{ship}B_{GPS}}^{B_{ship}}$ is the lever arm from the metacenter to the GPS antenna.

The time derivative of a rotational matrix is given by

$$\dot{\mathbf{R}}_{AB} = \mathbf{S}(\boldsymbol{\omega}_{AB}^A) \mathbf{R}_{AB} = \mathbf{R}_{AB} \mathbf{S}(\boldsymbol{\omega}_{AB}^B) \quad (46)$$

where $\mathbf{S}(\cdot)$ is the skew symmetric matrix such that for all $\mathbf{a}, \mathbf{b} \in \mathbb{R}^3$

$$\mathbf{S}(\mathbf{a})\mathbf{b} = \mathbf{a} \times \mathbf{b} = -\mathbf{b} \times \mathbf{a} \quad (47)$$

For a relatively large survey vessel, $\mathbf{p}_{B_{ship}B_{GPS}}^{B_{ship}}$ can be assumed constant. Use of equation (46) yields

$$\mathbf{v}_{EB_{GPS}}^E = \frac{d}{dt} \mathbf{p}_{EB_{ship}}^E + \mathbf{R}_{EB_{ship}} \mathbf{S}(\boldsymbol{\omega}_{EB_{ship}}^{B_{ship}}) \mathbf{p}_{B_{ship}B_{GPS}}^{B_{ship}} \quad (48)$$

We have $\mathbf{v}_{EB_{ship}}^E = \frac{d}{dt} \mathbf{p}_{EB_{ship}}^E$, and thus

$$\mathbf{v}_{EB_{GPS}}^E = \mathbf{v}_{EB_{ship}}^E + \mathbf{R}_{EB_{ship}} \mathbf{S}(\boldsymbol{\omega}_{EB_{ship}}^{B_{ship}}) \mathbf{p}_{B_{ship}B_{GPS}}^{B_{ship}} \quad (49)$$

Since $\bar{\boldsymbol{\omega}}_{EB_{ship}}^E \approx \bar{\boldsymbol{\omega}}_{NB_{ship}}^E$, we have

$$\mathbf{v}_{EB_{GPS}}^E = \mathbf{v}_{EB_{ship}}^E + \mathbf{R}_{EB_{ship}} \mathbf{S}(\boldsymbol{\omega}_{NB_{ship}}^{B_{ship}}) \mathbf{p}_{B_{ship}B_{GPS}}^{B_{ship}} \quad (50)$$

$$\mathbf{v}_{EB_{GPS}}^E = \mathbf{R}_{EB_{ship}} \left(\mathbf{v}_{EB_{ship}}^{B_{ship}} + \mathbf{S}(\boldsymbol{\omega}_{NB_{ship}}^{B_{ship}}) \mathbf{p}_{B_{ship}B_{GPS}}^{B_{ship}} \right) \quad (51)$$

Substitution of equation (51) into equation (43) yields

$$\tilde{\mathbf{p}}_{EB_{GPS}}^E = \mathbf{p}_{EB_{GPS}}^E + \mathbf{R}_{EB_{ship}} \left(\mathbf{v}_{EB_{ship}}^{B_{ship}} + \boldsymbol{\omega}_{NB_{ship}}^{B_{ship}} \times \mathbf{p}_{B_{ship}B_{GPS}}^{B_{ship}} \right) \delta t_{MBE} \quad (52)$$

where $\boldsymbol{\omega}_{NB_{ship}}^{B_{ship}}$ is angular velocity relative to N .

B.3 Error in orientation estimate at MBE measurement time

The orientation of the N relative to E , \mathbf{R}_{EN} , is calculated using the GPS position. It changes slowly (due to small position change in the considered time intervals) and we therefore assume that the orientation of N relative to E is equal at t_{MBE} and t_{INS} . Thus, no error in \mathbf{R}_{EN} due to timing errors is modeled:

$$\hat{\mathbf{R}}_{EN} = \mathbf{R}_{EN} \quad (53)$$

The orientation of B_{ship} relative to N , $\mathbf{R}_{NB_{ship}}$, changes with the body rotation rate. Since

$t_{INS} - t_{MBE}$ is small, we assume that $\frac{d}{dt} \mathbf{R}_{NB_{ship}}$ is constant (i.e. constant body rotation rate). The error in the orientation of the ship (B_{ship}) is equal to the rotation between t_{MBE} and t_{INS} and is given by

$$\hat{\mathbf{R}}_{NB_{ship}} - \mathbf{R}_{NB_{ship}} = \left(\frac{d}{dt} \mathbf{R}_{NB_{ship}} \right) (t_{INS} - t_{MBE}) \quad (54)$$

Substitution of equation (36) and (26) into equation (54) yields

$$\hat{\mathbf{R}}_{NB_{ship}} - \mathbf{R}_{NB_{ship}} = \left(\frac{d}{dt} \mathbf{R}_{NB_{ship}} \right) (\tilde{t}_{INS} - \delta t_{INS} - \tilde{t}_{MBE} + \delta t_{MBE}) \quad (55)$$

Since we assume $\tilde{t}_{INS} = \tilde{t}_{MBE}$, we get

$$\hat{\mathbf{R}}_{NB_{ship}} - \mathbf{R}_{NB_{ship}} = \left(\frac{d}{dt} \mathbf{R}_{NB_{ship}} \right) (\delta t_{MBE} - \delta t_{INS}) \quad (56)$$

Using equation (46) the measured orientation can be expressed as

$$\hat{\mathbf{R}}_{NB_{ship}} = \mathbf{R}_{NB_{ship}} + \mathbf{R}_{NB_{ship}} \mathbf{S}(\boldsymbol{\omega}_{NB_{ship}}^{B_{ship}}) (\delta t_{MBE} - \delta t_{INS}) \quad (57)$$

B.4 MBE measurement

There is no position error in the MBE beam due to timing error since the other sensors are referred to this measurement. Therefore

$$\tilde{\mathbf{p}}_{B_{MBE}M}^{B_{ship}} = \mathbf{p}_{B_{MBE}M}^{B_{ship}} \quad (58)$$

B.5 Total beam positioning error due to timing error

Substitution of equation (39), (52), (53), (57), and (58) into equation (8) yields

$$\begin{aligned} \mathbf{p}_{EM}^E + \delta \mathbf{p}_{EM}^E &= \mathbf{p}_{EB_{GPS}}^E + \left(\mathbf{v}_{EB_{ship}}^E + \mathbf{R}_{EB_{ship}} \mathbf{S}(\boldsymbol{\omega}_{NB_{ship}}^{B_{ship}}) \mathbf{p}_{B_{ship}B_{GPS}}^{B_{ship}} \right) \delta t_{MBE} \\ &+ \mathbf{R}_{EN} \left(\mathbf{R}_{NB_{ship}} + \mathbf{R}_{NB_{ship}} \mathbf{S}(\boldsymbol{\omega}_{NB_{ship}}^{B_{ship}}) (\delta t_{MBE} - \delta t_{INS}) \right) \left(\mathbf{p}_{B_{GPS}B_{MBE}}^{B_{ship}} + \mathbf{p}_{B_{MBE}M}^{B_{ship}} \right) \end{aligned} \quad (59)$$

Subtracting equation (38) from equation (59) yields

$$\begin{aligned} \delta \mathbf{p}_{EM}^E &= \mathbf{R}_{EB_{ship}} \left(\mathbf{v}_{EB_{ship}}^{B_{ship}} + \mathbf{S}(\boldsymbol{\omega}_{NB_{ship}}^{B_{ship}}) \mathbf{p}_{B_{ship}B_{GPS}}^{B_{ship}} \right) \delta t_{MBE} \\ &+ \mathbf{R}_{EB_{ship}} \mathbf{S}(\boldsymbol{\omega}_{NB_{ship}}^{B_{ship}}) \left(\mathbf{p}_{B_{GPS}B_{MBE}}^{B_{ship}} + \mathbf{p}_{B_{MBE}M}^{B_{ship}} \right) (\delta t_{MBE} - \delta t_{INS}) \end{aligned} \quad (60)$$

Using equation (47) we get

$$\begin{aligned} \delta \mathbf{p}_{EM}^E &= \mathbf{R}_{EB_{ship}} \left(\mathbf{v}_{EB_{ship}}^{B_{ship}} + \boldsymbol{\omega}_{NB_{ship}}^{B_{ship}} \times \mathbf{p}_{B_{ship}B_{GPS}}^{B_{ship}} \right) \delta t_{MBE} \\ &+ \mathbf{R}_{EB_{ship}} \left(\boldsymbol{\omega}_{NB_{ship}}^{B_{ship}} \times \left(\mathbf{p}_{B_{GPS}B_{MBE}}^{B_{ship}} + \mathbf{p}_{B_{MBE}M}^{B_{ship}} \right) \right) (\delta t_{MBE} - \delta t_{INS}) \end{aligned} \quad (61)$$

This can be written as

$$\begin{aligned} \delta \mathbf{p}_{EM}^E &= \mathbf{R}_{EB_{ship}} \mathbf{v}_{EB_{ship}}^{B_{ship}} \delta t_{MBE} \\ &+ \mathbf{R}_{EB_{ship}} \boldsymbol{\omega}_{NB_{ship}}^{B_{ship}} \times \mathbf{p}_{B_{ship}B_{GPS}}^{B_{ship}} \delta t_{MBE} \\ &+ \mathbf{R}_{EB_{ship}} \boldsymbol{\omega}_{NB_{ship}}^{B_{ship}} \times \mathbf{p}_{B_{GPS}B_{MBE}}^{B_{ship}} (\delta t_{MBE} - \delta t_{INS}) \\ &+ \mathbf{R}_{EB_{ship}} \boldsymbol{\omega}_{NB_{ship}}^{B_{ship}} \times \mathbf{p}_{B_{MBE}M}^{B_{ship}} (\delta t_{MBE} - \delta t_{INS}) \end{aligned} \quad (62)$$

where $\mathbf{v}_{EB_{ship}}^{B_{ship}}$ is translational ship velocity relative to Earth and $\boldsymbol{\omega}_{NB_{ship}}^{B_{ship}}$ is ship angular rate relative to the North-East-Down reference frame.

Equation (62) clearly shows how timing errors in the MBE and the INS contribute to MBE beam positioning error. Looking at MBE positioning error in the ship reference frame, $\delta \mathbf{p}_{EM}^{B_{ship}}$, the errors can be categorized as:

1. *Ship forward speed:* $\mathbf{v}_{EB_{ship}}^{B_{ship}} \delta t_{MBE}$
2. *Ship angular rate and lever arm between GPS and metacenter:* $\boldsymbol{\omega}_{NB_{ship}}^{B_{ship}} \times \mathbf{p}_{B_{ship}B_{GPS}}^{B_{ship}} \delta t_{MBE}$
3. *Ship angular rate and lever arm between GPS and MBE:*
 $\boldsymbol{\omega}_{NB_{ship}}^{B_{ship}} \times \mathbf{p}_{B_{GPS}B_{MBE}}^{B_{ship}} (\delta t_{MBE} - \delta t_{INS})$
4. *Ship angular rate and MBE beam:* $\boldsymbol{\omega}_{NB_{ship}}^{B_{ship}} \times \mathbf{p}_{B_{MBE}M}^{B_{ship}} (\delta t_{MBE} - \delta t_{INS})$

$\boldsymbol{\omega}_{NB_{ship}}^{B_{ship}}$ is angular velocity in three dimensions. The effect on $\delta \mathbf{p}_{EM}^{B_{ship}}$ from ship angular rate in x , y and z can be explored by defining the projection operators

$$\Pr_x = \begin{bmatrix} 1 & 0 & 0 \\ 0 & 0 & 0 \\ 0 & 0 & 0 \end{bmatrix}, \Pr_y = \begin{bmatrix} 0 & 0 & 0 \\ 0 & 1 & 0 \\ 0 & 0 & 0 \end{bmatrix}, \Pr_z = \begin{bmatrix} 0 & 0 & 0 \\ 0 & 0 & 0 \\ 0 & 0 & 1 \end{bmatrix} \quad (63)$$

In Table 12.1 the timing error is expressed as a velocity vector in three dimensions for each error source. The resulting positioning error is easily determined both in direction and magnitude by simply multiplying this vector with the timing error. In appendices D and E the direction and magnitude of timing errors for the small and large survey vessel examples are given in 3D plots.

Error source	Motion	Velocity error vector	Timing error
Ship forward speed	Forward velocity	$\mathbf{v}_{EB_{ship}}^{B_{ship}}$	δt_{MBE}
Ship angular rate and lever arm between GPS and metacenter	Roll	$\left(\Pr_x \boldsymbol{\omega}_{NB_{ship}}^{B_{ship}}\right) \times \mathbf{p}_{B_{ship}B_{GPS}}^{B_{ship}}$	δt_{MBE}
	Pitch	$\left(\Pr_y \boldsymbol{\omega}_{NB_{ship}}^{B_{ship}}\right) \times \mathbf{p}_{B_{ship}B_{GPS}}^{B_{ship}}$	δt_{MBE}
	Yaw	$\left(\Pr_z \boldsymbol{\omega}_{NB_{ship}}^{B_{ship}}\right) \times \mathbf{p}_{B_{ship}B_{GPS}}^{B_{ship}}$	δt_{MBE}
Ship angular rate and lever arm between GPS and MBE	Roll	$\left(\Pr_x \boldsymbol{\omega}_{NB_{ship}}^{B_{ship}}\right) \times \mathbf{p}_{B_{GPS}B_{MBE}}^{B_{ship}}$	$\delta t_{MBE} - \delta t_{INS}$
	Pitch	$\left(\Pr_y \boldsymbol{\omega}_{NB_{ship}}^{B_{ship}}\right) \times \mathbf{p}_{B_{GPS}B_{MBE}}^{B_{ship}}$	$\delta t_{MBE} - \delta t_{INS}$
	Yaw	$\left(\Pr_z \boldsymbol{\omega}_{NB_{ship}}^{B_{ship}}\right) \times \mathbf{p}_{B_{GPS}B_{MBE}}^{B_{ship}}$	$\delta t_{MBE} - \delta t_{INS}$
Ship angular rate and MBE beam	Roll	$\left(\Pr_x \boldsymbol{\omega}_{NB_{ship}}^{B_{ship}}\right) \times \mathbf{p}_{B_{MBE}M}^{B_{ship}}$	$\delta t_{MBE} - \delta t_{INS}$
	Pitch	$\left(\Pr_y \boldsymbol{\omega}_{NB_{ship}}^{B_{ship}}\right) \times \mathbf{p}_{B_{MBE}M}^{B_{ship}}$	$\delta t_{MBE} - \delta t_{INS}$
	Yaw	$\left(\Pr_z \boldsymbol{\omega}_{NB_{ship}}^{B_{ship}}\right) \times \mathbf{p}_{B_{MBE}M}^{B_{ship}}$	$\delta t_{MBE} - \delta t_{INS}$

Table 12.1 Timing errors for a surface survey system. The velocity vector determines direction and magnitude of the timing error in m/s. Multiply with timing error in s to get positioning error in m.

B.6 Covariance analysis

In Table 12.1 we have expressed how timing errors cause position errors in the MBE footprint because of ‘ship forward speed’, ‘ship angular rate and lever arm between GPS and metacenter’, ‘ship angular rate and lever arm between GPS and MBE’ and ‘ship angular rate and MBE beam’. The ten different error components are also illustrated graphically in appendices D and E. In order to consider all error components at the same time and derive specifications on MBE and INS timing errors, we apply the covariance analysis described in this section.

Equation (62) can be re-formulated as

$$\begin{aligned} \delta \mathbf{p}_{EM}^E &= \mathbf{R}_{EB_{ship}} \left(\mathbf{v}_{EB_{ship}}^{B_{ship}} + \boldsymbol{\omega}_{NB_{ship}}^{B_{ship}} \times \left(\mathbf{p}_{B_{ship}B_{MBE}}^{B_{ship}} + \mathbf{p}_{B_{MBE}M}^{B_{ship}} \right) \right) \delta t_{MBE} \\ &\quad - \mathbf{R}_{EB_{ship}} \boldsymbol{\omega}_{NB_{ship}}^{B_{ship}} \times \left(\mathbf{p}_{B_{GPS}B_{MBE}}^{B_{ship}} + \mathbf{p}_{B_{MBE}M}^{B_{ship}} \right) \delta t_{INS} \end{aligned} \quad (64)$$

As discussed in Section A.2, δt_{MBE} and δt_{INS} are stochastic variables. If we assume ship velocity $\mathbf{v}_{EB_{ship}}^{B_{ship}}$ and ship angular velocity $\boldsymbol{\omega}_{NB_{ship}}^{B_{ship}}$ to be deterministic variables, the covariance of $\delta \mathbf{p}_{EM}^{B_{ship}}$ is given by

$$\text{cov} \left(\delta \mathbf{p}_{EM}^{B_{ship}} \right) = \text{cov} \left(\mathbf{v}_1 \delta t_{MBE} + \mathbf{v}_2 \delta t_{INS} \right) \quad (65)$$

where

$$\begin{aligned}\mathbf{v}_1 &= \left(\mathbf{v}_{EB_{ship}}^{B_{ship}} + \boldsymbol{\omega}_{NB_{ship}}^{B_{ship}} \times \left(\mathbf{p}_{B_{ship}B_{MBE}}^{B_{ship}} + \mathbf{p}_{B_{MBE}M}^{B_{ship}} \right) \right) \\ \mathbf{v}_2 &= -\boldsymbol{\omega}_{NB_{ship}}^{B_{ship}} \times \left(\mathbf{p}_{B_{GPS}B_{MBE}}^{B_{ship}} + \mathbf{p}_{B_{MBE}M}^{B_{ship}} \right)\end{aligned}\quad (66)$$

The covariance of a vector \mathbf{x} is given as

$$\text{cov}(\mathbf{x}) = E \left\{ (\mathbf{x} - \bar{\mathbf{x}})(\mathbf{x} - \bar{\mathbf{x}})^T \right\} \quad (67)$$

where $\bar{\mathbf{x}} = E(\mathbf{x})$ is the mean value.

Since the mean value of δt_{INS} and δt_{MBE} is zero, equation (65) can be written

$$\text{cov}(\delta \mathbf{p}_{EM}^{B_{ship}}) = E \left\{ (\mathbf{v}_1 \delta t_{MBE} + \mathbf{v}_2 \delta t_{INS})(\mathbf{v}_1 \delta t_{MBE} + \mathbf{v}_2 \delta t_{INS})^T \right\} \quad (68)$$

$$\begin{aligned}\text{cov}(\delta \mathbf{p}_{EM}^{B_{ship}}) &= E \left\{ (\mathbf{v}_1 \delta t_{MBE})(\mathbf{v}_1 \delta t_{MBE})^T \right\} + E \left\{ (\mathbf{v}_2 \delta t_{INS})(\mathbf{v}_1 \delta t_{MBE})^T \right\} \\ &+ E \left\{ (\mathbf{v}_1 \delta t_{MBE})(\mathbf{v}_2 \delta t_{INS})^T \right\} + E \left\{ (\mathbf{v}_2 \delta t_{INS})(\mathbf{v}_2 \delta t_{INS})^T \right\}\end{aligned}\quad (69)$$

Since $\mathbf{v}_{EM,INS}^{B_{ship}}$ and $\mathbf{v}_{EM,MBE}^{B_{ship}}$ are deterministic variables we get

$$\begin{aligned}\text{cov}(\delta \mathbf{p}_{EM}^{B_{ship}}) &= \mathbf{v}_1 \mathbf{v}_1^T E \left\{ \delta t_{MBE}^2 \right\} + \mathbf{v}_2 \mathbf{v}_1^T E \left\{ \delta t_{INS} \delta t_{MBE} \right\} \\ &+ \mathbf{v}_1 \mathbf{v}_2^T E \left\{ \delta t_{MBE} \delta t_{INS} \right\} + \mathbf{v}_2 \mathbf{v}_2^T E \left\{ \delta t_{INS}^2 \right\}\end{aligned}\quad (70)$$

We assume uncorrelated timing errors δt_{INS} and δt_{MBE} , thus

$$\text{cov}(\delta \mathbf{p}_{EM}^{B_{ship}}) = \mathbf{v}_1 \mathbf{v}_1^T \text{cov}(\delta t_{MBE}) + \mathbf{v}_2 \mathbf{v}_2^T \text{cov}(\delta t_{INS}) \quad (71)$$

When deriving specifications on MBE and INS timing, we consider the diagonal elements of $\text{cov}(\delta \mathbf{p}_{EM}^{B_{ship}})$. These elements correspond to the covariance in surge, sway, and heave in the ship reference frame, B_{ship} . The bound for these components is dependent on the water depth and is specified in Section 9.2. We have

$$\sigma(\delta \mathbf{p}_{EM}^{B_{ship}}) = \sqrt{\text{diag}(\text{cov}(\delta \mathbf{p}_{EM}^{B_{ship}}))} < \begin{bmatrix} x_{spec} \\ y_{spec} \\ z_{spec} \end{bmatrix} \quad (72)$$

The square root sign means element-wise square root of each element in the vector.

Equal contribution to $\text{diag}(\text{cov}(\delta \mathbf{p}_{EM}^{B_{ship}}))$ from the terms $\mathbf{v}_1 \mathbf{v}_1^T \text{cov}(\delta t_{MBE})$ and $\mathbf{v}_2 \mathbf{v}_2^T \text{cov}(\delta t_{INS})$ is required. That means that MBE and INS timing errors contribute equally to $\delta \mathbf{p}_{EM}^{B_{ship}}$. $\text{cov}(\delta \mathbf{p}_{EM}^{B_{ship}})$ and values for $\text{cov}(\delta t_{MBE})$ and $\text{cov}(\delta t_{INS})$ are computed for every six dimensional combination of $\boldsymbol{\omega}_{NB_{ship}}^{B_{ship}}$ and $\mathbf{v}_{EB_{ship}}^{B_{ship}}$. The smallest calculated values of $\text{cov}(\delta t_{MBE})$ and $\text{cov}(\delta t_{INS})$ coincide with the combination of angular and linear velocity causing maximum position error, and hence these become the final specification on timing accuracy. Results for the large and small survey vessel cases in appendices D and E are presented in Section 9.2.

C TIMING ERRORS IN UNDERWATER SURVEY SYSTEMS

C.1 Introduction

As for the surface survey system, only the effects of sensor timing errors are modeled. That is, we assume that every sensor produces a perfect measurement, but with erroneous time stamp.

In Figure 12.4 a block diagram of an ROV underwater survey system is shown. For the survey vessel part we define

$$\begin{aligned}\tilde{t}_{GPS}^{UTC} &= t_{GPS}^{UTC} \\ \tilde{t}_{INS_{ship}}^{UTC} &= t_{INS_{ship}}^{UTC} + \delta t_{INS_{ship}}^{UTC} \\ \tilde{t}_{USBL}^{UTC} &= t_{USBL}^{UTC} + \delta t_{USBL}^{UTC}\end{aligned}\quad (73)$$

where the tilde embellishment (\sim) means measured time stamp, no embellishment means true value and δx means time stamp error for x . The UTC superscript means that a time is referred to the ship time reference. As in Appendix B, we assume error free time stamping of the GPS position measurement.

For the underwater vehicle we define

$$\begin{aligned}\tilde{t}_{TP}^{UTC} &= t_{TP}^{UTC} + \delta t_{USBL}^{UTC} \\ \tilde{t}_{INS_{UV}}^{UV} &= t_{INS_{UV}}^{UTC} + \delta t_{INS_{UV}}^{UV} + \delta t_{UVclock} \\ \tilde{t}_{MBE}^{UV} &= t_{MBE}^{UTC} + \delta t_{MBE}^{UV} + \delta t_{UVclock}\end{aligned}\quad (74)$$

The UV superscript means that a time is referred to the underwater vehicle time reference. $\delta t_{UVclock}$ is the difference between the UTC and UV time references. In an ROV or towfish survey system where all sensors normally remain synchronized to one single timeserver, $\delta t_{UVclock}$ should be close to zero. In an AUV survey system, the AUV time reference drifts from the ship time reference when the AUV is submerged, i.e. $|\delta t_{UVclock}|$ increases.

To relate the GPS-USBL time stamp discussion in Section 7.3 with the error modeling in this appendix, please observe $t_{USBL}^{UTC} = t_{Rx,ship}$ and $t_{TP}^{UTC} = t_{Tx,UV}$. The same timing error, δt_{USBL}^{UTC} , is assumed for both \tilde{t}_{USBL}^{UTC} and \tilde{t}_{TP}^{UTC} .

Following the argumentation in Sections A.2 and A.3, we assume equal time stamps (synchronous measurements) when deriving the error model

$$\tilde{t}_{MBE}^{UV} = \tilde{t}_{INS_{UV}}^{UV} = \tilde{t}_{TP}^{UTC} = \tilde{t}_{USBL}^{UTC} = \tilde{t}_{INS_{ship}}^{UTC} = \tilde{t}_{GPS}^{UTC}\quad (75)$$

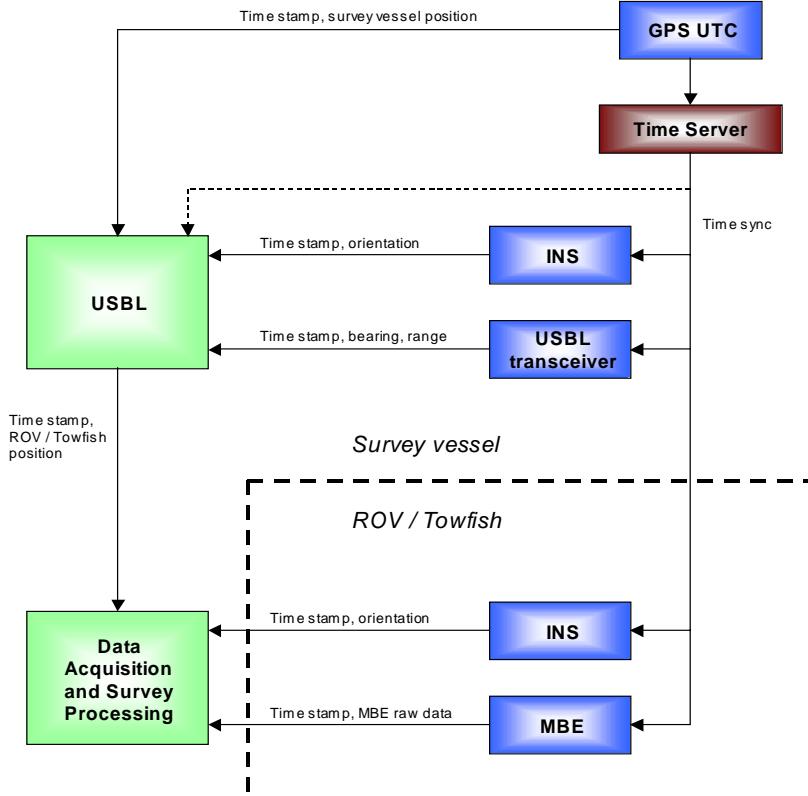


Figure 12.4 Block diagram of an ROV and towfish survey system where sensors in the survey vessel and the ROV / towfish are continually synchronized to the survey vessel Time Server. This is in contrast to an AUV survey system where the AUV is synchronized to the Time Server in the survey vessel only prior to launch. When the AUV is submerged, the AUV clock is dependent on an accurate oscillator to remain acceptably well synchronized.

C.2 Survey vessel

At $t = t_{USBL}^{UTC}$ the true position of the underwater vehicle USBL transponder, $\mathbf{p}_{EB_{TP}}^E$, is given by

$$\mathbf{p}_{EB_{TP}}^E = \mathbf{p}_{EB_{GPS}}^E + \mathbf{R}_{EN} \mathbf{R}_{NB_{ship}} \left(\mathbf{p}_{B_{GPS}B_{USBL}}^{B_{ship}} + \mathbf{p}_{B_{USBL}B_{TP}}^{B_{ship}} \right) \quad (76)$$

where $\mathbf{p}_{EB_{GPS}}^E$, \mathbf{R}_{EN} , $\mathbf{R}_{NB_{ship}}$, $\mathbf{p}_{B_{GPS}B_{USBL}}^{B_{ship}}$, and $\mathbf{p}_{B_{USBL}B_{TP}}^{B_{ship}}$ are true physical quantities at t_{USBL}^{UTC} .

The estimate of the position of the transponder in the underwater vehicle is given by

$$\hat{\mathbf{p}}_{EB_{TP}}^E = \mathbf{p}_{EB_{TP}}^E + \delta \mathbf{p}_{EB_{TP}}^E \quad (77)$$

where $\delta \mathbf{p}_{EB_{TP}}^E$ is the position error due to timing error. $\delta \mathbf{p}_{EB_{TP}}^E$ can be derived in a similar way to $\delta \mathbf{p}_{EM}^E$ in Section B.5 (equation (62)):

$$\begin{aligned}
\delta \mathbf{p}_{EB_{TP}}^E &= \mathbf{R}_{EB_{ship}} \mathbf{v}_{EB_{ship}}^{B_{ship}} \delta t_{USBL}^{UTC} \\
&+ \mathbf{R}_{EB_{ship}} \boldsymbol{\omega}_{NB_{ship}}^{B_{ship}} \times \mathbf{p}_{B_{ship}B_{GPS}}^{B_{ship}} \delta t_{USBL}^{UTC} \\
&+ \mathbf{R}_{EB_{ship}} \boldsymbol{\omega}_{NB_{ship}}^{B_{ship}} \times \mathbf{p}_{B_{GPS}B_{USBL}}^{B_{ship}} \left(\delta t_{USBL}^{UTC} - \delta t_{INS_{ship}}^{UTC} \right) \\
&+ \mathbf{R}_{EB_{ship}} \boldsymbol{\omega}_{NB_{ship}}^{B_{ship}} \times \mathbf{p}_{B_{USBL}B_{TP}}^{B_{ship}} \left(\delta t_{USBL}^{UTC} - \delta t_{INS_{ship}}^{UTC} \right)
\end{aligned} \tag{78}$$

where $\mathbf{v}_{EB_{ship}}^{B_{ship}}$ is ship metacenter velocity relative to Earth causing an underwater vehicle position offset error, and $\boldsymbol{\omega}_{NB_{ship}}^{B_{ship}}$ is angular ship rate relative to the North East down reference frame causing an underwater vehicle position ripple error.

C.3 Underwater vehicle

The true position of the footprint M relative to E , \mathbf{p}_{EM}^E , at $t = t_{MBE}^{UTC}$ is given by

$$\mathbf{p}_{EM}^E = \mathbf{p}_{EB_{TP}}^E + \mathbf{R}_{EN} \mathbf{R}_{NB_{UV}} \left(\mathbf{p}_{B_{TP}B_{MBE}}^{B_{UV}} + \mathbf{p}_{B_{MBE}M}^{B_{UV}} \right) \tag{79}$$

where $\mathbf{p}_{EB_{TP}}^E$, \mathbf{R}_{EN} , $\mathbf{R}_{NB_{UV}}$, $\mathbf{p}_{B_{TP}B_{MBE}}^{B_{UV}}$, and $\mathbf{p}_{B_{MBE}M}^{B_{UV}}$ are true physical quantities at t_{MBE}^{UTC} .

The estimate of the position of the footprint M is given by

$$\hat{\mathbf{p}}_{EM}^E = \mathbf{p}_{EM}^E + \delta \mathbf{p}_{EM}^E \tag{80}$$

where $\delta \mathbf{p}_{EM}^E$ is the position error due to timing error.

Equation (79) can be re-written as

$$\mathbf{p}_{EM}^E = \mathbf{p}_{EB_{TP}}^E + \mathbf{R}_{EN} \mathbf{R}_{NB_{UV}} \mathbf{p}_{B_{TP}B_{UV}}^{B_{UV}} + \mathbf{R}_{EN} \mathbf{R}_{NB_{UV}} \left(\mathbf{p}_{B_{UV}B_{MBE}}^{B_{UV}} + \mathbf{p}_{B_{MBE}M}^{B_{UV}} \right) \tag{81}$$

If the underwater vehicle has an integrated inertial navigation system located in B_{UV} , the inertial navigation system will be aided with the lever arm compensated position measurement

$$\tilde{\mathbf{p}}_{EB_{UV}}^E = \tilde{\mathbf{p}}_{EB_{TP}}^E + \hat{\mathbf{R}}_{EN} \hat{\mathbf{R}}_{NB_{UV}} \mathbf{p}_{B_{TP}B_{UV}}^{B_{UV}} \tag{82}$$

The MBE beam position relative to B_{UV} is given by

$$\hat{\mathbf{p}}_{B_{UV}M}^E = \hat{\mathbf{R}}_{EN} \hat{\mathbf{R}}_{NB_{UV}} \left(\mathbf{p}_{B_{UV}B_{MBE}}^{B_{UV}} + \mathbf{p}_{B_{MBE}M}^{B_{UV}} \right) \tag{83}$$

The re-formulation in equation (81) is introduced because the integrated inertial navigation system is able to filter some of the ripple noise from a timing error in $\tilde{\mathbf{p}}_{EB_{UV}}^E$. Thus, we can put less strict position error requirements on $\tilde{\mathbf{p}}_{EB_{UV}}^E$ than $\hat{\mathbf{p}}_{B_{UV}M}^E$, and consequently come up with less strict requirements on timing accuracy in the surface ship. The inertial navigation system has complementary information on the vehicle dynamics, which allows for filtering of $\tilde{\mathbf{p}}_{EB_{UV}}^E$. Of the seabed topography, $\hat{\mathbf{p}}_{B_{UV}M}^E$, no complementary information is normally available.

C.3.1 Error in GPS-USBL measurement at MBE measurement time

Timing related errors in $\hat{\mathbf{p}}_{EB_{TP}}^E$ has two components. The first component, $\delta \mathbf{p}_{EB_{TP}}^E$, is described in equation (78) and is due to timing errors in the surface vessel following the underwater vehicle.

The second error component is the distance the USBL transponder moves from its measurement time t_{TP}^{UTC} to the MBE measurement time, t_{MBE}^{UTC} . The error is given by

$$\hat{\mathbf{p}}_{EB_{TP}}^E - \mathbf{p}_{EB_{TP}}^E = \delta \mathbf{p}_{EB_{TP}}^E + \left(\frac{d}{dt} \mathbf{p}_{EB_{TP}}^E \right) (t_{TP}^{UTC} - t_{MBE}^{UTC}) \quad (84)$$

where $\hat{\mathbf{p}}_{EB_{TP}}^E$ is the GPS-USBL position modeled in equation (9) and $\mathbf{p}_{EB_{TP}}^E$ is the true position of B_{TP} at t_{TP}^{UTC} .

Inserting equation (74) and assuming synchronous measurements, $\tilde{t}_{MBE}^{UV} = \tilde{t}_{TP}^{UTC}$, we get

$$\hat{\mathbf{p}}_{EB_{TP}}^E = \mathbf{p}_{EB_{TP}}^E + \delta \mathbf{p}_{EB_{TP}}^E + \left(\frac{d}{dt} \mathbf{p}_{EB_{TP}}^E \right) (\delta t_{MBE}^{UV} - \delta t_{USBL}^{UTC} + \delta t_{UVclock}) \quad (85)$$

In equation (85), $\hat{\mathbf{p}}_{EB_{TP}}^E$ is a function of transponder velocity relative to Earth decomposed in Earth coordinates, $\frac{d}{dt} \mathbf{p}_{EB_{TP}}^E$. Instead we want to express $\hat{\mathbf{p}}_{EB_{TP}}^E$ as a function of velocity in the non-rotating underwater vehicle metacenter, $\mathbf{v}_{EB_{UV}}^E$. In Table 8.2, the origin of the UV reference frame, B_{UV} , is defined to be located in the metacenter. Since $\mathbf{p}_{EB_{TP}}^E = \mathbf{p}_{EB_{UV}}^E + \mathbf{R}_{EB_{UV}} \mathbf{p}_{B_{UV}B_{TP}}^{B_{UV}}$, where $\mathbf{p}_{B_{UV}B_{TP}}^{B_{UV}}$ is the lever arm from the UV metacenter to the USBL transponder, we have

$$\hat{\mathbf{p}}_{EB_{TP}}^E = \mathbf{p}_{EB_{TP}}^E + \delta \mathbf{p}_{EB_{TP}}^E + \frac{d}{dt} (\mathbf{p}_{EB_{UV}}^E + \mathbf{R}_{EB_{UV}} \mathbf{p}_{B_{UV}B_{TP}}^{B_{UV}}) (\delta t_{MBE}^{UV} - \delta t_{USBL}^{UTC} + \delta t_{UVclock}) \quad (86)$$

Since $t_{TP}^{UTC} - t_{MBE}^{UTC}$ is relatively small, we assume that $\frac{d}{dt} \mathbf{p}_{EB_{UV}}^E = \mathbf{v}_{EB_{UV}}^E$ is constant (i.e. constant underwater vehicle velocity). Likewise, we assume $\frac{d}{dt} \mathbf{R}_{EB_{UV}}$ constant (for large $\delta t_{UVclock}$ in AUVs, this assumption may actually fail. However, using maximum values for rotation rates, the estimated orientation error and thus ripple position error gets higher than the reality and thus we end up with more conservative timing requirements than strictly necessary). The USBL transponder position B_{TP} relative to the metacenter / UV body system B_{UV} , $\mathbf{p}_{B_{UV}B_{TP}}^{B_{UV}}$, is constant. Using this and equation (46) we get

$$\hat{\mathbf{p}}_{EB_{TP}}^E = \mathbf{p}_{EB_{TP}}^E + \delta \mathbf{p}_{EB_{TP}}^E + \mathbf{R}_{EB_{UV}} \left(\mathbf{v}_{EB_{UV}}^{B_{UV}} + \mathbf{S}(\boldsymbol{\omega}_{EB_{UV}}^{B_{UV}}) \mathbf{p}_{B_{UV}B_{TP}}^{B_{UV}} \right) (\delta t_{MBE}^{UV} - \delta t_{USBL}^{UTC} + \delta t_{UVclock}) \quad (87)$$

C.3.2 Error in underwater vehicle orientation estimate at MBE measurement time

The orientation of B_{UV} relative to N , $\mathbf{R}_{NB_{UV}}$, changes with the body rotation rate. The error in the orientation estimate is equal to the rotation of the UV from the time of the MBE measurement t_{MBE}^{UTC} to the time of the UV INS measurement $t_{INS_{UV}}^{UTC}$. Since $t_{INS_{UV}}^{UTC} - t_{MBE}^{UTC}$ is small, we assume that $\frac{d}{dt} \mathbf{R}_{NB_{UV}}$ is constant. The error is therefore given by

$$\delta \mathbf{R}_{NB_{UV}} = \hat{\mathbf{R}}_{NB_{UV}} - \mathbf{R}_{NB_{UV}} = \left(\frac{d}{dt} \mathbf{R}_{NB_{UV}} \right) (t_{INS_{UV}}^{UTC} - t_{MBE}^{UTC}) \quad (88)$$

Inserting equation (74) and using $\tilde{t}_{MBE}^{UV} = \tilde{t}_{INS_{UV}}^{UV}$, we get

$$\hat{\mathbf{R}}_{NB_{UV}} = \mathbf{R}_{NB_{UV}} + \left(\frac{d}{dt} \mathbf{R}_{NB_{UV}} \right) (\delta t_{MBE}^{UV} - \delta t_{INS_{UV}}^{UV}) \quad (89)$$

Using equation (46) the measured orientation of the UV can be expressed as

$$\hat{\mathbf{R}}_{NB_{UV}} = \mathbf{R}_{NB_{UV}} + \mathbf{R}_{NB_{UV}} \mathbf{S}(\boldsymbol{\omega}_{NB_{UV}}^{B_{UV}}) (\delta t_{MBE}^{UV} - \delta t_{INS_{UV}}^{UV}) \quad (90)$$

C.4 Total beam positioning error due to timing errors

12.1.1 Complete description

Substitution of equation (80), (87), and (90) into equation (11) yields

$$\begin{aligned} \mathbf{p}_{EM}^E + \delta \mathbf{p}_{EM}^E &= \mathbf{p}_{EB_{TP}}^E + \delta \mathbf{p}_{EB_{TP}}^E \\ &+ \mathbf{R}_{EB_{UV}} \left(\mathbf{v}_{EB_{UV}}^{B_{UV}} + \mathbf{S}(\boldsymbol{\omega}_{EB_{UV}}^{B_{UV}}) \mathbf{p}_{B_{UV}B_{TP}}^{B_{UV}} \right) (\delta t_{MBE}^{UV} - \delta t_{USBL}^{UTC} + \delta t_{UVclock}) \\ &+ \mathbf{R}_{EN} \left(\mathbf{R}_{NB_{UV}} + \mathbf{R}_{NB_{UV}} \mathbf{S}(\boldsymbol{\omega}_{NB_{UV}}^{B_{UV}}) (\delta t_{MBE}^{UV} - \delta t_{INS_{UV}}^{UV}) \right) \mathbf{p}_{B_{TP}B_{UV}}^{B_{UV}} \\ &+ \mathbf{R}_{EN} \left(\mathbf{R}_{NB_{UV}} + \mathbf{R}_{NB_{UV}} \mathbf{S}(\boldsymbol{\omega}_{NB_{UV}}^{B_{UV}}) (\delta t_{MBE}^{UV} - \delta t_{INS_{UV}}^{UV}) \right) (\mathbf{p}_{B_{UV}B_{MBE}}^{B_{UV}} + \mathbf{p}_{B_{MBE}M}^{B_{UV}}) \end{aligned} \quad (91)$$

Subtraction of true quantities in equation (81) from equation (91) yields an expression for the position error in an MBE beam footprint

$$\begin{aligned} \delta \mathbf{p}_{EM}^E &= \delta \mathbf{p}_{EB_{TP}}^E \\ &+ \mathbf{R}_{EB_{UV}} \mathbf{v}_{EB_{UV}}^{B_{UV}} (\delta t_{MBE}^{UV} - \delta t_{USBL}^{UTC} + \delta t_{UVclock}) \\ &+ \mathbf{R}_{EB_{UV}} \mathbf{S}(\boldsymbol{\omega}_{EB_{UV}}^{B_{UV}}) \mathbf{p}_{B_{UV}B_{TP}}^{B_{UV}} (\delta t_{MBE}^{UV} - \delta t_{USBL}^{UTC} + \delta t_{UVclock}) \\ &+ \mathbf{R}_{EN} \mathbf{R}_{NB_{UV}} \mathbf{S}(\boldsymbol{\omega}_{NB_{UV}}^{B_{UV}}) \mathbf{p}_{B_{TP}B_{UV}}^{B_{UV}} (\delta t_{MBE}^{UV} - \delta t_{INS_{UV}}^{UV}) \\ &+ \mathbf{R}_{EN} \mathbf{R}_{NB_{UV}} \mathbf{S}(\boldsymbol{\omega}_{NB_{UV}}^{B_{UV}}) (\mathbf{p}_{B_{UV}B_{MBE}}^{B_{UV}} + \mathbf{p}_{B_{MBE}M}^{B_{UV}}) (\delta t_{MBE}^{UV} - \delta t_{INS_{UV}}^{UV}) \end{aligned} \quad (92)$$

Assuming $\tilde{\boldsymbol{\omega}}_{EB} \approx \tilde{\boldsymbol{\omega}}_{NB}$ and using equation (47)

$$\begin{aligned} \delta \mathbf{p}_{EM}^E &= \delta \mathbf{p}_{EB_{TP}}^E \\ &+ \mathbf{R}_{EB_{UV}} \mathbf{v}_{EB_{UV}}^{B_{UV}} (\delta t_{MBE}^{UV} - \delta t_{USBL}^{UTC} + \delta t_{UVclock}) \\ &+ \mathbf{R}_{EB_{UV}} \boldsymbol{\omega}_{NB_{UV}}^{B_{UV}} \times \mathbf{p}_{B_{UV}B_{TP}}^{B_{UV}} (\delta t_{MBE}^{UV} - \delta t_{USBL}^{UTC} + \delta t_{UVclock}) \\ &+ \mathbf{R}_{EB_{UV}} \boldsymbol{\omega}_{NB_{UV}}^{B_{UV}} \times \mathbf{p}_{B_{TP}B_{UV}}^{B_{UV}} (\delta t_{MBE}^{UV} - \delta t_{INS_{UV}}^{UV}) \\ &+ \mathbf{R}_{EB_{UV}} \boldsymbol{\omega}_{NB_{UV}}^{B_{UV}} \times (\mathbf{p}_{B_{UV}B_{MBE}}^{B_{UV}} + \mathbf{p}_{B_{MBE}M}^{B_{UV}}) (\delta t_{MBE}^{UV} - \delta t_{INS_{UV}}^{UV}) \end{aligned} \quad (93)$$

Inserting the error in the GPS-USBL position estimate of the underwater vehicle transponder from the survey vessel in equation (78), equation (93) can be written as

$$\begin{aligned}
\delta \mathbf{p}_{EM}^E &= \mathbf{R}_{EB_{ship}} \mathbf{v}_{EB_{ship}}^{B_{ship}} \delta t_{USBL}^{UTC} \\
&+ \mathbf{R}_{EB_{ship}} \boldsymbol{\omega}_{NB_{ship}}^{B_{ship}} \times \mathbf{p}_{B_{ship}B_{GPS}}^{B_{ship}} \delta t_{USBL}^{UTC} \\
&+ \mathbf{R}_{EB_{ship}} \boldsymbol{\omega}_{NB_{ship}}^{B_{ship}} \times \mathbf{p}_{B_{GPS}B_{USBL}}^{B_{ship}} \left(\delta t_{USBL}^{UTC} - \delta t_{INS_{ship}}^{UTC} \right) \\
&+ \mathbf{R}_{EB_{ship}} \boldsymbol{\omega}_{NB_{ship}}^{B_{ship}} \times \mathbf{p}_{B_{USBL}B_{TP}}^{B_{ship}} \left(\delta t_{USBL}^{UTC} - \delta t_{INS_{ship}}^{UTC} \right) \\
&+ \mathbf{R}_{EB_{UV}} \mathbf{v}_{EB_{UV}}^{B_{UV}} \left(\delta t_{MBE}^{UV} - \delta t_{USBL}^{UTC} + \delta t_{UVclock} \right) \\
&+ \mathbf{R}_{EB_{UV}} \boldsymbol{\omega}_{NB_{UV}}^{B_{UV}} \times \mathbf{p}_{B_{UV}B_{TP}}^{B_{UV}} \left(\delta t_{MBE}^{UV} - \delta t_{USBL}^{UTC} + \delta t_{UVclock} \right) \\
&+ \mathbf{R}_{EB_{UV}} \boldsymbol{\omega}_{NB_{UV}}^{B_{UV}} \times \mathbf{p}_{B_{TP}B_{UV}}^{B_{UV}} \left(\delta t_{MBE}^{UV} - \delta t_{INS_{UV}}^{UV} \right) \\
&+ \mathbf{R}_{EB_{UV}} \boldsymbol{\omega}_{NB_{UV}}^{B_{UV}} \times \left(\mathbf{p}_{B_{UV}B_{MBE}}^{B_{UV}} + \mathbf{p}_{B_{MBE}M}^{B_{UV}} \right) \left(\delta t_{MBE}^{UV} - \delta t_{INS_{UV}}^{UV} \right)
\end{aligned} \tag{94}$$

$\boldsymbol{\omega}_{NB_{ship}}^{B_{ship}}$ and $\boldsymbol{\omega}_{NB_{UV}}^{B_{UV}}$ are three dimensional rotation vectors. The effect on $\delta \mathbf{p}_{EM}^E$ from ship and UV angular rate in x , y , and z can be explored by using the projection operators defined in equation (63). In Table 12.2 the timing error is expressed as a velocity vector in three dimensions for each error source in equation (94). The resulting positioning error is easily determined both in direction and magnitude by simply multiplying this velocity vector with the timing error. The 20 different error components are also illustrated graphically in appendices F and G for the AUV and ROV underwater survey system examples.

Error source	Motion	Velocity error vector	Timing error
Ship GPS antenna velocity	Forward ship velocity	$\mathbf{v}_{EB_{ship}}^{B_{ship}}$	δt_{USBL}^{UTC}
	Roll	$\left(Pr_x \boldsymbol{\omega}_{NB_{ship}}^{B_{ship}}\right) \times \mathbf{p}_{B_{ship}B_{GPS}}^{B_{ship}}$	δt_{USBL}^{UTC}
	Pitch	$\left(Pr_y \boldsymbol{\omega}_{NB_{ship}}^{B_{ship}}\right) \times \mathbf{p}_{B_{ship}B_{GPS}}^{B_{ship}}$	
	Yaw	$\left(Pr_z \boldsymbol{\omega}_{NB_{ship}}^{B_{ship}}\right) \times \mathbf{p}_{B_{ship}B_{GPS}}^{B_{ship}}$	
Ship angular rate and lever arm between GPS and USBL.	Roll	$\left(Pr_x \boldsymbol{\omega}_{NB_{ship}}^{B_{ship}}\right) \times \mathbf{p}_{B_{GPS}B_{USBL}}^{B_{ship}}$	$\delta t_{USBL}^{UTC} - \delta t_{INS_{ship}}^{UTC}$
	Pitch	$\left(Pr_y \boldsymbol{\omega}_{NB_{ship}}^{B_{ship}}\right) \times \mathbf{p}_{B_{GPS}B_{USBL}}^{B_{ship}}$	
	Yaw	$\left(Pr_z \boldsymbol{\omega}_{NB_{ship}}^{B_{ship}}\right) \times \mathbf{p}_{B_{GPS}B_{USBL}}^{B_{ship}}$	
Ship angular rate and relative USBL position	Roll	$\left(Pr_x \boldsymbol{\omega}_{NB_{ship}}^{B_{ship}}\right) \times \mathbf{p}_{B_{USBL}B_{TP}}^{B_{ship}}$	$\delta t_{USBL}^{UTC} - \delta t_{INS_{ship}}^{UTC}$
	Pitch	$\left(Pr_y \boldsymbol{\omega}_{NB_{ship}}^{B_{ship}}\right) \times \mathbf{p}_{B_{USBL}B_{TP}}^{B_{ship}}$	
	Yaw	$\left(Pr_z \boldsymbol{\omega}_{NB_{ship}}^{B_{ship}}\right) \times \mathbf{p}_{B_{USBL}B_{TP}}^{B_{ship}}$	
UV transponder velocity	Forward UV velocity	$\mathbf{v}_{EB_{UV}}^{B_{UV}}$	$\delta t_{MBE}^{UV} - \delta t_{USBL}^{UTC} - \delta t_{UV_{clock}}$
	Roll	$\left(Pr_x \boldsymbol{\omega}_{NB_{UV}}^{B_{UV}}\right) \times \mathbf{p}_{B_{UV}B_{TP}}^{B_{UV}}$	$\delta t_{MBE}^{UV} - \delta t_{USBL}^{UTC} - \delta t_{UV_{clock}}$
	Pitch	$\left(Pr_y \boldsymbol{\omega}_{NB_{UV}}^{B_{UV}}\right) \times \mathbf{p}_{B_{UV}B_{TP}}^{B_{UV}}$	
	Yaw	$\left(Pr_z \boldsymbol{\omega}_{NB_{UV}}^{B_{UV}}\right) \times \mathbf{p}_{B_{UV}B_{TP}}^{B_{UV}}$	
UV angular rate and lever arm between transponder and MBE	Roll	$\left(Pr_x \boldsymbol{\omega}_{NB_{UV}}^{B_{UV}}\right) \times \mathbf{p}_{B_{TP}B_{MBE}}^{B_{UV}}$	$\delta t_{MBE}^{UV} - \delta t_{INS_{UV}}^{UV}$
	Pitch	$\left(Pr_y \boldsymbol{\omega}_{NB_{UV}}^{B_{UV}}\right) \times \mathbf{p}_{B_{TP}B_{MBE}}^{B_{UV}}$	
	Yaw	$\left(Pr_z \boldsymbol{\omega}_{NB_{UV}}^{B_{UV}}\right) \times \mathbf{p}_{B_{TP}B_{MBE}}^{B_{UV}}$	
UV angular rate and MBE beam	Roll	$\left(Pr_x \boldsymbol{\omega}_{NB_{UV}}^{B_{UV}}\right) \times \mathbf{p}_{B_{MBE}M}^{B_{UV}}$	$\delta t_{MBE}^{UV} - \delta t_{INS_{UV}}^{UV}$
	Pitch	$\left(Pr_y \boldsymbol{\omega}_{NB_{UV}}^{B_{UV}}\right) \times \mathbf{p}_{B_{MBE}M}^{B_{UV}}$	
	Yaw	$\left(Pr_z \boldsymbol{\omega}_{NB_{UV}}^{B_{UV}}\right) \times \mathbf{p}_{B_{MBE}M}^{B_{UV}}$	

Table 12.2 Timing errors for an underwater survey system. The velocity vector determines direction and magnitude of the timing error in m/s. Multiply with timing error in s to get positioning error in m .

12.1.2 Categorization and simplification

Equation (94) can be categorized as

$$\delta \mathbf{p}_{EM}^E = \delta \mathbf{p}_{EB_{UV},offset}^E + \delta \mathbf{p}_{EB_{UV},ripple}^E + \delta \mathbf{p}_{B_{UV}M,ripple}^E \quad (95)$$

$\delta \mathbf{p}_{EB_{UV},offset}^E$ is given by

$$\begin{aligned} \delta \mathbf{p}_{EB_{UV},offset}^E &= \mathbf{R}_{EB_{ship}} \mathbf{v}_{EB_{ship}}^{B_{ship}} \delta t_{USBL}^{UTC} \\ &+ \mathbf{R}_{EB_{UV}} \mathbf{v}_{EB_{UV}}^{B_{UV}} \left(\delta t_{MBE}^{UV} - \delta t_{USBL}^{UTC} + \delta t_{UVclock} \right) \end{aligned} \quad (96)$$

$\delta \mathbf{p}_{EB_{UV},ripple}^E$ is given by

$$\begin{aligned} \delta \mathbf{p}_{EB_{UV},ripple}^E &= \mathbf{R}_{EB_{ship}} \boldsymbol{\omega}_{NB_{ship}}^{B_{ship}} \times \mathbf{p}_{B_{ship}B_{GPS}}^{B_{ship}} \delta t_{USBL}^{UTC} \\ &+ \mathbf{R}_{EB_{ship}} \boldsymbol{\omega}_{NB_{ship}}^{B_{ship}} \times \mathbf{p}_{B_{GPS}B_{USBL}}^{B_{ship}} \left(\delta t_{USBL}^{UTC} - \delta t_{INS_{ship}}^{UTC} \right) \\ &+ \mathbf{R}_{EB_{ship}} \boldsymbol{\omega}_{NB_{ship}}^{B_{ship}} \times \mathbf{p}_{B_{USBL}B_{TP}}^{B_{ship}} \left(\delta t_{USBL}^{UTC} - \delta t_{INS_{ship}}^{UTC} \right) \\ &+ \mathbf{R}_{EB_{UV}} \boldsymbol{\omega}_{NB_{UV}}^{B_{UV}} \times \mathbf{p}_{B_{UV}B_{TP}}^{B_{UV}} \left(\delta t_{INS_{UV}}^{UV} - \delta t_{USBL}^{UTC} + \delta t_{UVclock} \right) \\ &+ \mathbf{R}_{EB_{UV}} \boldsymbol{\omega}_{NB_{UV}}^{B_{UV}} \times \mathbf{p}_{B_{TP}B_{UV}}^{B_{UV}} \left(\delta t_{MBE}^{UV} - \delta t_{INS_{UV}}^{UV} \right) \end{aligned} \quad (97)$$

$\delta \mathbf{p}_{B_{UV}M,ripple}^E$ is given by

$$\begin{aligned} \delta \mathbf{p}_{B_{UV}M,ripple}^E &= \mathbf{R}_{EB_{UV}} \boldsymbol{\omega}_{NB_{UV}}^{B_{UV}} \times \mathbf{p}_{B_{UV}B_{MBE}}^{B_{UV}} \left(\delta t_{MBE}^{UV} - \delta t_{INS_{UV}}^{UV} \right) \\ &+ \mathbf{R}_{EB_{UV}} \boldsymbol{\omega}_{NB_{UV}}^{B_{UV}} \times \mathbf{p}_{B_{MBE}M}^{B_{UV}} \left(\delta t_{MBE}^{UV} - \delta t_{INS_{UV}}^{UV} \right) \end{aligned} \quad (98)$$

$\delta \mathbf{p}_{EB_{UV},offset}^E$ is only a practical problem in AUV applications where $\delta t_{UVclock} \gg \delta t_{USBL}^{UTC}$ and $\delta t_{UVclock} \gg \delta t_{MBE}^{UV}$. Thus, equation (96) can be simplified to:

$$\delta \mathbf{p}_{EB_{UV},offset}^E = \mathbf{R}_{EB_{UV}} \mathbf{v}_{EB_{UV}}^{B_{UV}} \delta t_{UVclock} \quad (99)$$

Since $\mathbf{p}_{B_{UV}B_{TP}}^{B_{UV}} \ll \mathbf{p}_{B_{USBL}B_{TP}}^{B_{ship}}$, $\mathbf{p}_{B_{UV}B_{TP}}^{B_{UV}} \ll \mathbf{p}_{B_{GPS}B_{USBL}}^{B_{ship}}$ and $\mathbf{p}_{B_{UV}B_{TP}}^{B_{UV}} \ll \mathbf{p}_{B_{ship}B_{GPS}}^{B_{ship}}$ equation (97) can be simplified to

$$\begin{aligned} \delta \mathbf{p}_{EB_{UV},ripple}^E &= \mathbf{R}_{EB_{ship}} \boldsymbol{\omega}_{NB_{ship}}^{B_{ship}} \times \mathbf{p}_{B_{ship}B_{GPS}}^{B_{ship}} \delta t_{USBL}^{UTC} \\ &+ \mathbf{R}_{EB_{ship}} \boldsymbol{\omega}_{NB_{ship}}^{B_{ship}} \times \mathbf{p}_{B_{GPS}B_{USBL}}^{B_{ship}} \left(\delta t_{USBL}^{UTC} - \delta t_{INS_{ship}}^{UTC} \right) \\ &+ \mathbf{R}_{EB_{ship}} \boldsymbol{\omega}_{NB_{ship}}^{B_{ship}} \times \mathbf{p}_{B_{USBL}B_{TP}}^{B_{ship}} \left(\delta t_{USBL}^{UTC} - \delta t_{INS_{ship}}^{UTC} \right) \end{aligned} \quad (100)$$

The reason for this categorization is to develop individual requirements for $\delta \mathbf{p}_{EB_{UV},offset}^E$, $\delta \mathbf{p}_{EB_{UV},ripple}^E$ and $\delta \mathbf{p}_{B_{UV}M,ripple}^E$ in order not to specify the timing accuracy requirements too strict.

The error contributions in $\delta \mathbf{p}_{EB_{UV},offset}^E$ are

1. *UV velocity and UV time drift:* $\mathbf{v}_{EB_{UV}}^{B_{UV}} \delta t_{UVclock}$

The effect of USBL and MBE timing errors to $\delta \mathbf{p}_{EB_{UV},offset}^E$ can be neglected.

The error contributions in $\delta \mathbf{p}_{EB_{UV},ripple}^E$ are

1. *Ship angular rate and lever arm between GPS antenna and metacenter:*

$$\boldsymbol{\omega}_{NB_{ship}}^{B_{ship}} \times \mathbf{p}_{B_{ship}B_{GPS}}^{B_{ship}} \delta t_{USBL}^{UTC}$$

2. *Ship angular rate and lever arm between GPS and USBL transducer:*

$$\boldsymbol{\omega}_{NB_{ship}}^{B_{ship}} \times \mathbf{p}_{B_{GPS}B_{USBL}}^{B_{ship}} \left(\delta t_{USBL}^{UTC} - \delta t_{INS_{ship}}^{UTC} \right)$$

3. *Ship angular rate and USBL measurement:* $\boldsymbol{\omega}_{NB_{ship}}^{B_{ship}} \times \mathbf{p}_{B_{USBL}B_{TP}}^{B_{ship}} \left(\delta t_{USBL}^{UTC} - \delta t_{INS_{ship}}^{UTC} \right)$

The effect of UV timing errors to $\delta \mathbf{p}_{EB_{UV},ripple}^E$ can be neglected due to comparatively small UV lever arms.

The error contributions in $\delta \mathbf{p}_{B_{UV}M,ripple}^E$ are

1. *UV angular rate and lever arm between underwater vehicle metacenter and MBE:*

$$\boldsymbol{\omega}_{NB_{UV}}^{B_{UV}} \times \mathbf{p}_{B_{UV}B_{MBE}}^{B_{UV}}$$

2. *UV angular rate and MBE beam:* $\boldsymbol{\omega}_{NB_{UV}}^{B_{UV}} \times \mathbf{p}_{B_{MBE}M}^{B_{UV}}$

The covariance analysis in Section C.5 is based on this simplified set of equations.

C.5 Covariance analysis

C.5.1.1 Derivation

In order to consider all error components at the same time and derive specifications on timing accuracy for all sensors involved in an underwater survey system, we apply the covariance analyses described in this section.

As discussed in Section A.2, $\delta t_{INS_{ship}}^{UTC}$, δt_{USBL}^{UTC} , δt_{MBE}^{UV} , δt_{TP} , $\delta t_{INS_{UV}}^{UTC}$ and $\delta t_{UVclock}$ are stochastic variables. We assume ship velocity $\mathbf{v}_{EB_{ship}}^{B_{ship}}$, ship angular velocity $\boldsymbol{\omega}_{NB_{ship}}^{B_{ship}}$, UV velocity $\mathbf{v}_{EB_{UV}}^{B_{UV}}$, and UV angular velocity $\boldsymbol{\omega}_{NB_{UV}}^{B_{UV}}$ to be deterministic variables.

The covariance analysis is based on the simplified set of equations (99), (100) and (98).

Reformulation gives:

$$\delta \mathbf{p}_{EB_{UV},offset}^E = \mathbf{R}_{EB_{UV}} \mathbf{v}_{EB_{UV}}^{B_{UV}} \delta t_{UVclock} \quad (101)$$

$$\begin{aligned} \delta \mathbf{p}_{EB_{UV},ripple}^E &= \mathbf{R}_{EB_{ship}} \boldsymbol{\omega}_{NB_{ship}}^{B_{ship}} \times \left(\mathbf{p}_{EB_{ship}B_{GPS}}^{B_{ship}} + \mathbf{p}_{B_{GPS}B_{USBL}}^{B_{ship}} + \mathbf{p}_{B_{USBL}B_{TP}}^{B_{ship}} \right) \delta t_{USBL}^{UTC} \\ &\quad - \mathbf{R}_{EB_{ship}} \boldsymbol{\omega}_{NB_{ship}}^{B_{ship}} \times \left(\mathbf{p}_{B_{GPS}B_{USBL}}^{B_{ship}} + \mathbf{p}_{B_{USBL}B_{TP}}^{B_{ship}} \right) \delta t_{INS_{ship}}^{UTC} \end{aligned} \quad (102)$$

$$\begin{aligned} \delta \mathbf{p}_{B_{UV}M,ripple}^E &= \mathbf{R}_{EB_{UV}} \boldsymbol{\omega}_{NB_{UV}}^{B_{UV}} \times \left(\mathbf{p}_{B_{UV}B_{MBE}}^{B_{UV}} + \mathbf{p}_{B_{MBE}M}^{B_{UV}} \right) \delta t_{MBE}^{UV} \\ &\quad - \mathbf{R}_{EB_{UV}} \boldsymbol{\omega}_{NB_{UV}}^{B_{UV}} \times \left(\mathbf{p}_{B_{UV}B_{MBE}}^{B_{UV}} + \mathbf{p}_{B_{MBE}M}^{B_{UV}} \right) \delta t_{INS_{UV}}^{UV} \end{aligned} \quad (103)$$

$\mathbf{R}_{EB_{ship}}$ and $\mathbf{R}_{EB_{UV}}$ are varying. The covariances of $\delta \mathbf{p}_{EB_{UV},offset}^{B_{UV}}$, $\delta \mathbf{p}_{EB_{UV},ripple}^{B_{ship}}$ and $\delta \mathbf{p}_{B_{UV}M,ripple}^{B_{UV}}$ are calculated. The covariance analysis is done in a similar way as in Section B.6:

$$\begin{aligned}
\text{cov}\left(\delta \mathbf{p}_{EB_{UV},offset}^{B_{UV}}\right) &= \mathbf{v}_{EB_{UV}}^{B_{UV}} \left(\mathbf{v}_{EB_{UV}}^{B_{UV}}\right)^T \text{cov}\left(\delta t_{UVclock}\right) \\
\text{cov}\left(\delta \mathbf{p}_{EB_{UV},ripple}^{B_{ship}}\right) &= \mathbf{v}_1 \mathbf{v}_1^T \text{cov}\left(\delta t_{USBL}^{UTC}\right) + \mathbf{v}_2 \mathbf{v}_2^T \text{cov}\left(\delta t_{INS_{ship}}^{UTC}\right) \\
\text{cov}\left(\delta \mathbf{p}_{B_{UV},M,ripple}^{B_{UV}}\right) &= \mathbf{v}_3 \mathbf{v}_3^T \text{cov}\left(\delta t_{MBE}^{UV}\right) + \mathbf{v}_3 \mathbf{v}_3^T \text{cov}\left(\delta t_{INS_{UV}}^{UV}\right)
\end{aligned} \tag{104}$$

where

$$\begin{aligned}
\mathbf{v}_1 &= \boldsymbol{\omega}_{NB_{ship}}^{B_{ship}} \times \left(\mathbf{p}_{B_{ship}B_{USBL}}^{B_{ship}} + \mathbf{p}_{B_{USBL}B_{TP}}^{B_{ship}}\right) \\
\mathbf{v}_2 &= \boldsymbol{\omega}_{NB_{ship}}^{B_{ship}} \times \left(\mathbf{p}_{B_{GPS}B_{USBL}}^{B_{ship}} + \mathbf{p}_{B_{USBL}B_{TP}}^{B_{ship}}\right) \\
\mathbf{v}_3 &= \boldsymbol{\omega}_{NB_{UV}}^{B_{UV}} \times \left(\mathbf{p}_{B_{UV}B_{MBE}}^{B_{UV}} + \mathbf{p}_{B_{MBE}M}^{B_{UV}}\right)
\end{aligned} \tag{105}$$

We consider underwater vehicle position offset ($\delta \mathbf{p}_{EB_{UV},offset}^{B_{UV}}$), underwater vehicle position ripples ($\delta \mathbf{p}_{EB_{UV},ripple}^{B_{ship}}$) and MBE ripples ($\delta \mathbf{p}_{B_{UV},M,ripple}^{B_{UV}}$) individually.

C.5.2 Underwater vehicle position offset

The diagonal elements of $\text{cov}\left(\delta \mathbf{p}_{EB_{UV},offset}^{B_{UV}}\right)$ are considered when deriving specifications on the clock accuracy between the surface vessel and the underwater vehicle. Obviously, the forward speed will determine the clock accuracy specification. The specification on position offset error due to timing error is given in Section 9.3:

$$\sigma\left(\delta \mathbf{p}_{EB_{UV},offset}^{B_{UV}}\right) = \sqrt{\text{diag}\left(\text{cov}\left(\delta \mathbf{p}_{EB_{UV},offset}^{B_{ship}}\right)\right)} < \begin{bmatrix} x_{offset_spec} \\ y_{offset_spec} \\ z_{offset_spec} \end{bmatrix} \tag{106}$$

The square root sign means element-wise square root of each element in the vector.

Depth of an underwater vehicle is normally determined by a pressure sensor, making the the z-component of $\sigma\left(\delta \mathbf{p}_{EB_{UV},offset}^{B_{UV}}\right)$ not applicable.

C.5.3 Underwater vehicle position ripples

The diagonal elements of $\text{cov}\left(\delta \mathbf{p}_{EB_{UV},ripple}^{B_{ship}}\right)$ are considered when deriving timing specifications for the surface ship, The diagonal elements correspond to the underwater vehicle position covariance in surge, sway, and heave in the ship reference frame due to ship timing errors in USBL and ship INS. The bound for these components is dependent on the water depth and is specified in Section 9.3:

$$\sigma\left(\delta \mathbf{p}_{EB_{UV},ripple}^{B_{ship}}\right) = \sqrt{\text{diag}\left(\text{cov}\left(\delta \mathbf{p}_{EB_{UV},ripple}^{B_{ship}}\right)\right)} < \begin{bmatrix} x_{ripple_spec} \\ y_{ripple_spec} \\ z_{ripple_spec} \end{bmatrix} \tag{107}$$

The square root sign means element-wise square root of each element in the vector.

Only the horizontal accuracy (the x and y components) is considered since the depth of an underwater vehicle normally is derived from a pressure sensor, not from an USBL measurement. Equal contribution to $\text{diag}\left(\text{cov}\left(\delta\mathbf{p}_{EB_{UV},ripple}^{B_{ship}}\right)\right)$ from the terms $\mathbf{v}_1\mathbf{v}_1^T \text{cov}\left(\delta t_{USBL}^{UTC}\right)$ and $\mathbf{v}_2\mathbf{v}_2^T \text{cov}\left(\delta t_{INS_{ship}}^{UTC}\right)$ is required. That means that USBL and ship INS timing errors contribute equally to $\delta\mathbf{p}_{EB_{UV},ripple}^{B_{ship}} \cdot \text{cov}\left(\delta\mathbf{p}_{EB_{UV},ripple}^{B_{ship}}\right)$ and values for $\text{cov}\left(\delta t_{INS_{ship}}^{UTC}\right)$ and $\text{cov}\left(\delta t_{USBL}^{UTC}\right)$ are computed for every six dimensional combination of $\boldsymbol{\omega}_{NB_{ship}}^{B_{ship}}$ and $\mathbf{v}_{EB_{ship}}^{B_{ship}}$. The smallest calculated values of $\delta t_{INS_{ship}}^{UTC}$ and δt_{USBL}^{UTC} become the final specification on timing accuracy.

C.5.4 MBE ripples

The diagonal elements of $\text{cov}\left(\delta\mathbf{p}_{B_{UV}M,ripple}^{B_{UV}}\right)$ are considered when deriving timing specifications for the underwater vehicle sensors. The diagonal elements correspond to covariance in x , y and z in attitude compensated MBE data due to timing errors in MBE and INS. The bound for these components is dependent on the altitude and is specified in Section 9.3:

$$\sigma\left(\delta\mathbf{p}_{B_{UV}M,ripple}^{B_{UV}}\right) = \sqrt{\text{diag}\left(\text{cov}\left(\delta\mathbf{p}_{B_{UV}M,ripple}^{B_{UV}}\right)\right)} < \begin{bmatrix} x_{ripple_spec} \\ y_{ripple_spec} \\ z_{ripple_spec} \end{bmatrix} \quad (108)$$

The square root sign means element-wise square root of each element in the vector.

Equal contribution to $\text{diag}\left(\text{cov}\left(\delta\mathbf{p}_{B_{UV}M,ripple}^{B_{UV}}\right)\right)$ from the terms, $\mathbf{v}_3\mathbf{v}_3^T \text{cov}\left(\delta t_{MBE}^{UV}\right)$ and $\mathbf{v}_3\mathbf{v}_3^T \text{cov}\left(\delta t_{INS_{UV}}^{UV}\right)$ is required. That means that MBE and UV INS timing errors contribute equally to $\delta\mathbf{p}_{B_{UV}M,ripple}^{B_{UV}} \cdot \text{cov}\left(\delta\mathbf{p}_{B_{UV}M,ripple}^{B_{UV}}\right)$ and values for $\text{cov}\left(\delta t_{MBE}^{UV}\right)$ and $\text{cov}\left(\delta t_{INS_{UV}}^{UV}\right)$ are computed for every six dimensional combination of $\boldsymbol{\omega}_{NB_{UV}}^{B_{UV}}$. The smallest calculated values of the timing errors become the final specification on timing accuracy.

Results for the ROV and AUV underwater survey system cases are presented in Section 9.3.

D LARGE SURVEY VESSEL EXAMPLE

D.1 Description



Figure 12.5 M/V Edda Fonn

D.2 Vessel coordinates

In Table 12.3 the vessel coordinates of the main sensors are listed. The Edda Fonn reference point is near the vessel centre of gravity. The sign convention is as follows:

- positive x: forward
- positive y: starboard
- positive z: down

	Coordinates		
	x (m)	y (m)	z (m)
Center of gravity	0	0	0
Metacenter			
Racal UKOOA GPS1	6.3880	5.511	-24.193
Starfix HP GPS2	6.380	5.511	-24.193
Starfix HP GPS2	3.386	5.502	-24.185
Ashtec GPS1	3.889	5.504	-24.135
Ashtec GPS2	5.893	5.513	-24.100
iXSea Octans motion sensor	-0.80	2.68	0.77
Kongsberg Maritime HiPAP starboard	5.965	7.126	10.297
Kongsberg Maritime HiPAP port	5.977	-7.144	10.284
Reson 8125 MBE	-1.918	2.484	9.822

Table 12.3 M/V Edda Fonn coordinates

D.3 Dynamics

Dynamic data on a large survey vessel is required to calculate timing accuracy requirements. In Table 12.4 M/V Edda Fonn example data is listed. The data come from (9). The ship velocity data is taken from normal operation specifications. The ship angular rate was obtained by derivation of attitude data. Since numerical derivation can introduce noise, the maximum value is a 99.9% value.

Data type	Maximum value
Ship velocity	
$v_{EB_{meta,ship},x}^{B_{ship}}$	2.5 m/s
$v_{EB_{meta,ship},y}^{B_{ship}}$	0 m/s
$v_{EB_{meta,ship},z}^{B_{ship}}$	0 m/s
Ship angular rate	
$\omega_{IB_{ship},x}^{B_{ship}}$	3.0°/s
$\omega_{IB_{ship},y}^{B_{ship}}$	3.0°/s
$\omega_{IB_{ship},z}^{B_{ship}}$	1.5°/s

Table 12.4 Large survey vessel example dynamics

D.4 Effect of timing errors

Error source	Motion	Velocity error vector	Timing error	Error magnitude
Ship forward speed	Forward velocity	$\mathbf{v}_{EB_{ship}}^{B_{ship}}$	δt_{MBE}	2.5 m/s
Ship angular rate and lever arm between GPS and metacenter	Roll	$\left(\text{Pr}_x \boldsymbol{\omega}_{NB_{ship}}^{B_{ship}} \right) \times \mathbf{p}_{B_{ship}B_{GPS}}^{B_{ship}}$	δt_{MBE}	1.3 m/s
	Pitch	$\left(\text{Pr}_y \boldsymbol{\omega}_{NB_{ship}}^{B_{ship}} \right) \times \mathbf{p}_{B_{ship}B_{GPS}}^{B_{ship}}$	δt_{MBE}	1.3 m/s
	Yaw	$\left(\text{Pr}_z \boldsymbol{\omega}_{NB_{ship}}^{B_{ship}} \right) \times \mathbf{p}_{B_{ship}B_{GPS}}^{B_{ship}}$	δt_{MBE}	0.22 m/s
Ship angular rate and lever arm between GPS and MBE	Roll	$\left(\text{Pr}_x \boldsymbol{\omega}_{NB_{ship}}^{B_{ship}} \right) \times \mathbf{p}_{B_{GPS}B_{MBE}}^{B_{ship}}$	$\delta t_{MBE} - \delta t_{INS}$	1.8 m/s
	Pitch	$\left(\text{Pr}_y \boldsymbol{\omega}_{NB_{ship}}^{B_{ship}} \right) \times \mathbf{p}_{B_{GPS}B_{MBE}}^{B_{ship}}$	$\delta t_{MBE} - \delta t_{INS}$	1.8 m/s
	Yaw	$\left(\text{Pr}_z \boldsymbol{\omega}_{NB_{ship}}^{B_{ship}} \right) \times \mathbf{p}_{B_{GPS}B_{MBE}}^{B_{ship}}$	$\delta t_{MBE} - \delta t_{INS}$	0.23 m/s
Ship angular rate and MBE beam	Roll	$\left(\text{Pr}_x \boldsymbol{\omega}_{NB_{ship}}^{B_{ship}} \right) \times \mathbf{p}_{B_{MBE}M}^{B_{ship}}$	$\delta t_{MBE} - \delta t_{INS}$	31 m/s
	Pitch	$\left(\text{Pr}_y \boldsymbol{\omega}_{NB_{ship}}^{B_{ship}} \right) \times \mathbf{p}_{B_{MBE}M}^{B_{ship}}$	$\delta t_{MBE} - \delta t_{INS}$	16 m/s
	Yaw	$\left(\text{Pr}_z \boldsymbol{\omega}_{NB_{ship}}^{B_{ship}} \right) \times \mathbf{p}_{B_{MBE}M}^{B_{ship}}$	$\delta t_{MBE} - \delta t_{INS}$	1.4 m/s

Table 12.5 Effect of timing errors for M/V Edda Fonn. The error magnitude is calculated using the vessel coordinates in Section D.2 and the error dynamics in Section D.3. Water depth is 300 m.

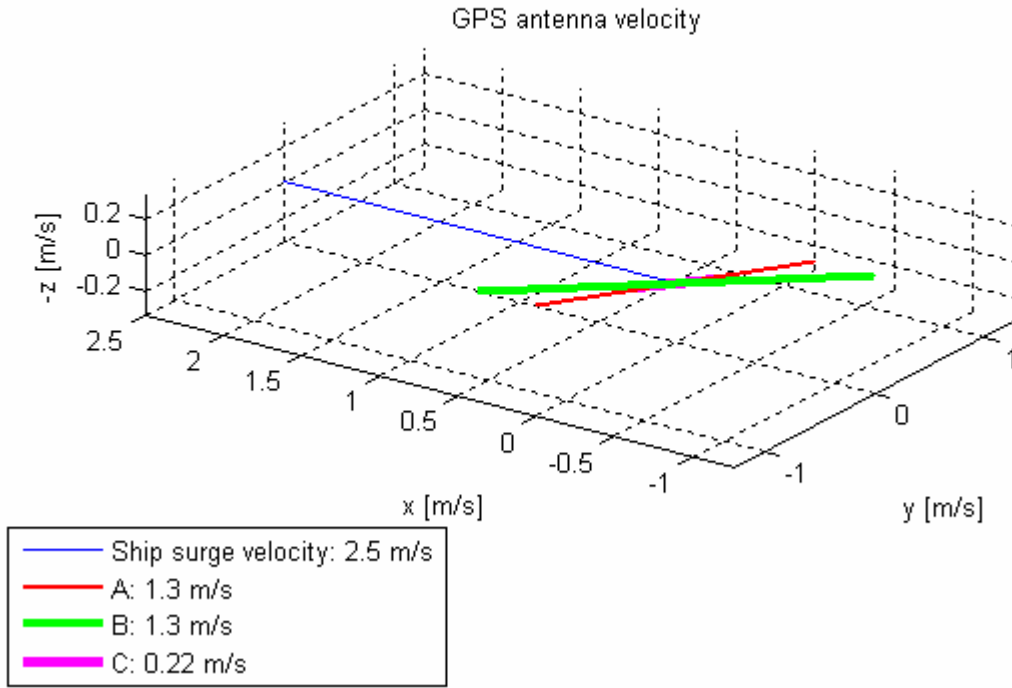


Figure 12.6 Sensitivity to MBE timing error because of ship GPS antenna velocity. Sensitivity is in ship reference frame in m/s. Multiply by timing error in s to get positioning error in m. $A = \left| \left(\text{Pr}_x \boldsymbol{\omega}_{NB_{ship}}^{B_{ship}} \right) \times \mathbf{p}_{B_{ship}B_{GPS}}^{B_{GPS}} \right|$, $B = \left| \left(\text{Pr}_y \boldsymbol{\omega}_{NB_{ship}}^{B_{ship}} \right) \times \mathbf{p}_{B_{ship}B_{GPS}}^{B_{GPS}} \right|$, and $C = \left| \left(\text{Pr}_z \boldsymbol{\omega}_{NB_{ship}}^{B_{ship}} \right) \times \mathbf{p}_{B_{ship}B_{GPS}}^{B_{GPS}} \right|$

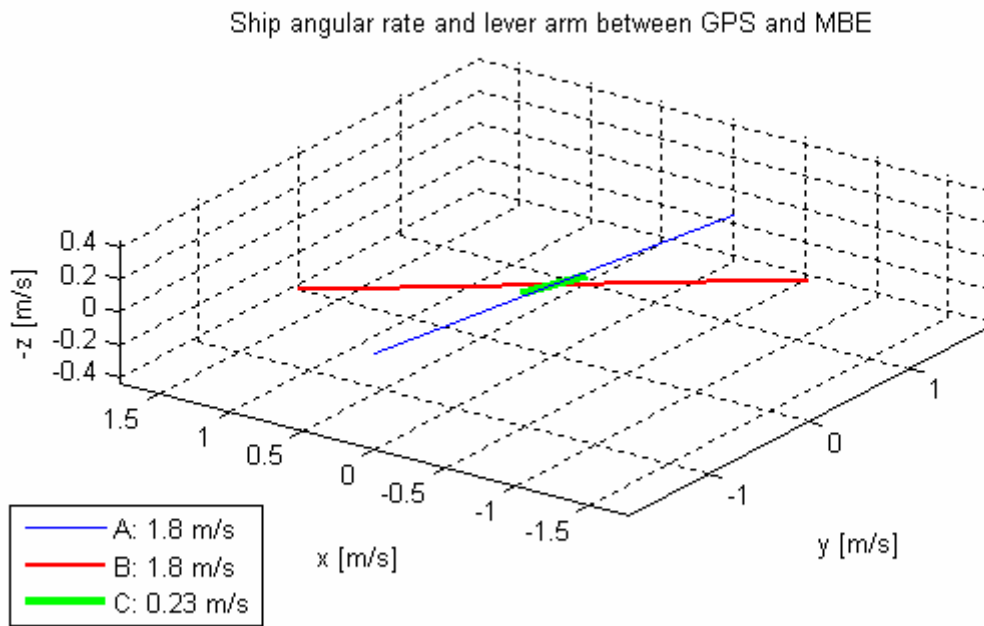


Figure 12.7 Sensitivity to MBE and INS timing errors because of ship angular rate and lever arm between GPS and MBE. Sensitivity is in ship reference frame in m/s. Multiply by timing error in s to get positioning error in m.

$$A = \left| \left(\text{Pr}_x \boldsymbol{\omega}_{NB_{ship}}^{B_{ship}} \right) \times \mathbf{p}_{B_{GPS}B_{MBE}}^{B_{ship}} \right|, \quad B = \left| \left(\text{Pr}_y \boldsymbol{\omega}_{NB_{ship}}^{B_{ship}} \right) \times \mathbf{p}_{B_{GPS}B_{MBE}}^{B_{ship}} \right|, \quad \text{and}$$

$$B = \left| \left(\text{Pr}_z \boldsymbol{\omega}_{NB_{ship}}^{B_{ship}} \right) \times \mathbf{p}_{B_{GPS}B_{MBE}}^{B_{ship}} \right|.$$

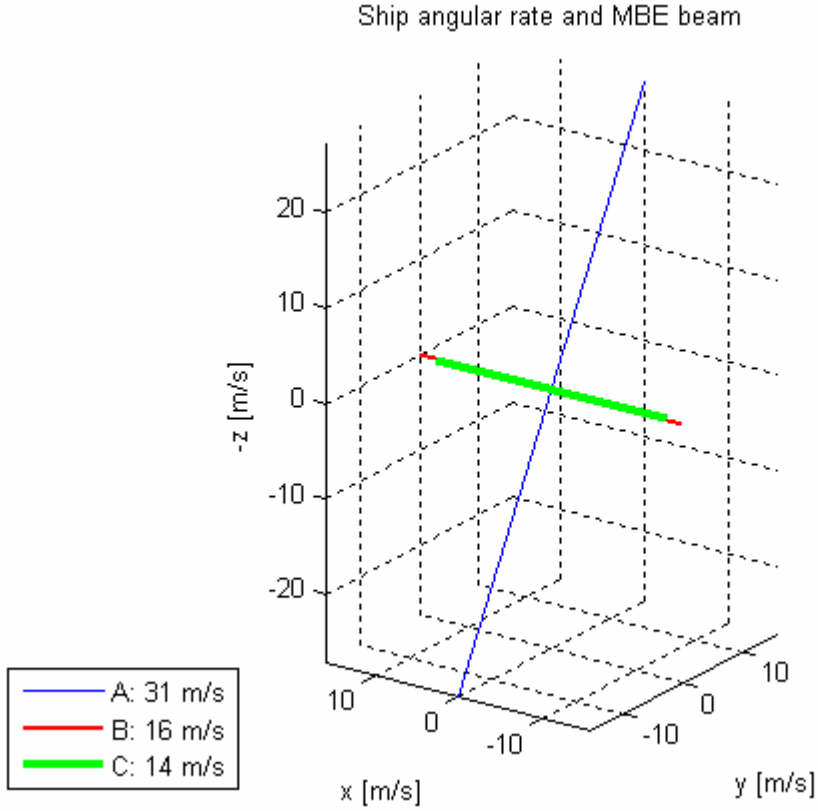


Figure 12.8 Sensitivity to MBE and INS timing errors because of ship angular rate and MBE beam. Sensitivity is in ship reference frame in m/s. Multiply by timing error in s to get positioning error in m. The figure shows the sensitivity for a 1000 m long MBE beam 60° out of the vertical. This explains the vertical component.

$$A = \left| \left(\text{Pr}_x \boldsymbol{\omega}_{NB_{ship}}^{B_{ship}} \right) \times \mathbf{p}_{B_{MBEM}}^{B_{ship}} \right|, \quad B = \left| \left(\text{Pr}_y \boldsymbol{\omega}_{NB_{ship}}^{B_{ship}} \right) \times \mathbf{p}_{B_{MBEM}}^{B_{ship}} \right|, \quad \text{and}$$

$$C = \left| \left(\text{Pr}_z \boldsymbol{\omega}_{NB_{ship}}^{B_{ship}} \right) \times \mathbf{p}_{B_{MBEM}}^{B_{ship}} \right|$$

E SMALL SURVEY VESSEL EXAMPLE

E.1 Description



Figure 12.9 S/L Sjøtroll

Some specifications for S/L Sjøtroll:

Built	1998
Hull	Fiberglass
Survey speed	8 knots
Weight	12 tons
Length	34'
Draught	1.2 m
Survey depth interval	1-1000 m

E.2 Vessel coordinates

In Table 12.6 the vessel coordinates of the main sensors are listed. The Sjøtroll reference point is near the vessel centre of gravity. The sign convention is as follows:

- positive x: forward
- positive y: starboard
- positive z: down

	Coordinates		
	x (m)	y (m)	z (m)
Center of gravity	0	0	0
Metacenter			
Kongsberg Maritime EM 3000D starboard transducer	-0.001	0.504	0.592
Kongsberg Maritime EM 3000D port transducer	0.005	-0.512	0.588
Kongsberg Maritime EM 1002 transducer	-0.728	-0.010	1.202
Kongsberg Seatex Seapath (MRU) reference point	0.484	1.056	-0.640
GPS antenna	-0.533	-0.048	-3.876

Table 12.6 S/L Sjøtroll coordinates

E.3 Dynamics

Dynamic data on a small survey vessel is required to calculate timing accuracy requirements. In Table 12.7 the S/L Sjøtroll example data is listed. The data come from (9). The ship velocity data is taken from normal operation specifications. The ship angular rate was obtained by derivation of attitude data. Since numerical derivation can introduce noise, the maximum value is a 99.9% value.

Data type	Maximum value
Ship velocity	
$v_{EB_{meta,ship},x}^{B_{ship}}$	4.0 m/s
$v_{EB_{meta,ship},y}^{B_{ship}}$	0 m/s
$v_{EB_{meta,ship},z}^{B_{ship}}$	0 m/s
Ship angular rate	
$\omega_{IB_{ship},x}^{B_{ship}}$	12.0°/s
$\omega_{IB_{ship},y}^{B_{ship}}$	9.0°/s
$\omega_{IB_{ship},z}^{B_{ship}}$	8°/s

Table 12.7 Small survey vessel example data

E.4 Effect of timing errors

Error source	Motion	Velocity error vector	Timing error	Error magnitude
Ship forward speed	Forward velocity	$\mathbf{v}_{EB_{ship}}^{B_{ship}}$	δt_{MBE}	4 m/s
Ship angular rate and lever arm between GPS and metacenter	Roll	$\left(\text{Pr}_x \boldsymbol{\omega}_{NB_{ship}}^{B_{ship}} \right) \times \mathbf{p}_{B_{ship}B_{GPS}}^{B_{ship}}$	δt_{MBE}	0.81 m/s
	Pitch	$\left(\text{Pr}_y \boldsymbol{\omega}_{NB_{ship}}^{B_{ship}} \right) \times \mathbf{p}_{B_{ship}B_{GPS}}^{B_{ship}}$	δt_{MBE}	0.61 m/s
	Yaw	$\left(\text{Pr}_z \boldsymbol{\omega}_{NB_{ship}}^{B_{ship}} \right) \times \mathbf{p}_{B_{ship}B_{GPS}}^{B_{ship}}$	δt_{MBE}	0.075 m/s
Ship angular rate and lever arm between GPS and MBE	Roll	$\left(\text{Pr}_x \boldsymbol{\omega}_{NB_{ship}}^{B_{ship}} \right) \times \mathbf{p}_{B_{GPS}B_{MBE}}^{B_{ship}}$	$\delta t_{MBE} - \delta t_{INS}$	1.1 m/s
	Pitch	$\left(\text{Pr}_y \boldsymbol{\omega}_{NB_{ship}}^{B_{ship}} \right) \times \mathbf{p}_{B_{GPS}B_{MBE}}^{B_{ship}}$	$\delta t_{MBE} - \delta t_{INS}$	0.8 m/s
	Yaw	$\left(\text{Pr}_z \boldsymbol{\omega}_{NB_{ship}}^{B_{ship}} \right) \times \mathbf{p}_{B_{GPS}B_{MBE}}^{B_{ship}}$	$\delta t_{MBE} - \delta t_{INS}$	0.028 m/s
Ship angular rate and MBE beam	Roll	$\left(\text{Pr}_x \boldsymbol{\omega}_{NB_{ship}}^{B_{ship}} \right) \times \mathbf{p}_{B_{MBE}M}^{B_{ship}}$	$\delta t_{MBE} - \delta t_{INS}$	42 m/s
	Pitch	$\left(\text{Pr}_y \boldsymbol{\omega}_{NB_{ship}}^{B_{ship}} \right) \times \mathbf{p}_{B_{MBE}M}^{B_{ship}}$	$\delta t_{MBE} - \delta t_{INS}$	16 m/s
	Yaw	$\left(\text{Pr}_z \boldsymbol{\omega}_{NB_{ship}}^{B_{ship}} \right) \times \mathbf{p}_{B_{MBE}M}^{B_{ship}}$	$\delta t_{MBE} - \delta t_{INS}$	2.4 m/s

Table 12.8 Effect of timing errors for Sjøtroll. The error magnitude is calculated using the vessel coordinates in Section E.2 and the error dynamics in Section E.3. Water depth is 100 m.

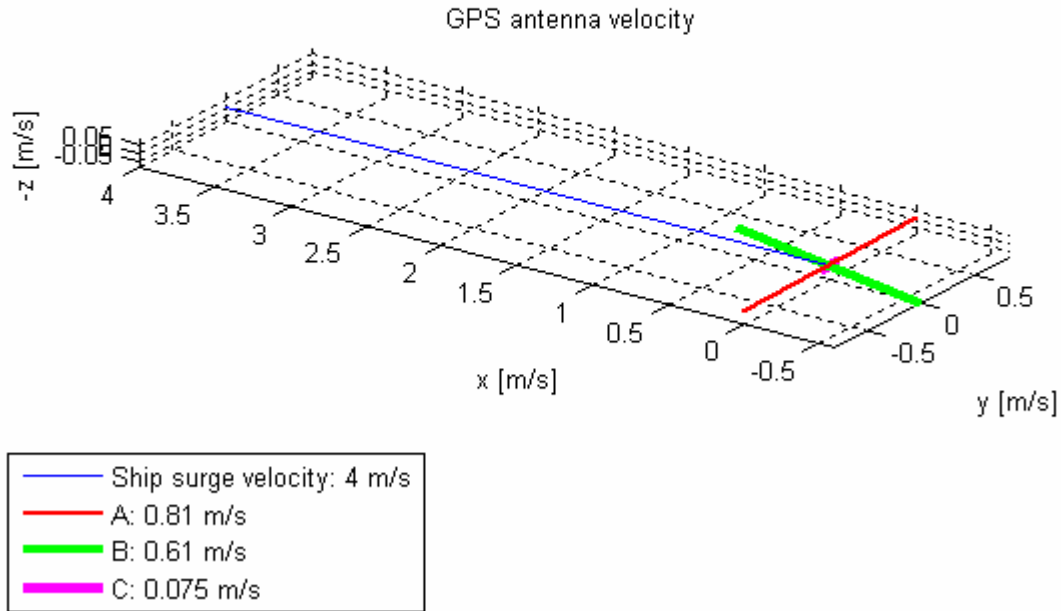


Figure 12.10 Sensitivity to MBE timing error because of ship GPS antenna velocity. Sensitivity is in ship reference frame in m/s. Multiply by timing error in s to get positioning error in m. $A = \left| \left(\text{Pr}_x \boldsymbol{\omega}_{NB_{ship}}^{B_{ship}} \right) \times \mathbf{p}_{B_{ship}B_{GPS}}^{B_{GPS}} \right|$, $B = \left| \left(\text{Pr}_y \boldsymbol{\omega}_{NB_{ship}}^{B_{ship}} \right) \times \mathbf{p}_{B_{ship}B_{GPS}}^{B_{GPS}} \right|$, and $C = \left| \left(\text{Pr}_z \boldsymbol{\omega}_{NB_{ship}}^{B_{ship}} \right) \times \mathbf{p}_{B_{ship}B_{GPS}}^{B_{GPS}} \right|$

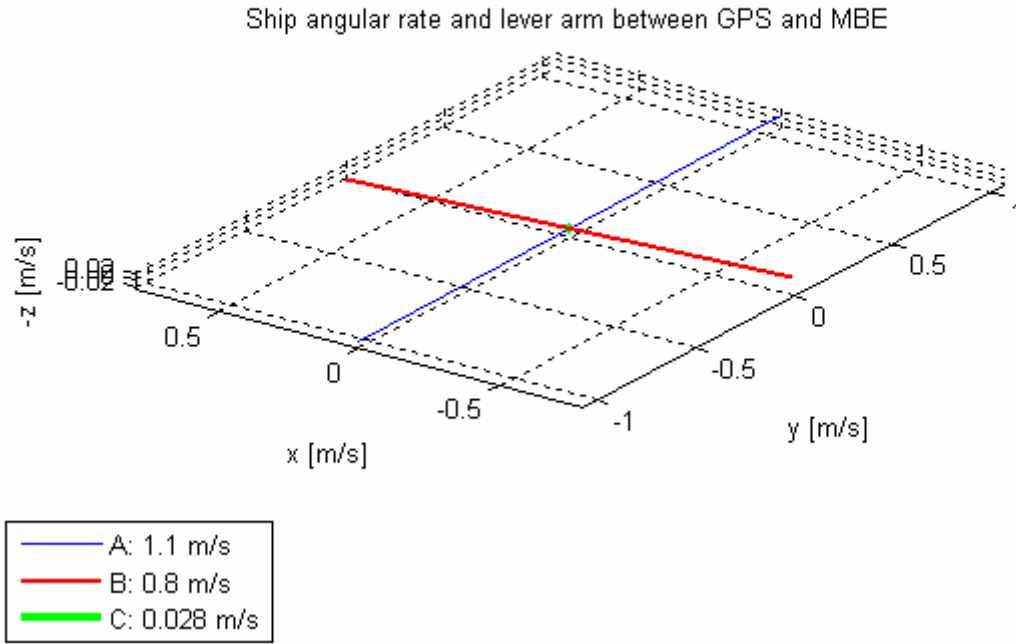


Figure 12.11 Sensitivity to MBE and INS timing errors because of ship angular rate and lever arm between GPS and MBE. Sensitivity is in ship reference frame in m/s. Multiply by timing error in s to get positioning error in m.

$$A = \left| \left(\text{Pr}_x \boldsymbol{\omega}_{NB_{ship}}^{B_{ship}} \right) \times \mathbf{p}_{B_{GPS}B_{MBE}}^{B_{ship}} \right|, \quad B = \left| \left(\text{Pr}_y \boldsymbol{\omega}_{NB_{ship}}^{B_{ship}} \right) \times \mathbf{p}_{B_{GPS}B_{MBE}}^{B_{ship}} \right|, \quad \text{and}$$

$$B = \left| \left(\text{Pr}_z \boldsymbol{\omega}_{NB_{ship}}^{B_{ship}} \right) \times \mathbf{p}_{B_{GPS}B_{MBE}}^{B_{ship}} \right|.$$

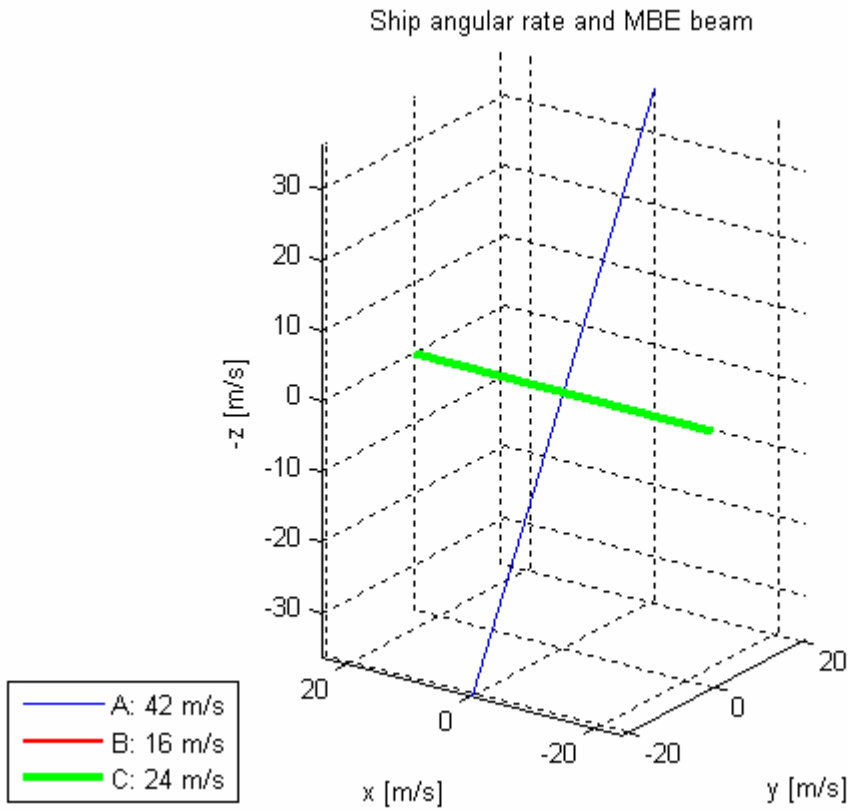


Figure 12.12 Sensitivity to MBE and INS timing errors because of ship angular rate and MBE beam. Sensitivity is in ship reference frame in m/s. Multiply by timing error in s to get positioning error in m. The figure shows the sensitivity for a 1000 m long MBE beam 60° out of the vertical. This explains the vertical component.

$$A = \left| \left(\text{Pr}_x \boldsymbol{\omega}_{NB_{ship}}^{B_{ship}} \right) \times \mathbf{p}_{B_{MBEM}}^{B_{ship}} \right|, \quad B = \left| \left(\text{Pr}_y \boldsymbol{\omega}_{NB_{ship}}^{B_{ship}} \right) \times \mathbf{p}_{B_{MBEM}}^{B_{ship}} \right|, \quad \text{and}$$

$$C = \left| \left(\text{Pr}_z \boldsymbol{\omega}_{NB_{ship}}^{B_{ship}} \right) \times \mathbf{p}_{B_{MBEM}}^{B_{ship}} \right|$$

F AUV EXAMPLE

F.1 Description

The HUGIN 3000 survey AUV is produced by Kongsberg Maritime and currently operated by C&C Technologies, Fugro and Geoconsult. Figure 12.13 shows a mechanical drawing of the vehicle.

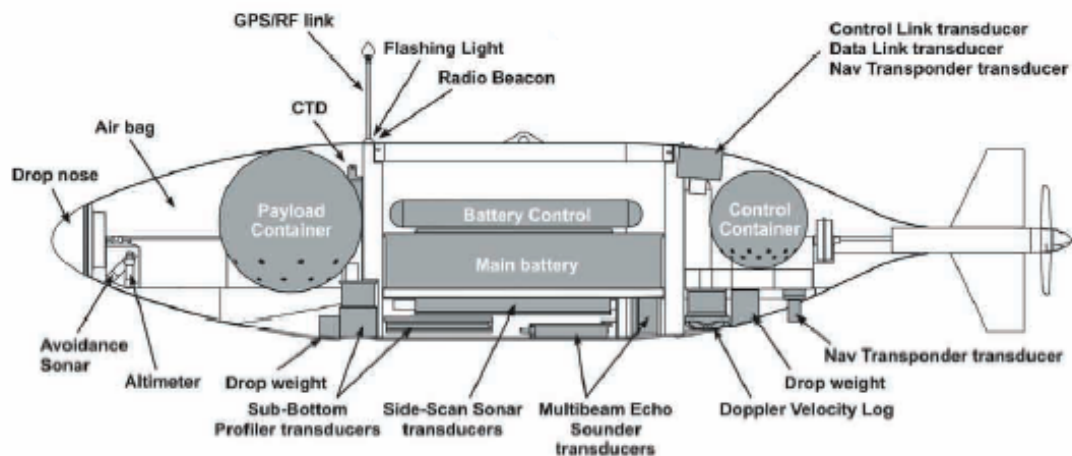


Figure 12.13 Mechanical outline of HUGIN 3000

HUGIN 3000 vehicle specifications:

Depth rating	3000 m
Length	5.35 m
Maximum diameter	1 m
Weight in air	1400 kg
Weight in water	Neutral
Nominal speed	4 knots
Vehicle endurance	50 – 60 hours, depending on speed and payload configuration

F.2 Vessel coordinates

In Table 12.9, the main HUGIN 3000-GC sensors and their vessel coordinates are listed. The arms are between the sensor reference points and the HUGIN 3000 reference point (B_{UV}). The HUGIN 3000 reference point is defined to be the tip of the nose cone. The sign convention is as follows:

- positive x: forward
- positive y: starboard
- positive z: down

	Coordinates		
	x (m)	y (m)	z (m)
Center of gravity	-2.202	0	0.05
Metacenter	-2.202	0	0
Kongsberg Maritime EM 2000 transmitter	-2.592	0.0	0.488
Kongsberg Maritime EM 2000 receiver	-2.910	0.0	0.490
Edgetech side scan sonar starboard (Not applicable in this document)	-2.242	0.363	0.362
SSS port	-2.242	-0.363	0.362
Edgetech sub bottom profiler transmitter (Not applicable in this document)	-1.570	0.0	0.486
SBP hydrophones	-1.978	0.0	0.446
iXSea IMU 90 inertial measurement unit	-3.678	0.123	-0.107
RDI WHN-300 Doppler velocity log	-3.355	0.0	0.448
Digiquartz pressure sensor	-3.485	-0.245	0.049
Kongsberg Maritime HiPAP transponder TP 324	-3.445	-0.215	-0.471
GPS receiver (Not applicable in this document)	-1.571	-0.022	-1.008

Table 12.9 HUGIN 3000 sensor coordinates

F.3 Deep-water dynamics

The AUV example data is taken from a HUGIN 3000 survey in the Gulf of Mexico March 27th 2001. The data is from a deep-water area with rough terrain. In Figure 12.14 a depth profile typical of the mission is shown. In Figure 12.15 AUV attitude data from the same profile is shown. At one instance, the pitch angle exceeds 40° as the AUV follows the seafloor at constant altitude. The example data includes four turns in heading. The roll angle is clearly affected by a turn.

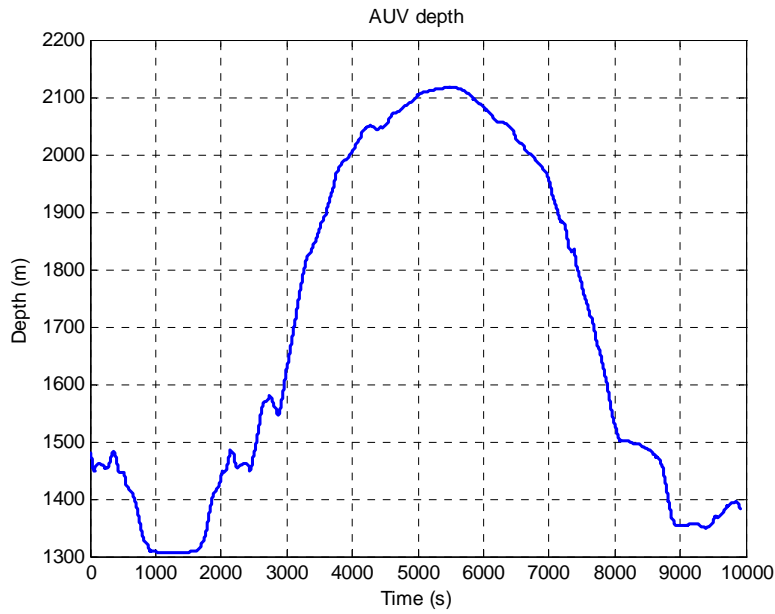


Figure 12.14 Depth profile from a HUGIN 3000 deep-water mission in rough terrain.

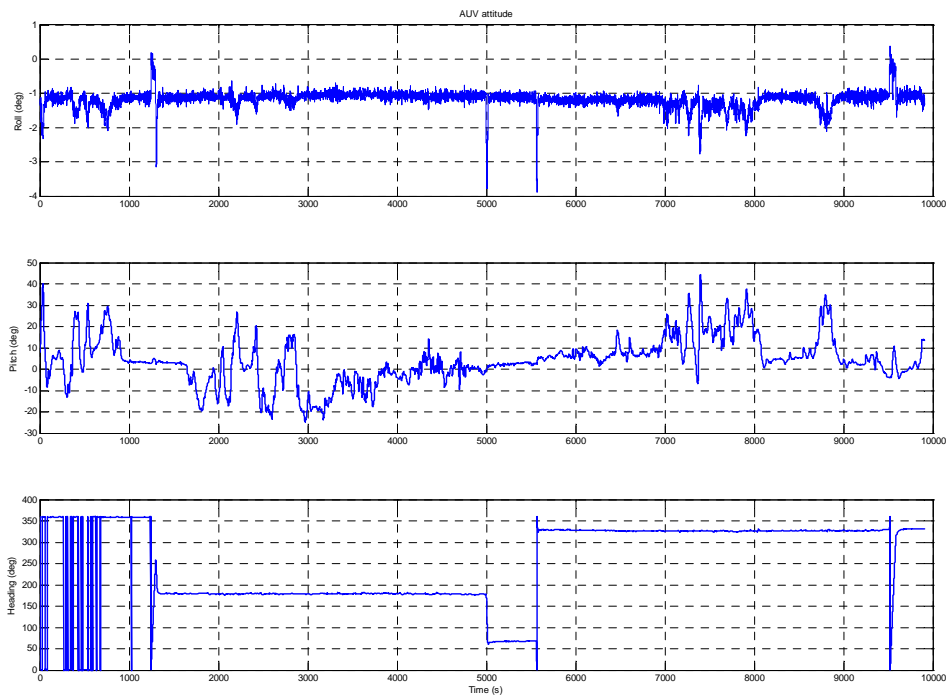


Figure 12.15 HUGIN 3000 attitude data from the same deep-water mission in rugged terrain as shown in Figure 12.14.

Dynamic data on an AUV is required to calculate timing accuracy requirements. In Table 12.10 the AUV example data is listed.

Data type	Maximum value
AUV velocity	
$v_{EB_{meta,UV},x}^{B_{UV}}$	2.1 m/s
$v_{EB_{meta,UV},y}^{B_{UV}}$	0.6 m/s
$v_{EB_{meta,UV},z}^{B_{UV}}$	0.4 m/s
AUV angular rate	
$\omega_{IB_{UV},x}^{B_{UV}}$	1.4°/s
$\omega_{IB_{UV},y}^{B_{UV}}$	3.0°/s
$\omega_{IB_{UV},z}^{B_{UV}}$	8.0°/s

Table 12.10 AUV example data

The AUV example data is based on the time series in Figure 12.16 and Figure 12.17. Angular rate around body y is dependent on the bottom topography. Maximum values for angular rate around x and z occur during turns. One can argue that picking maximum values from turns leads to too strict timing accuracy specifications. However, as discussed in Section 9.3.5 the goal was to arrive at timing accuracy specifications that does not compromise mapping accuracy at any time during a survey.

Maximum forward velocity in the example data is 2.1 m/s or 4 knots. After 5000 s, the propeller revolution speed is reduced, which explains the shift to a somewhat lower forward speed. Maximum values for sway speed (starboard) occur during turns. The constant positive down velocity is because HUGIN was a little negative buoyant in this mission. The negative buoyancy was compensated by a constant positive pitch angle offset. The maximum values in down velocity occur during rapid depth changes.

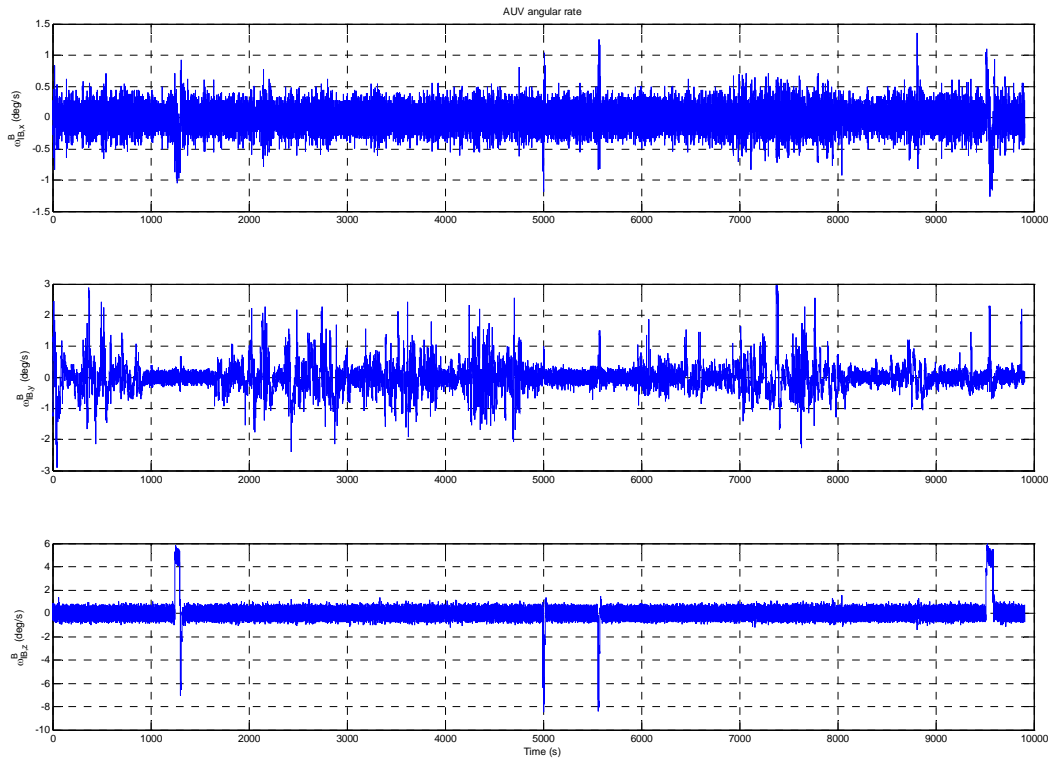


Figure 12.16 AUV Angular rate time series example

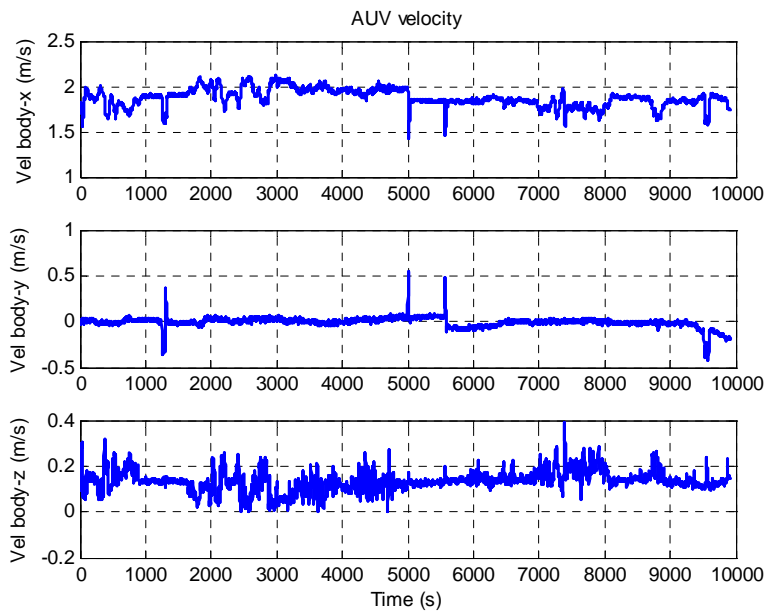


Figure 12.17 AUV velocity time series example

F.4 Effect of timing errors

Error source	Motion	Velocity error vector	Timing error	Error magnitude
Ship GPS antenna velocity	Forward ship velocity	$\mathbf{v}_{EB_{ship}}^{B_{ship}}$	δt_{USBL}^{UTC}	2.1 m/s
	Roll	$\left(\text{Pr}_x \boldsymbol{\omega}_{NB_{ship}}^{B_{ship}} \right) \times \mathbf{p}_{B_{ship}B_{GPS}}^{B_{ship}}$	δt_{USBL}^{UTC}	0.2 m/s
	Pitch	$\left(\text{Pr}_y \boldsymbol{\omega}_{NB_{ship}}^{B_{ship}} \right) \times \mathbf{p}_{B_{ship}B_{GPS}}^{B_{ship}}$		0.2 m/s
	Yaw	$\left(\text{Pr}_z \boldsymbol{\omega}_{NB_{ship}}^{B_{ship}} \right) \times \mathbf{p}_{B_{ship}B_{GPS}}^{B_{ship}}$		0.014 m/s
Ship angular rate and lever arm between GPS and USBL	Roll	$\left(\text{Pr}_x \boldsymbol{\omega}_{NB_{ship}}^{B_{ship}} \right) \times \mathbf{p}_{B_{GPS}B_{USBL}}^{B_{ship}}$	$\delta t_{USBL}^{UTC} - \delta t_{INS_{ship}}^{UTC}$	0.27 m/s
	Pitch	$\left(\text{Pr}_y \boldsymbol{\omega}_{NB_{ship}}^{B_{ship}} \right) \times \mathbf{p}_{B_{GPS}B_{USBL}}^{B_{ship}}$		0.27 m/s
	Yaw	$\left(\text{Pr}_z \boldsymbol{\omega}_{NB_{ship}}^{B_{ship}} \right) \times \mathbf{p}_{B_{GPS}B_{USBL}}^{B_{ship}}$		0.0052 m/s
Ship angular rate and relative USBL position	Roll	$\left(\text{Pr}_x \boldsymbol{\omega}_{NB_{ship}}^{B_{ship}} \right) \times \mathbf{p}_{B_{USBL}B_{TP}}^{B_{ship}}$	$\delta t_{USBL}^{UTC} - \delta t_{INS_{ship}}^{UTC}$	160 m/s
	Pitch	$\left(\text{Pr}_y \boldsymbol{\omega}_{NB_{ship}}^{B_{ship}} \right) \times \mathbf{p}_{B_{USBL}B_{TP}}^{B_{ship}}$		160 m/s
	Yaw	$\left(\text{Pr}_z \boldsymbol{\omega}_{NB_{ship}}^{B_{ship}} \right) \times \mathbf{p}_{B_{USBL}B_{TP}}^{B_{ship}}$		0 m/s
UV transponder velocity	Forward UV velocity	$\text{Pr}_x \mathbf{v}_{EB_{UV}}^{B_{UV}}$	$\delta t_{MBE}^{UV} - \delta t_{USBL}^{UTC} - \delta t_{UV_{clock}}$	2.1 m/s
	UV sway velocity	$\text{Pr}_y \mathbf{v}_{EB_{UV}}^{B_{UV}}$	$\delta t_{MBE}^{UV} - \delta t_{USBL}^{UTC} - \delta t_{UV_{clock}}$	0.6 m/s
	UV heave velocity	$\text{Pr}_z \mathbf{v}_{EB_{UV}}^{B_{UV}}$	$\delta t_{MBE}^{UV} - \delta t_{USBL}^{UTC} - \delta t_{UV_{clock}}$	0.4 m/s
	Roll	$\left(\text{Pr}_x \boldsymbol{\omega}_{NB_{UV}}^{B_{UV}} \right) \times \mathbf{p}_{B_{UV}B_{TP}}^{B_{UV}}$	$\delta t_{MBE}^{UV} - \delta t_{USBL}^{UTC} - \delta t_{UV_{clock}}$	0.013 m/s
	Pitch	$\left(\text{Pr}_y \boldsymbol{\omega}_{NB_{UV}}^{B_{UV}} \right) \times \mathbf{p}_{B_{UV}B_{TP}}^{B_{UV}}$		0.07 m/s
	Yaw	$\left(\text{Pr}_z \boldsymbol{\omega}_{NB_{UV}}^{B_{UV}} \right) \times \mathbf{p}_{B_{UV}B_{TP}}^{B_{UV}}$		0.18 m/s
UV angular rate and lever arm between transponder and MBE	Roll	$\left(\text{Pr}_x \boldsymbol{\omega}_{NB_{UV}}^{B_{UV}} \right) \times \mathbf{p}_{B_{TP}B_{MBE}}^{B_{UV}}$	$\delta t_{MBE}^{UV} - \delta t_{INS_{UV}}^{UV}$	0.024 m/s
	Pitch	$\left(\text{Pr}_y \boldsymbol{\omega}_{NB_{UV}}^{B_{UV}} \right) \times \mathbf{p}_{B_{TP}B_{MBE}}^{B_{UV}}$		0.34 m/s
	Yaw	$\left(\text{Pr}_z \boldsymbol{\omega}_{NB_{UV}}^{B_{UV}} \right) \times \mathbf{p}_{B_{TP}B_{MBE}}^{B_{UV}}$		0.89 m/s
UV angular rate and MBE beam	Roll	$\left(\text{Pr}_x \boldsymbol{\omega}_{NB_{UV}}^{B_{UV}} \right) \times \mathbf{p}_{B_{MBE}M}^{B_{UV}}$	$\delta t_{MBE}^{UV} - \delta t_{INS_{UV}}^{UV}$	1.5 m/s
	Pitch	$\left(\text{Pr}_y \boldsymbol{\omega}_{NB_{UV}}^{B_{UV}} \right) \times \mathbf{p}_{B_{MBE}M}^{B_{UV}}$		1.6 m/s
	Yaw	$\left(\text{Pr}_z \boldsymbol{\omega}_{NB_{UV}}^{B_{UV}} \right) \times \mathbf{p}_{B_{MBE}M}^{B_{UV}}$		7.3 m/s

Table 12.11 Effect of timing errors for an underwater survey system with a HUGIN 3000 AUV on M/V Edda Fonn. The error magnitude is calculated using the vessel coordinates in Section F.2 and the error dynamics in Section F.3. AUV depth is 3000 m and AUV altitude is 30 m.

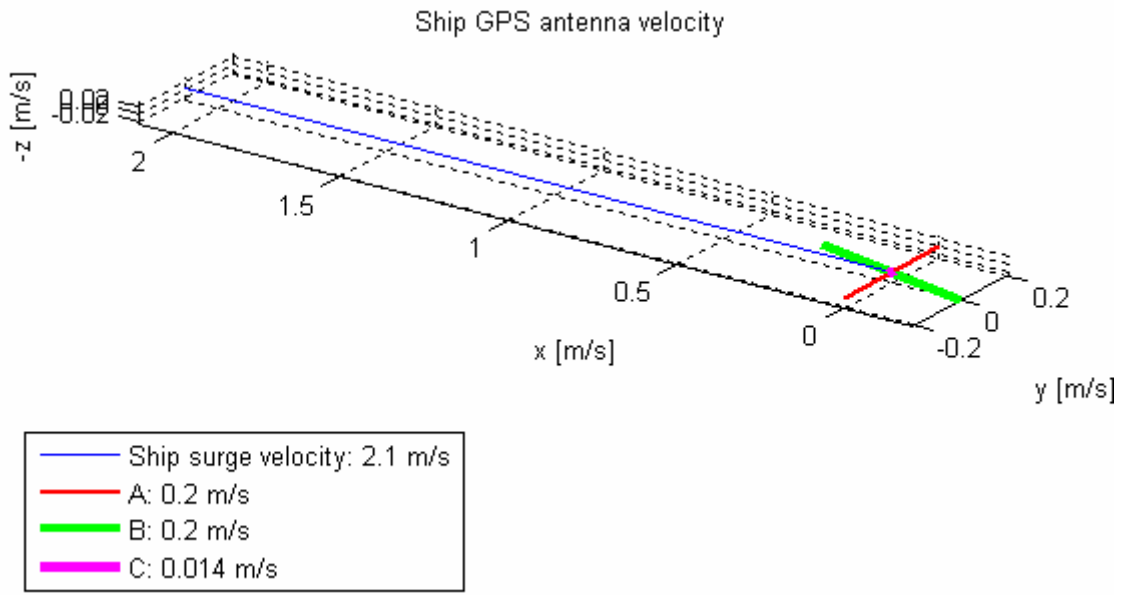


Figure 12.18 Illustration of sensitivity of the underwater vehicle transponder position error due to USBL timing error because of ship GPS antenna velocity. Sensitivity is in ship reference frame in m/s. Multiply by timing error in s to get transponder position error in m. $A = \left| \left(\text{Pr}_x \boldsymbol{\omega}_{NB_{ship}}^{B_{ship}} \right) \times \mathbf{p}_{B_{ship}B_{GPS}}^{B_{GPS}} \right|$, $B = \left| \left(\text{Pr}_y \boldsymbol{\omega}_{NB_{ship}}^{B_{ship}} \right) \times \mathbf{p}_{B_{ship}B_{GPS}}^{B_{GPS}} \right|$, and $C = \left| \left(\text{Pr}_z \boldsymbol{\omega}_{NB_{ship}}^{B_{ship}} \right) \times \mathbf{p}_{B_{ship}B_{GPS}}^{B_{GPS}} \right|$

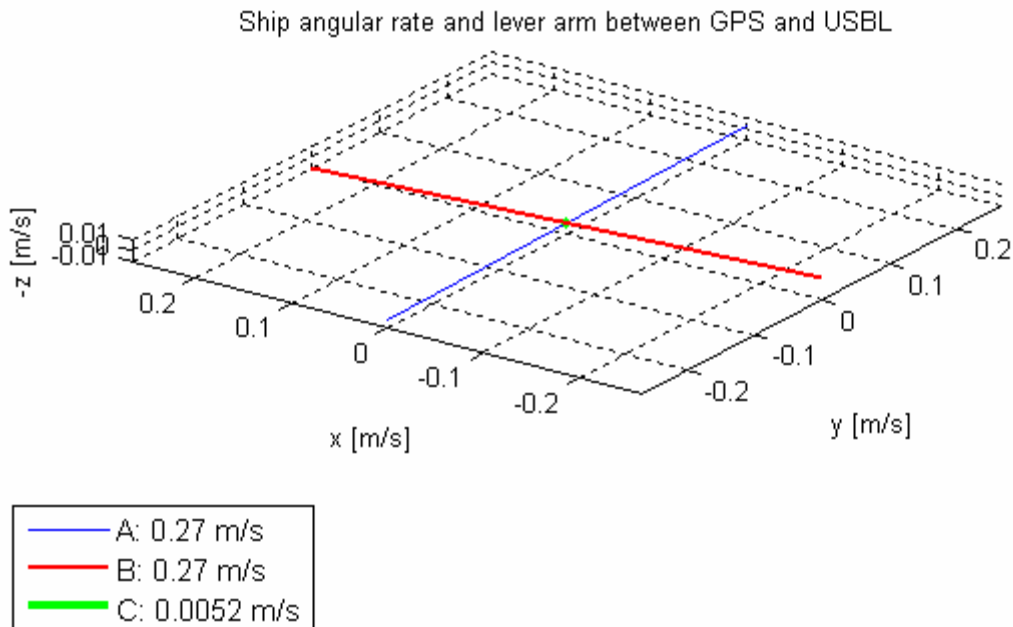


Figure 12.19 Illustration of sensitivity of the underwater vehicle transponder position error due to USBL and INS timing errors because of ship angular rate and GPS-USBL lever arm. Sensitivity is in ship reference frame in m/s. Multiply by timing error

in s to get transponder position error in m. $A = \left| \left(\text{Pr}_x \boldsymbol{\omega}_{NB_{ship}}^{B_{ship}} \right) \times \mathbf{p}_{B_{GPS}B_{USBL}}^{B_{ship}} \right|$,
 $B = \left| \left(\text{Pr}_y \boldsymbol{\omega}_{NB_{ship}}^{B_{ship}} \right) \times \mathbf{p}_{B_{GPS}B_{USBL}}^{B_{ship}} \right|$, and $C = \left| \left(\text{Pr}_z \boldsymbol{\omega}_{NB_{ship}}^{B_{ship}} \right) \times \mathbf{p}_{B_{GPS}B_{USBL}}^{B_{ship}} \right|$.

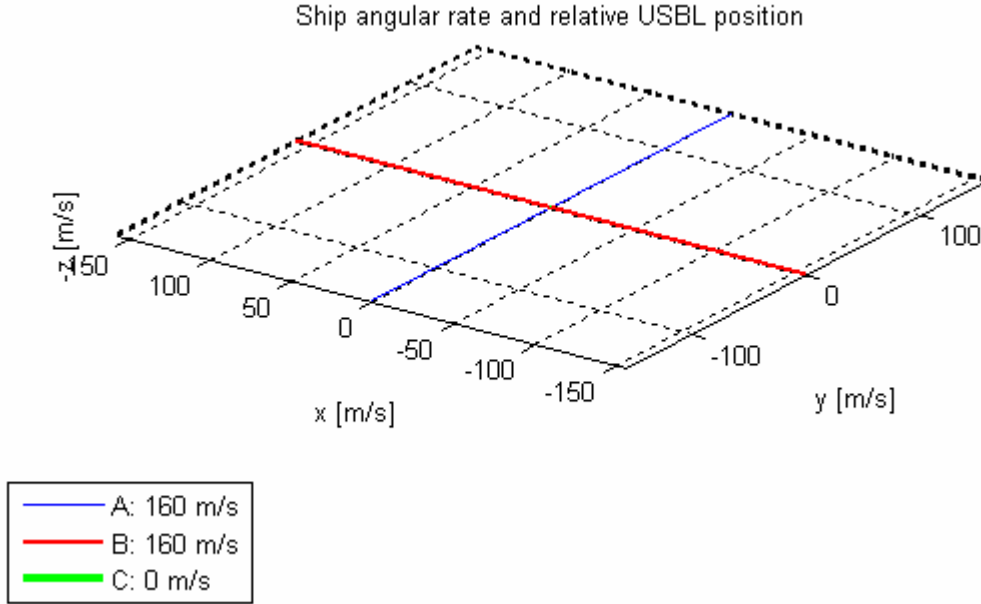


Figure 12.20 Illustration of sensitivity of the underwater vehicle transponder position error due to USBL and ship INS timing errors because of ship angular rate and relative position between surface ship and underwater vehicle. Sensitivity is in ship reference frame in m/s. Multiply by timing error in s to get transponder position error in m.

$A = \left| \left(\text{Pr}_x \boldsymbol{\omega}_{NB_{ship}}^{B_{ship}} \right) \times \mathbf{p}_{B_{USBL}B_{TP}}^{B_{ship}} \right|$, $B = \left| \left(\text{Pr}_y \boldsymbol{\omega}_{NB_{ship}}^{B_{ship}} \right) \times \mathbf{p}_{B_{USBL}B_{TP}}^{B_{ship}} \right|$, and
 $C = \left| \left(\text{Pr}_z \boldsymbol{\omega}_{NB_{ship}}^{B_{ship}} \right) \times \mathbf{p}_{B_{USBL}B_{TP}}^{B_{ship}} \right|$

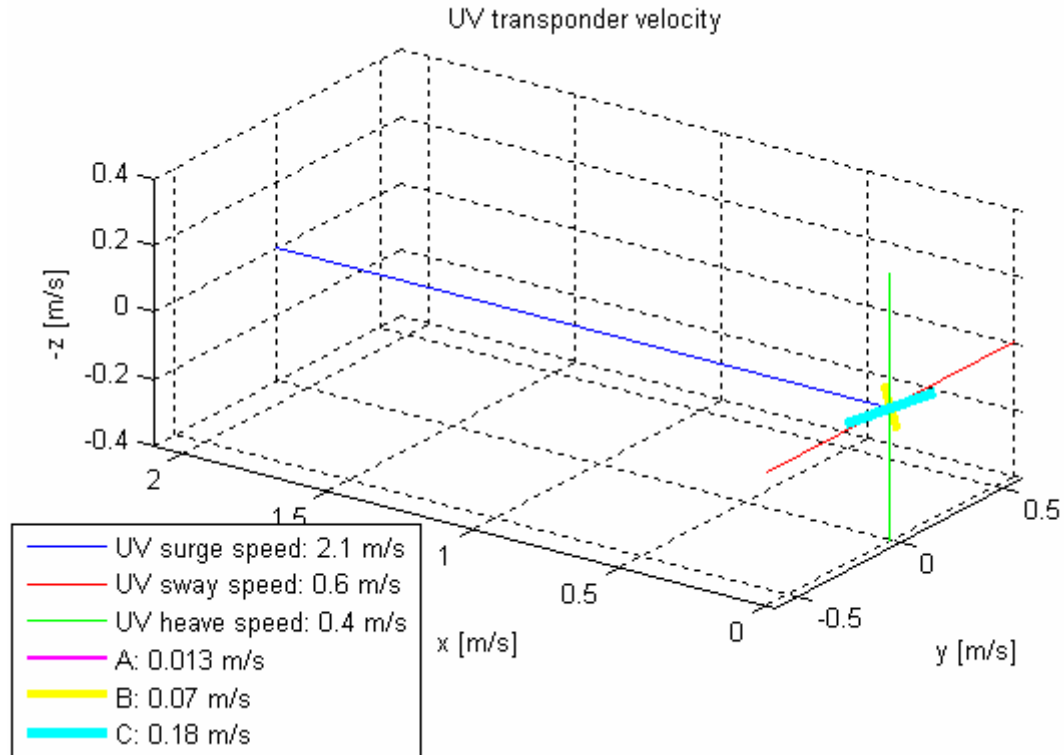


Figure 12.21 Illustration of sensitivity of MBE positioning error due to USBL, INS, and UV clock timing errors because of UV transponder velocity. Sensitivity is in underwater vehicle reference frame in m/s. Multiply by timing error in s to get positioning error in m. $A = \left| \left(\text{Pr}_x \boldsymbol{\omega}_{NB_{UV}}^{B_{UV}} \right) \times \mathbf{p}_{B_{UV}B_{TP}}^{B_{UV}} \right|$, $B = \left| \left(\text{Pr}_y \boldsymbol{\omega}_{NB_{UV}}^{B_{UV}} \right) \times \mathbf{p}_{B_{UV}B_{TP}}^{B_{UV}} \right|$, and $C = \left| \left(\text{Pr}_z \boldsymbol{\omega}_{NB_{UV}}^{B_{UV}} \right) \times \mathbf{p}_{B_{UV}B_{TP}}^{B_{UV}} \right|$.

UV angular rate and lever arm between transponder and MBE

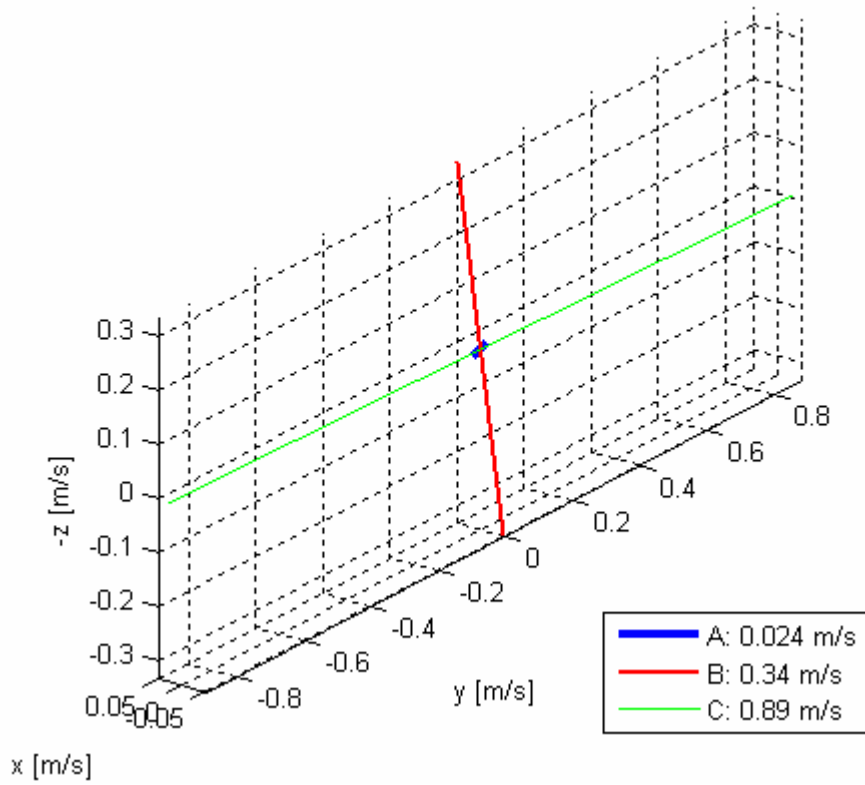


Figure 12.22 Illustration of sensitivity of MBE positioning error due to MBE and UV INS timing errors because of UV angular rate and lever arm between transponder and MBE. Sensitivity is in underwater vehicle reference frame in m/s. Multiply by timing error in s to get positioning error in m. The figure shows the sensitivity for a 600 m MBE beam 60° out of the vertical (Depth 300 m). This explains the vertical component. $A = \left| \left(\text{Pr}_x \boldsymbol{\omega}_{NB_{UV}}^{B_{UV}} \right) \times \mathbf{p}_{B_{TP}B_{MBE}}^{B_{UV}} \right|$, $B = \left| \left(\text{Pr}_y \boldsymbol{\omega}_{NB_{UV}}^{B_{UV}} \right) \times \mathbf{p}_{B_{TP}B_{MBE}}^{B_{UV}} \right|$, and $C = \left| \left(\text{Pr}_z \boldsymbol{\omega}_{NB_{UV}}^{B_{UV}} \right) \times \mathbf{p}_{B_{TP}B_{MBE}}^{B_{UV}} \right|$.

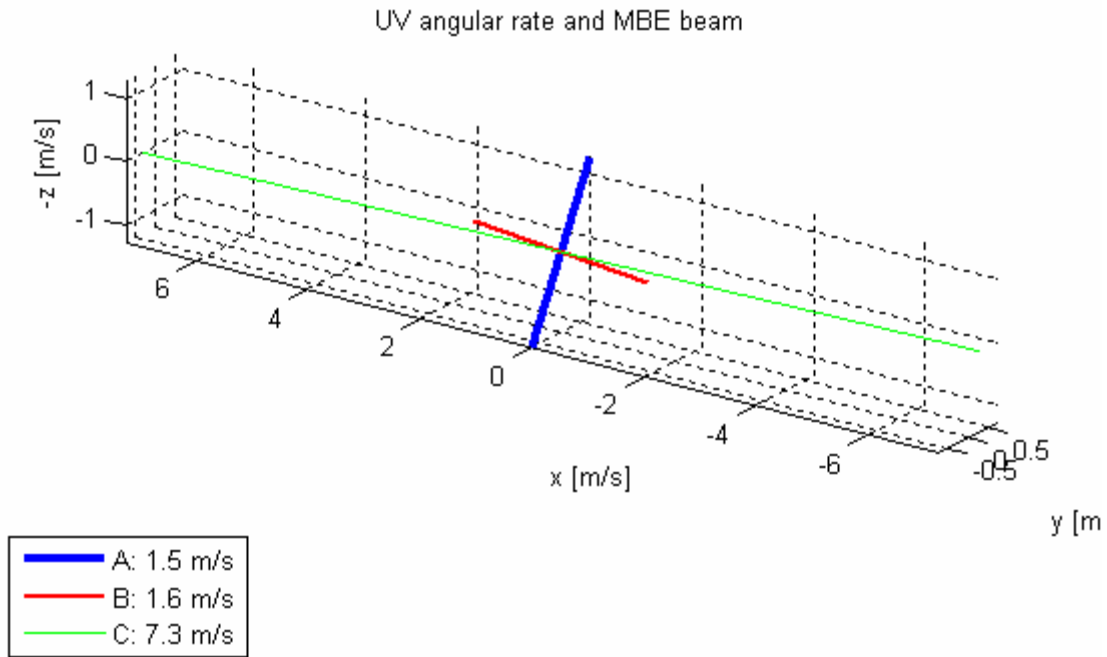


Figure 12.23 Illustration of sensitivity of MBE positioning error due to MBE and UV INS timing errors because of UV angular rate and MBE beam. Sensitivity is in underwater vehicle reference frame in m/s. Multiply by timing error in s to get positioning error in m. The figure shows the sensitivity for a 600 m MBE beam 60° out of the vertical (Depth 300 m). This explains the vertical component. $A = \left| \left(\text{Pr}_x \boldsymbol{\omega}_{NB_{UV}}^{B_{UV}} \right) \times \mathbf{p}_{B_{MBE}M}^{B_{UV}} \right|$, $B = \left| \left(\text{Pr}_y \boldsymbol{\omega}_{NB_{UV}}^{B_{UV}} \right) \times \mathbf{p}_{B_{MBE}M}^{B_{UV}} \right|$, and $C = \left| \left(\text{Pr}_z \boldsymbol{\omega}_{NB_{UV}}^{B_{UV}} \right) \times \mathbf{p}_{B_{MBE}M}^{B_{UV}} \right|$

G ROV EXAMPLE

G.1 Description



Figure 12.24 HiROV 3000 from Deep Ocean inspecting a pipeline. The DVL can be seen on the aft of the ROV.

G.2 Vessel coordinates

In Table 12.12, the main HiROV sensors and their coordinates are listed. The coordinates define the sensor reference points in the ROV reference frame (B_{UV}). The HiROV reference point is defined to be the front center of the survey frame. The sign convention is as follows:

- positive x: forward
- positive y: starboard
- positive z: down

	Coordinates		
	x (m)	y (m)	z (m)
Center of gravity			
Metacenter (FFI assumption)	-2	0	1
RDI WHN-600 Doppler velocity log	-4.351	0.017	0.348
Responder B25	-0.250	-0.010	-0.160
Kongsberg Maritime HiPAP transponder B71	-0.243	-0.565	-0.155
Reson Seabat Head 2 Starboard	-0.324	0.983	0.250
Reson Seabat Head 1 Port	-0.337	-0.969	0.278
DigiQuartz 700	-0.135	0.458	0.156
SSS Port	0.190	0.450	1.730
SSS Starboard	0.190	0.450	1.730
iXSea Octans motion sensor	-0.110	-0.399	0.096

Table 12.12 HiROV 3000 vessel coordinates

G.3 Dynamics

Dynamic data on an ROV is required to calculate timing accuracy requirements. In Table 12.13 the S/L HiROV 3000 example data is listed. The data come from (9). The ship velocity data is taken from normal operation specifications. The ship angular rate was obtained by derivation of attitude data. Since numerical derivation can introduce noise, the maximum value is a 99.9% value.

Data type	Maximum value
ROV velocity	
$v_{EB_{meta.UV},x}^{B_{UV}}$	1.5 m/s
$v_{EB_{meta.UV},y}^{B_{UV}}$	0 m/s
$v_{EB_{meta.UV},z}^{B_{UV}}$	0 m/s
ROV angular rate	
$\omega_{IB_{UV},x}^{B_{UV}}$	4.0°/s
$\omega_{IB_{UV},y}^{B_{UV}}$	8.0°/s
$\omega_{IB_{UV},z}^{B_{UV}}$	3.0°/s

Table 12.13 ROV example data

G.4 Effect of timing errors

Error source	Motion	Velocity error vector	Timing error	Error magnitude
Ship GPS antenna velocity	Forward ship velocity	$\mathbf{v}_{EB_{ship}}^{B_{ship}}$	δt_{USBL}^{UTC}	1.5 m/s
	Roll	$\left(\Pr_x \boldsymbol{\omega}_{NB_{ship}}^{B_{ship}}\right) \times \mathbf{p}_{B_{ship}B_{GPS}}^{B_{ship}}$	δt_{USBL}^{UTC}	0.2 m/s
	Pitch	$\left(\Pr_y \boldsymbol{\omega}_{NB_{ship}}^{B_{ship}}\right) \times \mathbf{p}_{B_{ship}B_{GPS}}^{B_{ship}}$		0.2 m/s
	Yaw	$\left(\Pr_z \boldsymbol{\omega}_{NB_{ship}}^{B_{ship}}\right) \times \mathbf{p}_{B_{ship}B_{GPS}}^{B_{ship}}$		0.014 m/s
Ship angular rate and lever arm between GPS and USBL	Roll	$\left(\Pr_x \boldsymbol{\omega}_{NB_{ship}}^{B_{ship}}\right) \times \mathbf{p}_{B_{GPS}B_{USBL}}^{B_{ship}}$	$\delta t_{USBL}^{UTC} - \delta t_{INS_{ship}}^{UTC}$	0.27 m/s
	Pitch	$\left(\Pr_y \boldsymbol{\omega}_{NB_{ship}}^{B_{ship}}\right) \times \mathbf{p}_{B_{GPS}B_{USBL}}^{B_{ship}}$		0.27 m/s
	Yaw	$\left(\Pr_z \boldsymbol{\omega}_{NB_{ship}}^{B_{ship}}\right) \times \mathbf{p}_{B_{GPS}B_{USBL}}^{B_{ship}}$		0.0052 m/s
Ship angular rate and relative USBL position	Roll	$\left(\Pr_x \boldsymbol{\omega}_{NB_{ship}}^{B_{ship}}\right) \times \mathbf{p}_{B_{USBL}B_{TP}}^{B_{ship}}$	$\delta t_{USBL}^{UTC} - \delta t_{INS_{ship}}^{UTC}$	160 m/s
	Pitch	$\left(\Pr_y \boldsymbol{\omega}_{NB_{ship}}^{B_{ship}}\right) \times \mathbf{p}_{B_{USBL}B_{TP}}^{B_{ship}}$		160 m/s
	Yaw	$\left(\Pr_z \boldsymbol{\omega}_{NB_{ship}}^{B_{ship}}\right) \times \mathbf{p}_{B_{USBL}B_{TP}}^{B_{ship}}$		0 m/s
UV transponder velocity	Forward UV velocity	$\Pr_x \mathbf{v}_{EB_{UV}}^{B_{UV}}$	$\delta t_{MBE}^{UV} - \delta t_{USBL}^{UTC} - \delta t_{UVclock}$	1.5 m/s
	UV sway velocity	$\Pr_y \mathbf{v}_{EB_{UV}}^{B_{UV}}$	$\delta t_{MBE}^{UV} - \delta t_{USBL}^{UTC} - \delta t_{UVclock}$	0 m/s
	UV heave velocity	$\Pr_z \mathbf{v}_{EB_{UV}}^{B_{UV}}$	$\delta t_{MBE}^{UV} - \delta t_{USBL}^{UTC} - \delta t_{UVclock}$	0 m/s
	Roll	$\left(\Pr_x \boldsymbol{\omega}_{NB_{UV}}^{B_{UV}}\right) \times \mathbf{p}_{B_{UV}B_{TP}}^{B_{UV}}$	$\delta t_{MBE}^{UV} - \delta t_{USBL}^{UTC} - \delta t_{UVclock}$	0.09 m/s
	Pitch	$\left(\Pr_y \boldsymbol{\omega}_{NB_{UV}}^{B_{UV}}\right) \times \mathbf{p}_{B_{UV}B_{TP}}^{B_{UV}}$		0.29 m/s
	Yaw	$\left(\Pr_z \boldsymbol{\omega}_{NB_{UV}}^{B_{UV}}\right) \times \mathbf{p}_{B_{UV}B_{TP}}^{B_{UV}}$		0.097 m/s
UV angular rate and lever arm between transponder and MBE	Roll	$\left(\Pr_x \boldsymbol{\omega}_{NB_{UV}}^{B_{UV}}\right) \times \mathbf{p}_{B_{TP}B_{MBE}}^{B_{UV}}$	$\delta t_{MBE}^{UV} - \delta t_{INS_{UV}}^{UV}$	0.11 m/s
	Pitch	$\left(\Pr_y \boldsymbol{\omega}_{NB_{UV}}^{B_{UV}}\right) \times \mathbf{p}_{B_{TP}B_{MBE}}^{B_{UV}}$		0.058 m/s
	Yaw	$\left(\Pr_z \boldsymbol{\omega}_{NB_{UV}}^{B_{UV}}\right) \times \mathbf{p}_{B_{TP}B_{MBE}}^{B_{UV}}$		0.081 m/s
UV angular rate and MBE beam	Roll	$\left(\Pr_x \boldsymbol{\omega}_{NB_{UV}}^{B_{UV}}\right) \times \mathbf{p}_{B_{MBE}M}^{B_{UV}}$	$\delta t_{MBE}^{UV} - \delta t_{INS_{UV}}^{UV}$	4.2 m/s
	Pitch	$\left(\Pr_y \boldsymbol{\omega}_{NB_{UV}}^{B_{UV}}\right) \times \mathbf{p}_{B_{MBE}M}^{B_{UV}}$		4.1 m/s
	Yaw	$\left(\Pr_z \boldsymbol{\omega}_{NB_{UV}}^{B_{UV}}\right) \times \mathbf{p}_{B_{MBE}M}^{B_{UV}}$		2.7 m/s

Table 12.14 Effect of timing errors for an underwater survey system with a HiROV 3000 on M/V Edda Fonn. The error magnitude is calculated using the vessel coordinates in Section G.2 and the error dynamics in Section G.3. ROV depth is 3000 m and ROV altitude is 30 m.

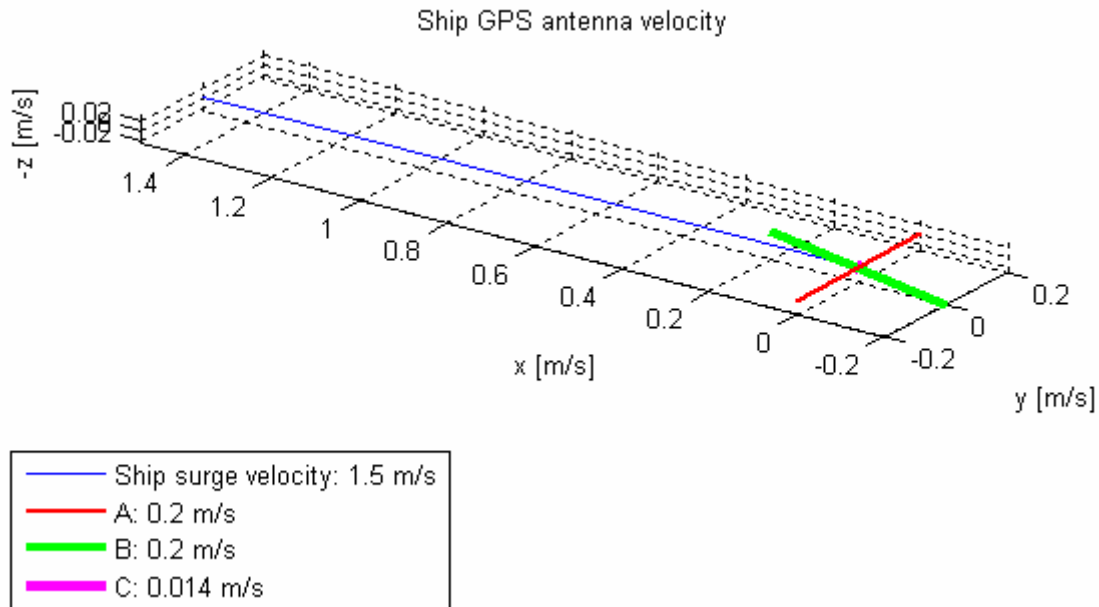


Figure 12.25 Illustration of sensitivity of the underwater vehicle transponder position error due to USBL timing error because of ship GPS antenna velocity. Sensitivity is in ship reference frame in m/s. Multiply by timing error in s to get transponder position error in m. $A = \left| \left(\text{Pr}_x \boldsymbol{\omega}_{NB_{ship}}^{B_{ship}} \right) \times \mathbf{p}_{B_{ship}B_{GPS}}^{B_{GPS}} \right|$, $B = \left| \left(\text{Pr}_y \boldsymbol{\omega}_{NB_{ship}}^{B_{ship}} \right) \times \mathbf{p}_{B_{ship}B_{GPS}}^{B_{GPS}} \right|$, and

$$C = \left| \left(\text{Pr}_z \boldsymbol{\omega}_{NB_{ship}}^{B_{ship}} \right) \times \mathbf{p}_{B_{ship}B_{GPS}}^{B_{GPS}} \right|$$

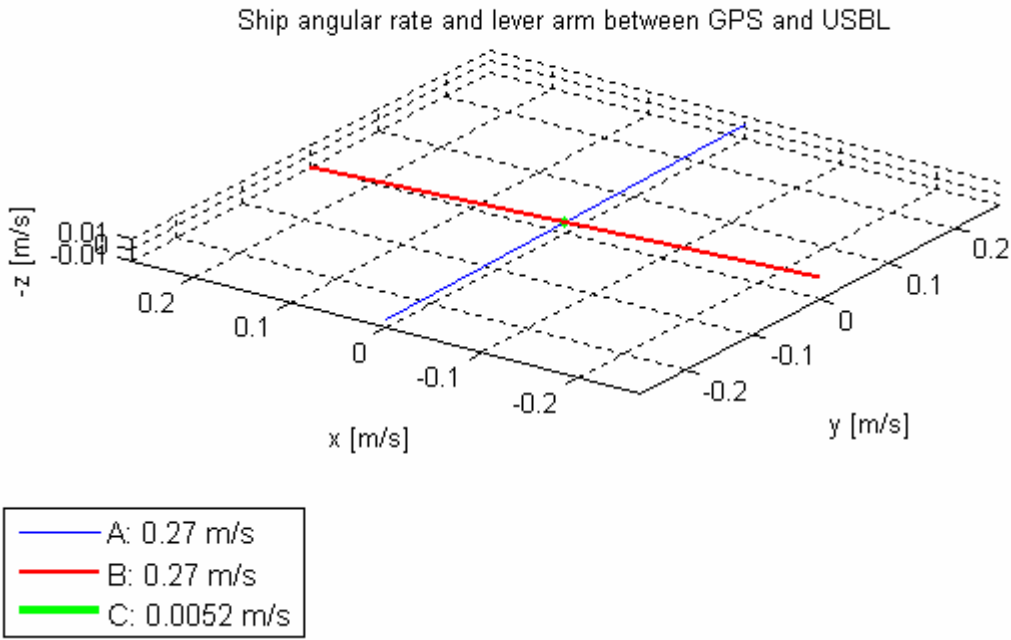


Figure 12.26 Illustration of sensitivity of the underwater vehicle transponder position error due to USBL and INS timing errors because of ship angular rate and GPS-USBL lever arm. Sensitivity is in ship reference frame in m/s. Multiply by timing error

in s to get transponder position error in m. $A = \left| \left(\Pr_x \boldsymbol{\omega}_{NB_{ship}}^{B_{ship}} \right) \times \mathbf{p}_{B_{GPS}B_{USBL}}^{B_{ship}} \right|$,
 $B = \left| \left(\Pr_y \boldsymbol{\omega}_{NB_{ship}}^{B_{ship}} \right) \times \mathbf{p}_{B_{GPS}B_{USBL}}^{B_{ship}} \right|$, and $C = \left| \left(\Pr_z \boldsymbol{\omega}_{NB_{ship}}^{B_{ship}} \right) \times \mathbf{p}_{B_{GPS}B_{USBL}}^{B_{ship}} \right|$.

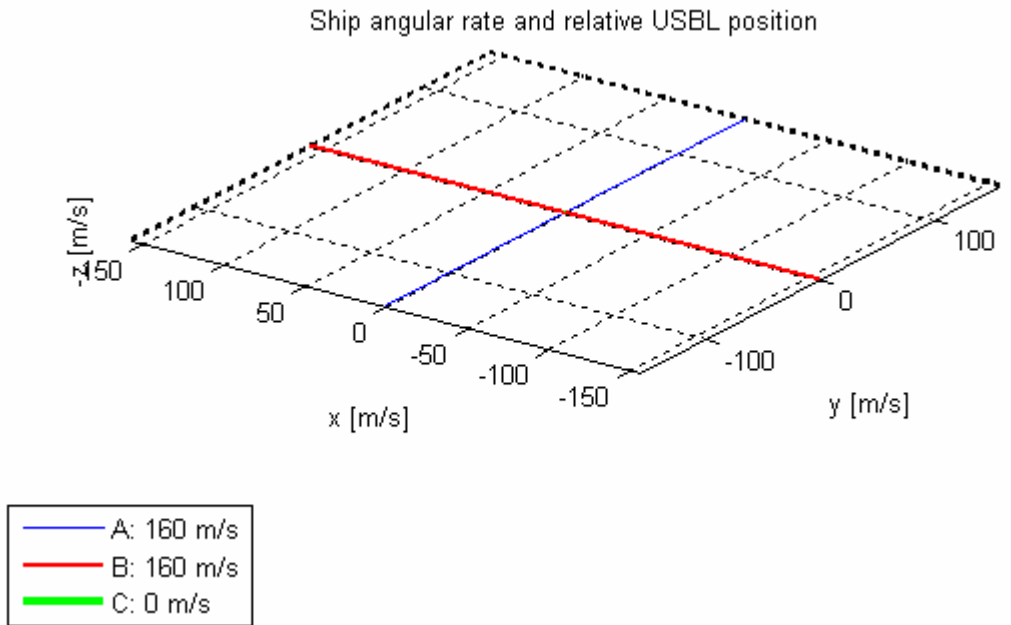


Figure 12.27 Illustration of sensitivity of the underwater vehicle transponder position error due to USBL and ship INS timing errors because of ship angular rate and relative position between surface ship and underwater vehicle. Sensitivity is in ship reference frame in m/s. Multiply by timing error

position error in m. $A = \left| \left(\text{Pr}_x \boldsymbol{\omega}_{NB_{ship}}^{B_{ship}} \right) \times \mathbf{p}_{B_{USBL}B_{TP}}^{B_{ship}} \right|$, $B = \left| \left(\text{Pr}_y \boldsymbol{\omega}_{NB_{ship}}^{B_{ship}} \right) \times \mathbf{p}_{B_{USBL}B_{TP}}^{B_{ship}} \right|$, and $C = \left| \left(\text{Pr}_z \boldsymbol{\omega}_{NB_{ship}}^{B_{ship}} \right) \times \mathbf{p}_{B_{USBL}B_{TP}}^{B_{ship}} \right|$

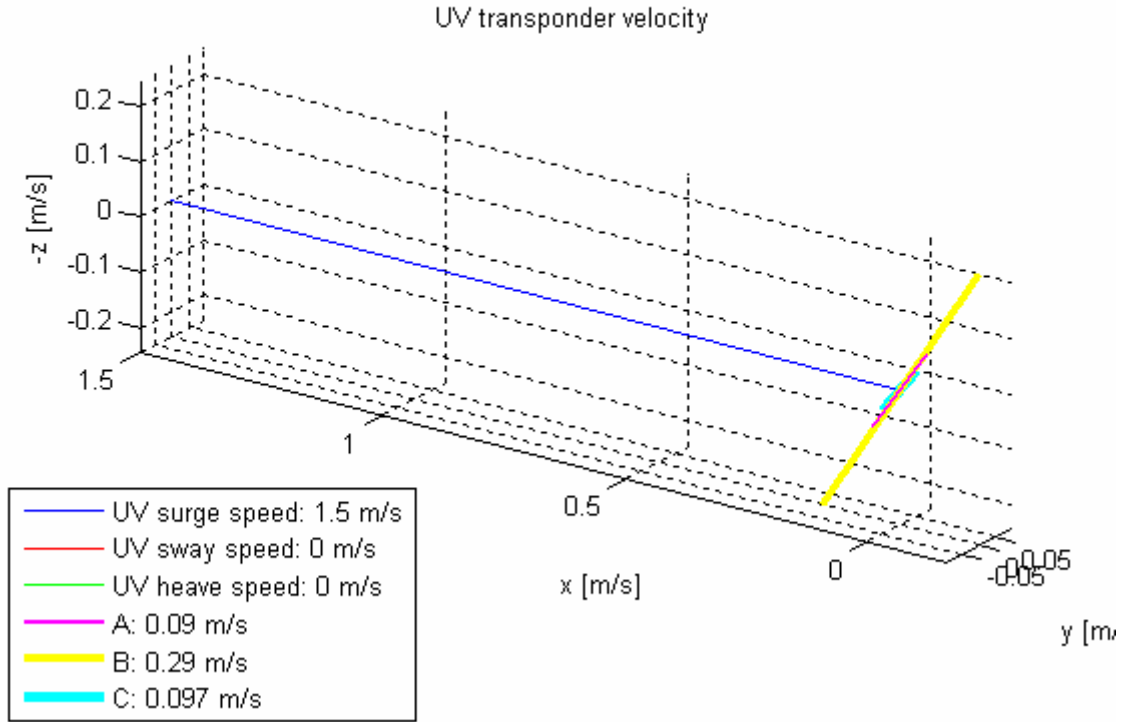


Figure 12.28 Illustration of sensitivity of MBE positioning error due to USBL, INS, and UV clock timing errors because of UV transponder velocity. Sensitivity is in underwater vehicle reference frame in m/s. Multiply by timing error in s to get positioning error in m. $A = \left| \left(\text{Pr}_x \boldsymbol{\omega}_{NB_{UV}}^{B_{UV}} \right) \times \mathbf{p}_{B_{UV}B_{TP}}^{B_{UV}} \right|$, $B = \left| \left(\text{Pr}_y \boldsymbol{\omega}_{NB_{UV}}^{B_{UV}} \right) \times \mathbf{p}_{B_{UV}B_{TP}}^{B_{UV}} \right|$, and $C = \left| \left(\text{Pr}_z \boldsymbol{\omega}_{NB_{UV}}^{B_{UV}} \right) \times \mathbf{p}_{B_{UV}B_{TP}}^{B_{UV}} \right|$.

UV angular rate and lever arm between transponder and MBE

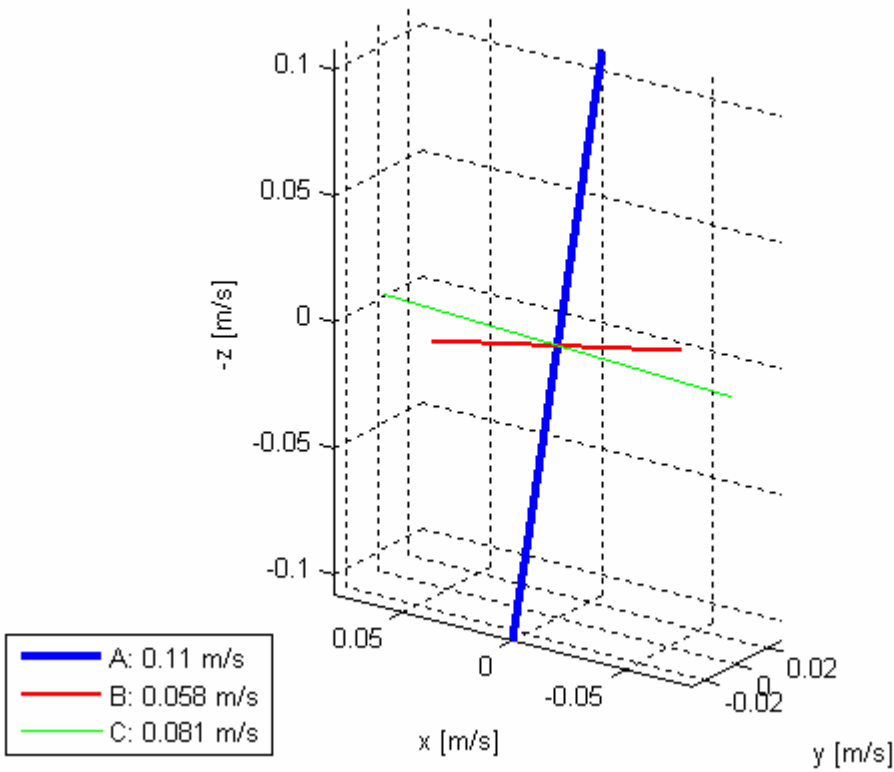


Figure 12.29 Illustration of sensitivity of MBE positioning error due to MBE and UV INS timing errors because of UV angular rate and lever arm between transponder and MBE. Sensitivity is in underwater vehicle reference frame in m/s. Multiply by timing error in s to get positioning error in m. The figure shows the sensitivity for a 600 m MBE beam 60° out of the vertical (Depth 300 m). This explains the vertical component. $A = \left| \left(\text{Pr}_x \boldsymbol{\omega}_{NB_{UV}}^{B_{UV}} \right) \times \mathbf{p}_{B_{TP}B_{MBE}}^{B_{UV}} \right|$, $B = \left| \left(\text{Pr}_y \boldsymbol{\omega}_{NB_{UV}}^{B_{UV}} \right) \times \mathbf{p}_{B_{TP}B_{MBE}}^{B_{UV}} \right|$, and $C = \left| \left(\text{Pr}_z \boldsymbol{\omega}_{NB_{UV}}^{B_{UV}} \right) \times \mathbf{p}_{B_{TP}B_{MBE}}^{B_{UV}} \right|$.

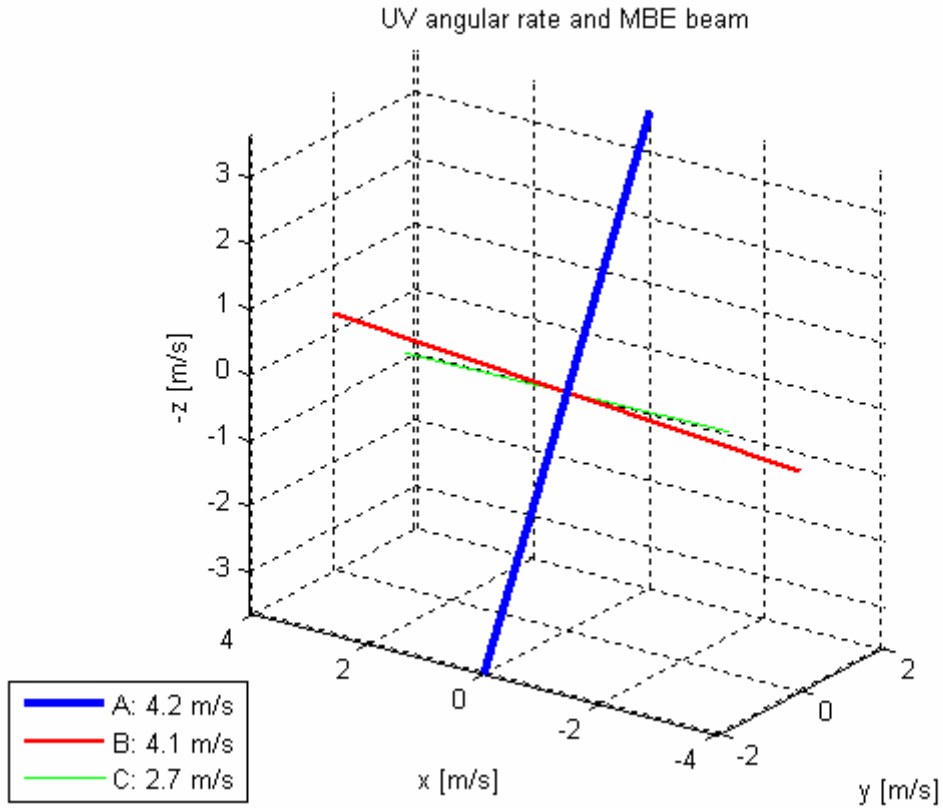


Figure 12.30 Illustration of sensitivity of MBE positioning error due to MBE and UV INS timing errors because of UV angular rate and MBE beam. Sensitivity is in underwater vehicle reference frame in m/s. Multiply by timing error in s to get positioning error in m. The figure shows the sensitivity for a 600 m MBE beam 60° out of the vertical (Depth 300 m). This explains the vertical

component. $A = \left| \left(\text{Pr}_x \boldsymbol{\omega}_{NB_{UV}}^{B_{UV}} \right) \times \mathbf{p}_{B_{MBE}M}^{B_{UV}} \right|$, $B = \left| \left(\text{Pr}_y \boldsymbol{\omega}_{NB_{UV}}^{B_{UV}} \right) \times \mathbf{p}_{B_{MBE}M}^{B_{UV}} \right|$, and

$$C = \left| \left(\text{Pr}_z \boldsymbol{\omega}_{NB_{UV}}^{B_{UV}} \right) \times \mathbf{p}_{B_{MBE}M}^{B_{UV}} \right|.$$

H WORK GROUP MEMBERS

Name	Organization	Contact information
Arne Indreeide	Statoil	ARIN@statoil.com www.statoil.com
Arne Ofstad	Sjøkartverket	arne.ofstad@statkart.no www.statkart.no
Jan Didrik Andersen	Deep Ocean	jda@deepocean.no www.deepocean.no
Rolf Arne Ueland	Blom	rue@blom.no http://maritime.blom.no/
Tor Arne Paulsen	Acergy	tor.arne.paulsen@stoltoffshore.no www.acergy-group.com
Jan Arvid Ingulfsen	Geoconsult	jai@geoconsult.no www.geoconsult.no
Bjørn Jalving	FFI	Bjorn.jalving@ffi.no www.ffi.no